FACULTY OF SCIENCE AND TECHNOLOGY

MASTER THESIS

Study programme / specialisation:
Master of Science Structural and Mechanical Engineering

The spring semester, **2022**

Open / ~~Confidential~~

Author: **Victor FAGNON**

Course coordinator: **Dimitrios PAVLOU**

Supervisor(s): **Dimitrios PAVLOU**

.....
(signature author)

Thesis title:

Techno-economic assessment of flexible composite pipelines for decentralised production of H2 with electrolysers integrated in wind turbine

Credits (ECTS): **30**

Keywords: **FRP, Hydrogen, Pipe, Pipeline, Energy, H2 production, H2 transportation, H2 costs.**

Pages: **88**

+ appendix: **30**

Stavanger, **15/06/2022**

Abstract

Hydrogen gas, H_2, is currently creating a lot of attention from governments and companies. The potential applications bring a lot of attention and, even too much when regarding in details the situation. Liquid hydrogen appears irrelevant to satisfy a global hydrogen network due to the extreme conditions required and its huge energy loss to obtain this phase.

Since hydrogen is not an energy, it must receive power to be produced and this is currently driven by fossil energies at 95%. Electrolysis of water has been analysed and is found to be an interesting way of H_2 production with an acceptable efficiency, no CO_2 emissions and a decent adaptability to intermittent renewable sources of energy such as wind. However, it still keeps a high cost with a ratio from 2 to 3 times the price from using fossil fuels instead.

About the pipeline transportation, GFRP and GRE seem to be the most sustainable FRP pipes regarding the energy and carbon footprint. From an actual hydrogen pipe and other similar pipe products, the features are usually composed of a diameter up to 6" (152mm), a temperature and pressure resistance around 80°C and [40 ; 80] bar with a lifetime between 20 to 50 years and made of either glass or aramid fibres for the reinforcement.

Regarding the economy, on one hand, hydrogen produced from electrolysis has costs in the range [2.5 ; 5.5]€·kg^{-1}. The compression stage costs [0.9 ; 1.75]€·kg^{-1} where the actual compressor price is between 45 000€ to 90 000€. In comparison, fossil fuel energies produce hydrogen at a cost of [1.5 ; 2]€·kg^{-1} which fade the cost competitiveness away.

On the other hand, the hydrogen transportation costs are found in the order of [0.139 ; 0.261]€·kg^{-1} for a minimum demand of 5 million of tonnes per year. In a recent report, costs for offshore pipeline are estimated to reach [0.17 ; 0.32]€·(kg·1000km)$^{-1}$. In addition, the price of FRP pipeline is globally comprised between 32\$·m^{-1} and 46\$·m^{-1} and could reach a maximum of 66\$·m^{-1} for difficult installation conditions.

For strategic purpose, it is important to remind that hydrogen is an energy carrier and requires a huge amount of energy to be produced, process mainly done by fossil fuel today. An interesting way for decarbonising the society would first to replace this major production by a renewable production of hydrogen which would need a transportation assured by pipelines for reducing environmental footprint, costs, times and increasing quantity with efficiency.

Acknowledgement

This master thesis is written as my final project of the master´s degree in structures and materials at the Faculty of Science and Technology in the University of Stavanger, in Norway. This work has been carried out during the spring semester of 2021.

I wish to express my sincere gratitude to Dimitrios Pavlou, my supervisor at the University of Stavanger during this master's thesis, for assistance and supervision throughout the duration of the thesis. His advices, guidelines during discussions at the beginning and middle parts of the semester were crucial, periods when uncertainties arise.

I would also like to thank:
- Ramin Moslemian from *DNV* for taking the time to have Teams meetings before discussing about this interesting topic for the master's thesis in accordance to the current hydrogen trend and needs; and also for his guidance to orient me in order to contact companies that manufacture reinforced composite pipes.
- Mark breed from *Teijin aramid* for sharing his work method for the economic and environmental comparison between aramid reinforced pipes and steel pipes.
- Robbert Laan and Peter Cloos from *Soluforce* for their time for a Teams meeting, viewpoint and description of the H2t pipe made for hydrogen.
- Mark Heckman from *Future Pipe* for his time to have a Teams meeting, his precious descriptions and explanations as well as documents shared about the Future Pipe products.
- Last but not least, Frits Kronenburg from *Strohm* for sharing highly relevant documents with a precious value regarding the topic of my thesis.

I finally would like to thank my student friends sitting at IL during all this semester and sharing doubts, moments and stress together.

Stavanger, June 2022

Victor Fagnon

Table of Contents

List of Tables

List of Figures

List of abbreviation

- °C = Degree Celsius
- AWE = Alkaline Water Electrolysis
- CH_4 = Methane
- CO_2 = Carbon dioxyde
- FEM = Finite Element Element
- FRP = Fibre Reinforced Polymer
- GHG = Greenhouse gases
- GPa = Giga Pascal (Pressure, 10^9Pa)
- GRE = Glass Fibre Reinforced Epoxy
- Gt = Gigaton (10^9 ton = 10^{12} kg)
- GW = Giga Watt
- H_2 = (Di)hydrogen
- HP = High Pressure
- K = degree Kelvin
- LCOH = Levelised Cost Of Hydrogen
- LP = Low Pressure
- MPa = Mega Pascal (Pressure, 10^6 Pa)
- Mt = Mega ton
- MW = Mega Watt
- NH_3 = Ammonia
- PEM(EC) = Polymer Electrolyte Membrane (Electrolysis)
- SiO_2 = Silica
- SMR = Steam Methane Reforming

- SOEC = Solid Oxide Electrolysis
- TCP = Thermoplastic Composite Pipe

Introduction

Hydrogen is one of the major elements in the universe and represents a fundamental atom regarding the composition of molecules. It has, indeed, a huge role in the origin of life by creating suitable particles at the beginning of the atmosphere formation on Earth. A few basic examples are water vapour or liquid, H_2O, containing two hydrogen atoms for one oxygen atom; organic molecules, where carbon atoms are the base for this type; other chemical compounds such as ammonia, NH_3, or methane, CH_4. Hydrogen, alone, is found usually, for ambient temperature and atmospheric pressure, as a gas called dihydrogen, H_2. The phase diagram of hydrogen can be found in this document, see Figure 2, which makes visible the difficulties to obtain hydrogen at another state than gas. For solid or liquid hydrogen, extreme low temperatures must be reached at a minimum of approximately -240°C. [121]

Recently, hydrogen appears very attractive by the potential utilisation that can be done with it. One of the main properties which are featured is the clean aspect of hydrogen by not emitting any CO_2 emissions when used to power a system. The product resulting of the hydrogen usage is basically water by the unification of the hydrogen and oxygen atoms. However, the production of hydrogen is still mostly produced from fossil energy sources which, unfortunately, emit greenhouse gases (GHG) such as CO_2. Thus, the ideal solution is now partly focused on producing hydrogen from *green energy sources*, renewable energies and nuclear power, which will not emit those GHG. In addition, the interest is not just a scientific or technological fact but also an economic engagement proved by important investments done by governments in several countries for financing hydrogen projects. [27]

The whole hydrogen demand reached about 90 mega-tonnes (Mt) in 2020 with 70 Mt directly dedicated to be pure hydrogen. The major demands for hydrogen goes to the oil refining process and then to industry in general like chemical production of ammonia or methanol. Nevertheless, due to the increasing interest for this gas, the demand will potentially be more diversified. Moreover, including more renewable energies in the production of hydrogen would change the location for production sites such as offshore wind farms for, this thesis, that are placed in the sea. That is why, transportation is becoming a relevant topic to achieve the goals of reducing GHG emissions set by the companies, industries and governments. Pipelines seem fully relevant for one part of the solution, especially for long distance, but classic steel pipelines suffer from hydrogen embrittlement. Thus, transportation by pipelines made in reinforced composite materials will be investigated, as a literature review, in this document. [58], [57]

Composite pipelines, or Fibre Reinforced Polymer (FRP) pipes, have been and are already being used for other transport applications such as petroleum, water and gas. The motivation to chose this option instead of a steel pipe is both a cost reduction as well as the lack of corrosion of the pipe. Additionally to this, other mechanical advantages are non-negligible including: weight to strength ratios due to the lighter mass, good stiffness and durability, satisfying pressure resistance and cost benefit together with an improved environmental footprint. However, today, there exists only a few projects for actual hydrogen pipe developed with fibre reinforced materials. That is linked to an almost non-existent market for this new product but interest is growing with more projects being created and developed for the next future years giving hope for this branch. [8]

Therefore, composite reinforced materials could help to solve the challenge of transporting hydrogen via pipeline under certain characteristics. The purpose of this thesis is, thus, to present an overview and general outlook of the technical characteristics as well as a cost perspective for hydrogen gas, its production and transportation via pipelines. To achieve this goal, information from papers, studies, reports and other documents from the scientific literature as well as from companies themselves will be summarised and included through this thesis.

This master's thesis include some limitations. Hydrogen is not a new gas and is pretty well known but producing it with electrolysers along with the transportation via composite reinforced pipelines represent new challenges. It means that scientific studies for finding good materials, dimensions, aspects and other details have to be performed. Then, standards can guide industries and manufacturers to make products by satisfying safety rules and proper designs. However, there are only a few projects based on transportation of hydrogen by FRP pipelines and current company groups and networks are working together to produce standards and collaborations in order to facilitate the cooperation and share of information, e.g. HyREADY (JIP: Joint Industry Project) and see section IV in Appendix C. The main limitations were to access, find and analyse data as well as relevant results because they either do not exist yet or are not available for secrecy reasons. That is why contacting several companies and industries helped a little in the process of bringing additional information. The lack of standards for this technology is also a crucial point both for this work but also for companies which would like to develop this product. Limitations regarding the economy sections include the lack of information and also the specificity of each project when information becomes very detailed. Including that aspect, driving conclusions can be done either, for a general situation from global information as it has been done in this thesis or, for a specific project with more detailed and precise data.

First, the theoretical features, main calculations and important mathematical expressions of composite pipelines will be listed in Part I *Design aspects of flexible multi-layered pipelines*. Then, hydrogen gas and composite materials will be further introduced and detailed together with the information provided and shared by pipe manufacturers in Part II *Materials and technologies for H2 transportation*. After that, the cost aspects regarding both the production and the transportation by pipelines of hydrogen will be described and presented in Part III *Production, demand and transportation costs of hydrogen gas and pipelines*. Finally, the properties, characteristics and results obtained and expressed in this master's thesis will be interpreted and discussed in the last chapter, Part IV *Conclusion*.

Part I
Design aspects of flexible multi-layered pipelines

Solid mechanic equations applied to laminae and laminates

Mechanical aspects of laminae and laminates

The main purpose of the whole part is to describe the fundamental equations related to the mechanics of composite pipeline. To do that, the main source that will be used for the notation of variables and as a guideline is [87].

In order to treat correctly the design aspects of FRP composite pipes, only the macroscopic scale of the system will be investigated without taking into account the smaller effects, i.e. the microscopic view. To justify this choice, by assuming that all the analysis can be performed with including all the microscopic effects acting in addition to the macroscopic ones, numerical simulations would engage too much time, effort and money. So in order to perform a good analysis, only the macro-effects are considered and, in fact they actually represent larger effects and order of magnitude on calculations.

To do so, the equations linking stress and strains are used and defined first for a material with a plane of elastic symmetry. Furthermore, it is obvious that a composite pipeline is a cylindrical structure, thus it has two mutual orthogonal planes of elastic symmetry. This means that the materials constants C_{14}, C_{24}, C_{34}, C_{41}, C_{42}, C_{43}, C_{56} and C_{65} are also equal to zero. By applying these simplifications and the symmetry of the stiffness tensor C_{ij}, the equation (1), from Hooke's law in [87], states the stress-strain matrix relation of unidirectional composite lamina. The parameters C_{ij} and S_{ij} are expressed in appendix A with the equations (36)-(39) and (40)-(43), from [87] and [46].

$$\begin{Bmatrix} \sigma_1 \\ \sigma_2 \\ \sigma_3 \\ \tau_{23} \\ \tau_{13} \\ \tau_{12} \end{Bmatrix} = [C] \begin{Bmatrix} \varepsilon_1 \\ \varepsilon_2 \\ \varepsilon_3 \\ \gamma_{23} \\ \gamma_{13} \\ \gamma_{12} \end{Bmatrix} \approx \begin{bmatrix} C_{11} & C_{12} & C_{13} & 0 & 0 & 0 \\ C_{12} & C_{22} & C_{23} & 0 & 0 & 0 \\ C_{13} & C_{23} & C_{33} & 0 & 0 & 0 \\ 0 & 0 & 0 & C_{44} & 0 & 0 \\ 0 & 0 & 0 & 0 & C_{55} & 0 \\ 0 & 0 & 0 & 0 & 0 & C_{66} \end{bmatrix} \begin{Bmatrix} \varepsilon_1 \\ \varepsilon_2 \\ \varepsilon_3 \\ \gamma_{23} \\ \gamma_{13} \\ \gamma_{12} \end{Bmatrix} \tag{1}$$

The previous relation can also be written as an expression giving the strains according to the stresses by inverting the stiffness matrix $[C_{ij}]$, which gives the compliance matrix $[S_{ij}] = [C_{ij}]^{-1}$.

$$\begin{Bmatrix} \varepsilon_1 \\ \varepsilon_2 \\ \varepsilon_3 \\ \gamma_{23} \\ \gamma_{13} \\ \gamma_{12} \end{Bmatrix} = [S] \begin{Bmatrix} \sigma_1 \\ \sigma_2 \\ \sigma_3 \\ \tau_{23} \\ \tau_{13} \\ \tau_{12} \end{Bmatrix} \approx \begin{bmatrix} S_{11} & S_{12} & S_{13} & 0 & 0 & 0 \\ S_{12} & S_{22} & S_{23} & 0 & 0 & 0 \\ S_{13} & S_{23} & S_{33} & 0 & 0 & 0 \\ 0 & 0 & 0 & S_{44} & 0 & 0 \\ 0 & 0 & 0 & 0 & S_{55} & 0 \\ 0 & 0 & 0 & 0 & 0 & S_{66} \end{bmatrix} \begin{Bmatrix} \sigma_1 \\ \sigma_2 \\ \sigma_3 \\ \tau_{23} \\ \tau_{13} \\ \tau_{12} \end{Bmatrix} \tag{2}$$

By forming layers of composite materials for pipeline, the analysis can be reduced to two dimensions since there is one side much smaller than the two others. Regarding the previous matrix equations, it transforms the previous strain and stress vectors to the 2D strain and stress form by also reducing the number of dimension in the compliance/stiffness matrix. The equations (1) and (2), as proved by [87] and [46], are reduced as follow:

$$\begin{Bmatrix} \sigma_1 \\ \sigma_2 \\ \tau_{12} \end{Bmatrix} = [Q] \begin{Bmatrix} \varepsilon_1 \\ \varepsilon_2 \\ \gamma_{12} \end{Bmatrix} \approx \begin{bmatrix} Q_{11} & Q_{12} & 0 \\ Q_{12} & Q_{22} & 0 \\ 0 & 0 & Q_{66} \end{bmatrix} \begin{Bmatrix} \varepsilon_1 \\ \varepsilon_2 \\ \gamma_{12} \end{Bmatrix} \tag{3}$$

$$\begin{Bmatrix} \varepsilon_1 \\ \varepsilon_2 \\ \gamma_{12} \end{Bmatrix} = [S] \begin{Bmatrix} \sigma_1 \\ \sigma_2 \\ \tau_{12} \end{Bmatrix} \approx \begin{bmatrix} S_{11} & S_{12} & 0 \\ S_{12} & S_{22} & 0 \\ 0 & 0 & S_{66} \end{bmatrix} \begin{Bmatrix} \sigma_1 \\ \sigma_2 \\ \tau_{12} \end{Bmatrix} \tag{4}$$

The parameters of the reduced compliance matrix S_{ij} are still the same while the reduced stiffness parameters are modified and expressed in Appendix A by the equation (44)-(45), from [87].

In addition to the basic expression of the strains in equations (1) and (2), thermal and moisture effects can be taken into account. It will simply add the terms $-\alpha_i \Delta T$ and $-\beta_i \Delta M$ to ε_1, ε_2 and ε_3. The coefficient of thermal expansion is α and the one for moisture expansion is β. [17], [124], [93]

Oriented fibres with an angle

Since the fibres direction x_1 and x_2 can create an angle θ with the axis of the plate, the transformation matrix $[T]$, as expressed by the equation (46) in Appendix A, is used in equations (5), from [87] and [46], to define the stresses and strains by taking into account this rotation:

$$\begin{Bmatrix} \sigma_1 \\ \sigma_2 \\ \tau_{12} \end{Bmatrix} = [T] \begin{Bmatrix} \sigma_x \\ \sigma_y \\ \tau_{xy} \end{Bmatrix} \quad ; \quad \begin{Bmatrix} \varepsilon_1 \\ \varepsilon_2 \\ \frac{1}{2}\gamma_{12} \end{Bmatrix} = [T] \begin{Bmatrix} \varepsilon_x \\ \varepsilon_y \\ \frac{1}{2}\gamma_{xy} \end{Bmatrix} \tag{5}$$

Thus, the transformed reduced compliance matrix $\overline{S}_{ij}$ is used to obtain the strains from the stresses with the equation $\{\varepsilon\}_{3\times1} = [\overline{S}]_{3\times3}\{\sigma\}_{3\times1}$; and the transformed reduced stiffness matrix $\overline{Q}_{ij}$ to obtain the stresses from the strains with the equation $\{\sigma\}_{3\times1} = [\overline{Q}]_{3\times3}\{\varepsilon\}_{3\times1}$. The expressions of those parameters are also stated in appendix A through the equations (47)-(58), from [87]. From the equations, it can be easily deduced that the transformed reduced compliances and stiffnesses values depend highly on the angle made by the fibre orientation. [46]

A laminate perspective

A sequence of several fibre-reinforced laminae constitutes the overall structure of composite laminates. That is why the characteristics defining by each lamina such as the layer sequence with the fibre orientation and the total number of layers can produce a significant effect on the whole composite pipeline. A change among these criteria creates another structure with different properties. Thus, it is important to be aware of the potential changes when a design needs to be review or modified.

To analyse a laminate, the use of Kirchhoff assumption is relevant. It states that potential straight lines which are perpendicular, i.e. normal, to the plane xy of the composite surface would stay in this position to the mi-surface after deformation. Therefore, this statement is particularly relevant and helpful since it allows to neglect both the shear and transverse normal effects. In order to display the stresses of a laminate, its strains need to be found. This can be done by defining the displacement in x and y directions in equation (6), as given in [87]. In the equation, w^0 is the vertical movement and its derivative represents the slope after deformation. And thanks to the strain-displacement relations expressed in appendix A by equations (59)-(60) from [116], equation (7) of stresses for a laminate is obtained from [87].

$$u = u^0 - z\frac{\partial w^0}{\partial x} \quad ; \quad v = v^0 - z\frac{\partial w^0}{\partial y} \tag{6}$$

$$\begin{Bmatrix} \sigma_x \\ \sigma_y \\ \tau_{xy} \end{Bmatrix} = \begin{bmatrix} \overline{Q}_{11} & \overline{Q}_{12} & \overline{Q}_{13} \\ \overline{Q}_{21} & \overline{Q}_{22} & \overline{Q}_{23} \\ \overline{Q}_{31} & \overline{Q}_{32} & \overline{Q}_{33} \end{bmatrix} \begin{Bmatrix} \varepsilon_x^0 + zk_x^0 \\ \varepsilon_y^0 + zk_y^0 \\ \gamma_{xy}^0 + zk_{xy}^0 \end{Bmatrix} \tag{7}$$

From this last equation,

- $k_x^0 = -\frac{\partial^2 w^0}{\partial x^2}$, $k_y^0 = -\frac{\partial^2 w^0}{\partial y^2}$ and $k_{xy}^0 = -2\frac{\partial^2 w^0}{\partial x \partial y}$ are the *curvatures of the reference surface in the x and y directions* together with *the reference twisting curvature.*

- $\varepsilon_x^0 = \frac{\partial u}{\partial x}$, $\varepsilon_y^0 = \frac{\partial v}{\partial y}$ and $\gamma_{xy}^0 = \frac{\partial v^0}{\partial x} + \frac{\partial u}{\partial y}$ are *reference surface extensional strain in the x and y direction* together with *the reference surface in-plane shear strain.*

- The elements $\overline{Q}_{ij}$ of the transformed reduced stiffness matrix $[Q]$ are given in appendix A by equations (53)-(58), from [87].

After calculation of force and moment resultants, the results can be combined in a matrix format, as presented by [87]:

$$\begin{Bmatrix} N_x \\ N_y \\ N_{xy} \\ M_x \\ M_y \\ M_{xy} \end{Bmatrix} = \begin{bmatrix} A_{11} & A_{12} & A_{16} & B_{11} & B_{12} & B_{16} \\ A_{12} & A_{22} & A_{26} & B_{12} & B_{22} & B_{26} \\ A_{16} & A_{26} & A_{66} & B_{16} & B_{26} & B_{66} \\ B_{11} & B_{12} & B_{16} & D_{11} & D_{12} & D_{16} \\ B_{12} & B_{22} & B_{26} & D_{12} & D_{22} & D_{26} \\ B_{16} & B_{26} & B_{66} & D_{16} & D_{26} & D_{66} \end{bmatrix} \begin{Bmatrix} \varepsilon_x^0 \\ \varepsilon_y^0 \\ \gamma_{xy}^0 \\ k_x^0 \\ k_y^0 \\ k_{xy}^0 \end{Bmatrix} \tag{8}$$

It reveals the ABD matrix, regrouping the terms A_{ij}, B_{ij} and D_{ij}, which is also called the laminate stiffness matrix. In the same way as before, the inverse of the previous matrix can be deduced and is defined as matrix $[a] = [A]^{-1}$. [109], [116]

Failure criterion

The information that the engineer usually obtains from experiments are forces and moments at the boundaries. The purpose is then, regarding the multi-layered composite pipeline, to compute the stress on each layer as a way to apply a failure criterion. From the moment it exists a loss of integrity in the material, there is an actual risk of failure. The safety factors are thus very useful in this field and correspond to one of the main goal to achieve. For isotropic materials, the most common failure criterion is probably the *Von Mises criterion.* However, in this type of material, anisotropy must be taken into account and the most relevant failure criterion for that is *Tsai-Wu criterion* which is based on a similar logic as the *Von Mises.*

The equation (9) is expressing the Tsai-Wu failure criterion where the parameters F_{ij} are put in appendix A by equations (61)-(62), as proved by [119].

$$F_1\sigma_1 + F_2\sigma_2 + F_{11}\sigma_1^2 + F_{22}\sigma_2^2 + F_{66}\tau_{12}^2 - \sqrt{F_{11}F_{22}}\sigma_1\sigma_2 \leq 1 \tag{9}$$

The final calculation of the principal stresses

All the previous calculations and results summarised are useful in order to obtain one of the main information of any design problem: the principal stresses.

In order to do so, and as mentioned above, the input data are the forces and moments N_x, N_y, N_{xy}, M_x, M_y, M_{xy} and will then be used to obtain the strains and curvature quantities ϵ_x^0, ϵ_y^0, γ_{xy}^0, k_x^0, k_y^0, k_{xy}^0 through the ABD matrix, or to be more precise through its inverse, the abd matrix. Then, the kirchhoff assumption allows to deduce the strains ϵ_x, ϵ_y and γ_{xy} which gives the principal strains by making use of the transformation matrix $[T]$. Ultimately, thanks to the stress-strain relations, the principal stresses σ_1, σ_2 and σ_{12} can be obtained.

Categories of materials for fibre reinforced composite pipes

The matrix

For choosing the composite matrix material for the pipeline, there is mainly two options. The first one includes a type of resin called *thermosets* (e.g. epoxies) which does not vary or change its form during a period of time when heating is increased. The second one is called *thermoplastics* and acts in the opposite way. When temperature is high, it does modify the shape by being more flexible. An additional information concerns the second heating sequence which allows this type of resin to be reform again thus, meaning that repairing can be performed. Once the matrix of the composite structure is chosen, the fibres need to be selected. Among the different categories, *carbon*, *glass* and *synthetic fibres* are the most used thanks to their good strength, thermal stability and low density. Graphite fibres is also including in carbon type and kevlar fibres are a part of the synthetics. [100], [87], [124]

Thermosets

Thermosets is the usual resin utilised for matrix in composites. This is due to good points such as good chemical resistance, stability, fibre impregnation, price and low processing temperatures. It includes the following types, as stated by [87] and [100]:

- polyester resins
- vinyl ester resins
- bisphenol fumerate resins
- liquid epoxy resins
- solid epoxy resins

- polyurethane resins
- furane resins
- phenolic resins
- chlorenic resins

Thermoplastics

One particularity of the thermoplastic resins is to not be *cross-linked*, this means that there is no polymer chains linked to each other in order to have a network. This specificity is very interesting in the fact that the process can be manufactured quickly which reduces the cost. A main difference compared to thermosets is the quantity of deformation to apply before the apparition of the final fracture, incidentally deformation is dependent on time because of creep. Indeed, thermoplastics can tolerate larger deformation which is defined as having a higher toughness. [124], [87]

The fibres

The **glass fibres** are composed mainly of SiO_2, silica, and thus will not melt easily. In addition, they are cheap and relevant concerning piping applications such as transport of high corrosive fluid. To give a few examples, *E-Glass* and *C-Glass* can carry water and mild conditions thanks to a very good corrosion resistance, though the second type is long-lasting for acids and alkalis. *S-Glass* is another one that is improved regarding strength and stiffness, it is then appropriate for high-performance applications.

Compared to the previous type, **carbon fibres** have a better density than the glass by keeping a similar diameter and also a higher tensile modulus which directly means a greater stiffness. However, glass fibres can allow a better elongation as well as a higher tensile strength which implies that they will be able to carry more load than the carbon fibres.

An other range of fibre is the **synthetic** ones also called sometimes **polymeric fibres**. They are quite competitive regarding the manufacturing of FRP materials. This can be explained by their good density and especially chemical resistance. Among this family of fibres, Kevlar is probably the most famous and well-known synthetic fibre. But, the most problematic point is their poor temperature resistance. By comparison with the two previous fibres, about tensile strength and elongation *Kevlar-49* is similar than glass. For the tensile modulus, this characteristic is slightly larger than glass but still much less than carbon. Finally, for a diameter a bit larger, the density is still significantly reduced. [124], [87]

Technologies for the production

There are two techniques to make a FRP composite pipe called filament winding and filament placement. The last one consists of applying pre-impregnated tapes of distinct fibres on the mandrel's surface.

Regarding the filament winding, the matrix and fibres can be composed of the materials described above in the previous sections. To perform the filament winding process, two patterns exist. First, the helical pattern is created by wounding over a mandrel which is rotating. and this pattern is suitable for pipe production. Some examples of winding angles can be stated: at a winding angle of $\frac{\pi}{2} rad$, i.e. 90°, the process is suitable for pipes which are long and contain internal pressure; on the other hand with an angle around $0 rad$, i.e. 0°, the process better fits situation including axial tension or bending. Second, the polar pattern results of a mandrel static with the payout head rotating around. This type is used for axisymmetric composite shells and mainly in axisymmetric pressure vessels.

Both methods, either filament winding or filament placement, are lightweight and high-strength products which make them a potential good technology in many pipeline applications. [50], [87]

Mechanical design

Difference between loads

Installation loads

The loading is one of the main parameter in designing the pipelines and include the installation as well as the in-service period of time. Small variations, changes and unexpected behaviour might occur during the operation phase of the composite pipelines, however, the most important loads usually occur while the pipes are installed. Bending, external pressure, axial tension, torsion and combination of them can happen for example. Two methods for the installation of composite pipelines are: [66], [87]

- *S-Lay* installation which consists to distribute the pipes offshore horizontally from the boat until the bottom of the sea by forming a "S" shape.

- *J-Lay* technique is, on the other hand, using a vertical installation of the pipes forming a "J" shape.

Operation loads

The types of load varies from the installation, where there are mainly pseudo-static loads, to the operation stage, where an addition of static and dynamic

loading situations can appear. Static loading has a constant value while pseudo-static loading includes some changes but stay constant over time; then, dynamic loading represents vibrations or impacts for instance.

For the design, instead of using a failure criteria, which is mostly developed for static loads, it appears more relevant to do the analysis with a fatigue damage accumulation due to the variable loading cases stated above which can occur during the whole life time of the pipelines. [66], [87]

Summary of main results for pure bending

Failure analysis

Among the loading cases stated previously, bending is a typical load especially during the installation of pipelines following the procedures stated: S-Lay and J-lay. One of the most important aspect to consider in analysis concerning this type of loading is to determine the bending moment or the minimum radius of curvature. In addition, the stress analysis of composite pipelines is simplified by using only elasticity equations since the plastic behaviour of this type of material is nearly absent.

In the principal coordinate system, the engineering properties (elasticity and shear modulus; Poisson's ratio; longitudinal, transverse an in-plane stress) of the pipe's are found once the material has been defined and chosen, i.e. E_1, E_2, G_{12}, ν_{12}, σ_1^T, σ_1^C, σ_2^T, σ_2^C, τ_{12}^F. [87]

Single layered pipe

The single-layered pipe's stresses is given by using the Lekhnitskii formalism for stress and displacements. [68]

$$\begin{aligned}
\sigma_r &= \left[C_1 r^{n-1} - C_2 r^{-n-1} + \frac{C_3}{r} + Agr\right] \sin\varphi \\
\sigma_\varphi &= \left[C_1 (n+1) r^{n-1} + C_2 (n-1) r^{-n-1} + \frac{C_3}{r} + 3Agr\right] \sin\varphi \\
\sigma_z &= Ar \sin\varphi - \frac{1}{S_{33}} (S_{13}\sigma_r + S_{23}\sigma_\varphi) \\
\tau_{r\varphi} &= -\left[r^{n-1} C_1 - r^{-n-1} C_2 + r^{-1} C_3 + grA\right] \cos\varphi
\end{aligned} \tag{10}$$

A represents the area where the elementary area of the pipe is defined as $dA = rd\phi dr$. C_1, C_2, C_3 are simply representing constants in the equations. The reference [94] gives the first four equations (11) between the stresses and strains

in cylindrical directions while the last four equations, from [68], correlate strains and displacements in r and φ directions:

$$\begin{aligned}
\epsilon_z &= \overline{S}_{11}\sigma_z + \overline{S}_{12}\sigma_\varphi + \overline{S}_{13}\sigma_r \\
\epsilon_\varphi &= \overline{S}_{21}\sigma_z + \overline{S}_{22}\sigma_\varphi + \overline{S}_{23}\sigma_r \\
\epsilon_r &= \overline{S}_{31}\sigma_z + \overline{S}_{32}\sigma_\varphi + \overline{S}_{33}\sigma_r \\
\gamma_{r\varphi} &= \frac{1}{2}\overline{S}_{44}\tau_{r\varphi}
\end{aligned} \quad ; \quad
\begin{aligned}
\epsilon_z &= \frac{\partial u_z}{\partial z} \\
\epsilon_\varphi &= \frac{u_r}{r} + \frac{1}{r}\frac{\partial u_\varphi}{\partial \varphi} \\
\epsilon_r &= \frac{\partial u_r}{\partial r} \\
\gamma_{r\varphi} &= \frac{1}{r}\frac{\partial u_r}{\partial \varphi} + \frac{\partial u_\varphi}{\partial r} - \frac{u_\varphi}{r}
\end{aligned} \tag{11}$$

The following expressions (12) can be obtained for the displacements and stresses. The calculations and the elements λ and μ are detailed in [87]:

$$\begin{aligned}
u_r &= \sin\varphi\,(\lambda_1 C_1 + \lambda_2 C_2 + \lambda_3 A) \\
u_\varphi &= \cos\varphi\,(\lambda_4 C_1 + \lambda_5 C_2 + \lambda_6 A) \\
\sigma_r &= \sin\varphi\,(\mu_1 C_1 + \mu_2 C_2 + \mu_3 A) \\
\sigma_\varphi &= \sin\varphi\,(\mu_4 C_1 + \mu_5 C_2 + 3\mu_3 A) \\
\sigma_z &= \frac{\sin\varphi}{S_{33}}\,(\mu_1 C_1 + \mu_2 C_2 + \mu_3 A) \\
\tau_{r\varphi} &= -\cos\varphi\,(\mu_1 C_1 + \mu_2 C_2 + \mu_3 A)
\end{aligned} \tag{12}$$

Multi-layered pipe

The above equations mentioned are describing the stresses and displacements of a single layered pipe. However, in reality a pipe is composed of several layers of composite materials. Thus, it is necessary to describe the stresses σ_r, σ_ϕ, σ_z, $\tau_{r\phi}$ and afterwards the constants C_1, C_2, A for all the layers k which compose the pipe when this one can be subjected to bending for example. In order to do that, the equilibrium equations on interfaces, compatibility equations, boundary conditions both on exterior cylindrical surfaces and on the cross-sections at the ends of the pipe must be set.

If the previous example, i.e. when the multi-layered pipe with stacking sequence $(\pm\theta)_{NP}$ is subjected to bending, is analysed after having set the system of matrix equation, it has to be solved. Thus, it will give the value of the constants C_1, C_2 and A for all layers from $k = 1$ to $k = N$. Once these are obtained, the critical exterior layer's constant values should be used to obtain the stresses which will give the possibility to know the principal stresses from a similar expression than

equation (5), from [87] and [46]. Ultimately, all this procedure will give afterwards, by using a failure criterion, the possible bending moment that was desired. [87]

Summary of main results for external pressure

Failure analysis

Let assume that the pipe is in fact not subjected to bending but to an external pressure acting on it. By keeping the same characteristics, so the stacking sequence $[\pm\theta_{NP}]$, diameter D and thickness h, the pipe is supposed to be well designed in order to resist to this external pressure p_z. By following a similar procedure, it is set, in this example, that the external loads are defined as: $N_x = N_{xy} = M_x = M_y = M_{xy} = 0$ except for N_y giving by the equilibrium equation of the half pipe: $2N_yL = pDL$. Then, by using ABD matrix and Kirchhoff hypothesis , the strains can be obtained as well as the stresses by the stress-strain relation from equation . Then, using the $[T]$ matrix, principal stresses are deduced giving the allowable external pressure by using the Tsai-Wu failure criterion. [91]

Summary of main results for combination of both bending and external pressure

Failure analysis

For the presence of both bending and external pressure, the principal stresses are obtained with the following formulas in (13), from [87]:

$$\begin{aligned}
\sigma_1 &= \left(\sigma_x^M + \sigma_x^P\right)\cos^2\theta + \left(\sigma_y^M + \sigma_y^P\right)\sin^2\theta \\
\sigma_2 &= \left(\sigma_x^M + \sigma_x^P\right)\sin^2\theta + \left(\sigma_y^M + \sigma_y^P\right)\cos^2\theta \\
\tau_{12} &= \left[\left(\sigma_y^M + \sigma_y^P\right) - \left(\sigma_x^M + \sigma_x^P\right)\right](\cos\theta\sin\theta) + \left(\tau_{xy}^M + \tau_{xy}^P\right)\left(\cos^2\theta - \sin^2\theta\right)
\end{aligned} \tag{13}$$

where

$\begin{Bmatrix} \sigma_x^M \\ \sigma_y^M \\ \tau_{xy}^M \end{Bmatrix} = \begin{Bmatrix} \frac{1}{S_{33}}\left(\mu_6 C_1 + \mu_7 C_2 + \mu_8 A\right) \\ \mu_4 C_1 + \mu_5 C_2 + 3\mu_3 A \\ 0 \end{Bmatrix}$ are the stresses due to the external pressure.

$\begin{Bmatrix} \sigma_x^P \\ \sigma_y^P \\ \tau_{xy}^P \end{Bmatrix} = \left[\overline{Q}_{ij}(\theta)\right] \begin{Bmatrix} a_{12} + \frac{h}{2}b_{21} \\ a_{22} + \frac{h}{2}b_{22} \\ a_{26} + \frac{h}{2}b_{26} \end{Bmatrix} \frac{\rho D}{2}$ are the stresses due to bending.

Summary of main results for combination of both bending and axial tension

Failure analysis

To give a last example among the several others introduced in [87], the multi-layered pipe can also be analysed under axial tension. This condition means that, this time, only the load per unit length N_x is different than 0 while $N_y = N_{xy} = M_x = M_y = M_{xy} = 0$ and $N_x = \frac{N}{\pi D}$. Furthermore, when bending is adding to this axial tension, the principal stresses (14), from [87], are similar to the previous principal stresses in equation (13). The stresses σ^N from the axial tension are just replacing the term σ^P corresponding to the external pressure. It gives the following principal stresses :

$$\begin{aligned}
\sigma_1 &= \left(\sigma_x^M + \sigma_x^N\right)\cos^2\theta + \left(\sigma_y^M + \sigma_y^N\right)\sin^2\theta \\
\sigma_2 &= \left(\sigma_x^M + \sigma_x^N\right)\sin^2\theta + \left(\sigma_y^M + \sigma_y^N\right)\cos^2\theta \\
\tau_{12} &= \left[\left(\sigma_y^M + \sigma_y^N\right) - \left(\sigma_x^M + \sigma_x^N\right)\right](\cos\theta\sin\theta) + \left(\tau_{xy}^M + \tau_{xy}^N\right)\left(\cos^2\theta - \sin^2\theta\right)
\end{aligned} \tag{14}$$

where the stresses due to bending are unchanged and those from axial tension are now defined as follow, from [87]: $\begin{Bmatrix}\sigma_x^N \\ \sigma_y^N \\ \tau_{xy}^N\end{Bmatrix} = \left[\overline{Q}_{ij}(\theta)\right]\begin{Bmatrix}a_{11} + \frac{h}{2}b_{11} \\ a_{12} + \frac{h}{2}b_{12} \\ a_{16} + \frac{h}{2}b_{16}\end{Bmatrix}\frac{Nx}{\pi D}$

By following the same logic as earlier, the allowable axial force N as well as bending moment M are found by using the Tsai-Wu failure criterion. [119]

Dynamic analysis

Free vibration study

Structural aspects

A key parameter is the stiffness of the pipe EI_{yy}, with respect to axis y for example, and this represents the structural variable which controls vibrations of the system. Being aware of that and knowing that the stiffness of a beam during bending is given by $EI_{yy} = M_y \cdot \rho_y$, the expression bending moment M_y is required. Indeed, by using the elementary bending moment as well as the relationships between the strains and curvatures with the forces and moments, M_y acting in the cross-section of the composite pipeline can be calculated. This allows to develop the expression of the stiffness of a multilayered composite pipe with the following equation (15), from [87]:

$$EI_{yy} = \frac{\pi D}{2}\left(\frac{D}{2a_{11}} + \frac{1}{d_{11}}\right) \tag{15}$$

where the parameters a_{11} and d_{11} can be calculated from the stiffness matrix of the laminated wall: $[a]_{6\times6} = [A]^{-1}_{6\times6}$

In order to obtain the stiffness of a multilayered composite pipe EI_{yy}, several important steps need to be followed. First, the material properties, fibre orientation, number of layers and their locations are used to obtain the matrix elements of the transformed reduced stiffness $\overline{Q}_{ij}$. These elements will be utilised to obtain the stiffness matrix elements of the laminated wall $[A]_{6\times6}$ which will be useful for obtaining the parameters a_{11} and d_{11} as described previously. Finally, with the diameter of the pipe, the calculation of the final stiffness defined in equation (15) can be done.

Forces and moments

For a fixed pipe at both ends, many stresses, forces and moments act on it. Regarding an elementary section, those consist of shear stresses q and forces Q; reaction F, gravity and vertical dynamic forces; tension T and bending moment M_y. They are used to obtain the following equilibrium of forces and moments in equation (16, from [87], acting on an elementary section of pipe:

$$\begin{aligned} \frac{\partial T}{\partial x} + \pi D q - F\frac{\partial w}{\partial x} &= 0 \\ \frac{\partial Q}{\partial x} + F + \frac{\partial}{\partial x}\left(T\frac{\partial w}{\partial x}\right) + \pi D q \frac{\partial w}{\partial x} + mg &= ma_z^p \\ \frac{\partial M_y}{\partial x} = -Q \Longleftrightarrow Q &= -EI_{yy}\frac{\partial^3 w}{\partial x^3} \end{aligned} \tag{16}$$

The last form of the equations (16) is obtained by using $EI_{yy} = M_y \cdot \rho_y$ and the relation between the deflection w and curvature $\frac{1}{\rho_y} = \frac{\partial^2 w}{\partial x^2}$.

Regarding an elementary section of fluid now, the forces acting on this fluid element are due to pressure p, shear q, horizontal and vertical dynamic forces, reaction F, gravity. The equilibrium equations (17) of forces acting on a fluid element are then expressed, from [87], as:

$$\begin{aligned} -A\frac{\partial p}{\partial x} - q\pi D + F\frac{\partial w}{\partial x} &= Ma_x^f \\ -F - A\frac{\partial}{\partial x}\left(p\frac{\partial w}{\partial x}\right) - q\pi D\frac{\partial w}{\partial x} - Mg &= Ma_z^f \end{aligned} \tag{17}$$

The equation of motion

From the previous equilibrium equations, quantities related to tension, pressurisation and gravity are neglected; then, the simplified equations are combined in order to deduce the equation of motion (18), from [87], below:

$$EI_{yy}\frac{\partial^4 w}{\partial x^4} + MU^2\frac{\partial^2 w}{\partial x^2} + 2MU\frac{\partial^2 w}{\partial x \partial t} + (M+m)\frac{\partial^2 w}{\partial t^2} = 0 \tag{18}$$

Effect of an elastic foundation:
When pipes are installed and fixed on the bottom of the sea, analysing the dynamic behaviour of an elastic foundation can be relevant. This gives a new form of the equation of motion 19, from [86], by simply adding the new parameter kw:

$$EI_{yy}\frac{\partial^4 w}{\partial x^4} + MU^2\frac{\partial^2 w}{\partial x^2} + 2MU\frac{\partial^2 w}{\partial x \partial t} + (M+m)\frac{\partial^2 w}{\partial t^2} + kw = 0 \tag{19}$$

In the above equation (18) of free vibrations from a composite pipe, the terms represent different types of instability:

- the elastic flexural restoring force with $EI_{yy}\frac{d^4 w}{dx^4}$;
- the Coriolis force with $2MU\frac{\partial^2 w}{\partial x \partial t}$; This force dominates when small values of U occur since it is proportional to the linear value of U. The Coriolis forces act to the pipe in an opposite direction of the motion from the fluid. The system is then subjected to flow-induced damping [3].
- the centrifugal force of the fluid in curve with U constant with $MU^2\frac{d^2 w}{dx^2}$; This force is also influenced by the flow velocity and especially by higher values since it depends on the square value of U. If the system is subjected to more centrifugal force than the amount of the Coriolis damping effect, the whole system can lose stability.
- the inertia effects of the masses of fluid and pipe with $(M+m)\frac{\partial^2 w}{\partial t^2}$;

Boundary conditions depend on the type of support and they are primordial to solve the equation (18). A good table of the equations related to the several types of support is presented at page 118 in reference [87]. Furthermore, in order to prevent instability in the composite pipe conveying fluids, the calculation of the eigenfrequencies ω as well as critical values of the fluid velocity should be calculated. As mentioned previously, in the calculation, it will be particularly important to know whether and how the pipe is supported. From equation (18),

obtaining the eigenvalues and a direct solution is difficult, even with good numerical methods. Therefore, the use of other methods such as FEM will be needed to approach the correct results from the actual system.

Influence of temperature

The effect of temperature on offshore pipeline is also an important aspect concerning the design of those ones. Along the whole structure, the temperature can vary and change significantly, therefore increasing the stress acting on the pipeline through the strain created.

The first equation of (20), from [97], below reminds the global heat conduction in cylindrical coordinates, so applied to pipes. The axial and circumferential terms are neglected by considering the huge length of the pipeline and gives the simplified form in (20). The heat flux Q_r per unit length is, then, deduced in equation (21), still from [97]. The heat flux from the convection phenomena generated through the inner and external surfaces is also expressed in equation (22), [97].

$$\begin{aligned} &\frac{\partial}{r\partial r}\left(kr\frac{\partial T}{\partial r}\right)+\frac{\partial}{r^2\partial\theta}\left(k\frac{\partial T}{\partial\theta}\right)+\frac{\partial}{\partial z}\left(k\frac{\partial T}{\partial z}\right)+\dot{q}=\rho C_p\frac{\partial T}{\partial t} \\ \implies &\frac{\partial}{r\partial r}\left(kr\frac{\partial T}{\partial r}\right)=\rho C_p\frac{\partial T}{\partial t} \end{aligned} \tag{20}$$

$$Q_r^{conduction}=-2\pi rk\frac{dT}{dr} \tag{21}$$

$$Q_r^{convection}=2\pi r_ih_i(T_i-T_1)=2\pi r_eh_e(T_n-T_e) \tag{22}$$

From the heat consequence, it implies thermal load effects for the pipe. If the pipeline is fixed at both ends, the longitudinal strain is zero, so an axial tension force T_{axial} exists. Using the equilibrium of forces both acting on an elementary section of pipe, equation (16), and acting on a fluid element, equation (17), and assuming a constant flow velocity as well as an independent pressure along x, the tension T_{axial} becomes constant. This implies that there is a constant longitudinal stress. $\sigma_x=\frac{(T/NP)}{\pi Dh}$ is the longitudinal stress of each ply for a composite pipe of NP plies, with thickness h and diameter D and $\sigma_y=\frac{D(P/NP)}{2h}$ is the stress caused by an internal pressure P.

The longitudinal strain equation can be obtained implying the deduction of the axial tension force T_{axial}. By using them, with the fact that no longitudinal movement is allowed and that the axial tension has the same value at any point x of the pipe, the following equation (23), from [87], can be obtained to express the thermal effect:

$$EI_{yy}\frac{\partial^4 w}{\partial x^4} + 2MU\frac{\partial^2 w}{\partial x \partial t} + (M+m)\frac{\partial^2 w}{\partial t^2} + \left[MU^2 + \frac{\pi D}{\overline{S}_{11}}\left(\frac{D \cdot P \cdot \overline{S}_{12}}{2} + NP \cdot h\left(a_1 \cos^2\theta + a_2 \sin^2\theta\right)\Delta T_{axial}\right)\right]\frac{\partial^2 w}{\partial x^2} = 0 \tag{23}$$

where the expressions of $\overline{S}_{11}$ and $\overline{S}_{12}$ are expressed by equation (63) in appendix.

Effect of both thermal and elastic foundation

Furthermore, to finally take into account both the thermal effect and the elastic foundation on the composite pipeline, basically, the sum of both equation (23) and kw is considered.

However, if the problem is simplified by neglecting thermal loads as well as elastic foundation effects, some values for critical velocity in divergence instability can be found depending on the type of fixation at both ends according to the Table 1, equations and results of critical velocity values from the type of supports from [87].

Type of supports	Fixed-fixed pipe	Pinned-pinned pipe	Fixed-pinned pipe
U_{cr}	$\frac{4\pi}{L}\sqrt{\frac{EI_{yy}}{M}}$	$\frac{\pi}{L}\sqrt{\frac{EI_{yy}}{M}}$	$\frac{4.49}{L}\sqrt{\frac{EI_{yy}}{M}}$

Table 1: Critical values of velocity depending on the type of supports

Part II
Materials and technologies for H2 transportation

Global theory, overview and production of hydrogen gas

Hydrogen: history, characteristics and properties

The hydrogen element was termed by Lavoisier, who also identified during the same period nitrogen and oxygen, as it is a part of a list of other elements and it was recognised as a distinct substance by Cavendish in 1766.

It is known today that this element contributes to a major part of the several different reactions, e.g. proton-proton reaction and carbon-nitrogen cycle, which can exist in the sun and many other stars. It also represents three quarter of the whole mass in the universe and consists of three different types called isotopes which are:

- protium (H), it is the typical and primary isotope of hydrogen.
- deuterium (D or 2H), it is a stable isotope of hydrogen but much less present in natural state where it can reach only $0,015\%$.
- tritium (3H), it is an unstable isotope of hydrogen and is also present in natural hydrogen with an even smaller ratio.[49], [14]

According to the table from Mendeleev, hydrogen is the lightest atom which gives the property to hydrogen gas to be also the lightest of all gases. Regarding that phase of hydrogen, it is good to remember that, under normal conditions, this gas is a mix between "ortho and para hydrogen". Without going too deep in details, those kinds of molecules are different by looking at the spins of their electrons and nuclei. The composition is usually made of one fourth from the type "para" and the rest of "ortho" in ordinary conditions. [54], [53], [60]

On Earth, more than ninety percent of the atoms are hydrogen. A very common example to this fact is the composition of the water, which is formed with one atom of oxygen and two of hydrogen and which represents a crucial criteria to have life on Earth (to be more precise, the exact factors are: *Na-poor water* and *Non-toxic water environment*).
Of course, the implication of hydrogen in the production and existence of molecules is not limited to water since it also contributes mainly to several organic compo-

nents such as oil and gas, coal, vegetation and so on... The production of the gas from water can be done by electrolysis and precautions need to be taken since it is an extreme flammable gas. Indeed, hydrogen, with the molecular formula H_2, owns the following characteristics at standard temperature and pressure conditions: odourless, colourless, tasteless, non-metallic, non-toxic, and as stated previously highly combustible. The utilisation concerns for example rocket fuel, welding, acid HCl and also tritium, created in nuclear reactors, to be used in the hydrogen bomb. Different than gas, hydrogen can also be used as a liquid. In order to do so, the hydrogen gas is cooled down at an extreme low temperature of 20°Kelvin which gives -253.15°Celsius. For comparison, the coldest temperature registered on the Earth was -89.2°Celsius. Cryogenics and superconductivity studies use liquid hydrogen since it has several interesting properties below this extreme melting point of a few degrees Kelvin. [75], [120], [117], [84], [3]

Although its concentration in a volume of air is of the order of hardly one part per million (ppm), this atom is by far the most abundant element and probably one of the most important as well. By using renewable energies, such as wind or solar power, the hydrogen production can occur by electrolysis of water in remote areas and thus the transport of this gas can be performed by pipelines. This represents one of the main options regarding the hydrogen future uses.

Another very interesting topic concerns what is going to be performed by this form of energy storage, in other words the applications of hydrogen. The studies for using hydrogen are currently emerging these days. To quote some examples for new applications, the societies care about replacing transport modes using fuels by using hydrogen instead, steel industries and metallurgy are thinking to switch the production method for a cleaner option and trash could be converted into ethylene and methane with it. In addition, chemical, gas and some other industries are still having a frequent need of hydrogen supply as well. There is a high potential to use it but it is important to think carefully about the applications for H_2 due to the lack of time society has to meet the environmental changes. Moreover, the global constant decrease of conventional world oil production is happening currently and more sources are stating that the international peak oil has probably already occurred where Norway, for example, has already passed the peak oil in 2001. However, a lot of scientific papers still continue to ignore these natural limits in the energy production sector to estimate future trends, e.g. "increase in energy demand (by 14% in 2030) and the continuing reliance on fossil fuels" [78] with percentage based on the european report [39].

This huge consumption of fossil fuel implies a perpetual increase of greenhouse gas, thus (CO_2) among them, estimated at around 900 Mt CO_2 per year which is approximately 50 % higher than in 1990. H_2 utilisation in specific fields can

reduce drastically CO_2 emissions while in others, it might only play an artificial and green-washing economic role without strong significant impact. [57], [40], [85], [54], [53], [52]

Production of hydrogen via electrolysis

The production of Hydrogen is a key aspect of the whole chain process and comes before any transportation modes. In order to meet requirements for less carbon dioxide emissions, transport as well as production of the gas is important. H2 is perceived as an appealing, adaptable and clean energy vector. Its high potential in a non-CO_2 emissions goal is principally the ability to be produced from primary renewable energy which will result in a decarbonised fuel. However, a lower cost together with a higher production efficiency are needed in addition to find suitable ways for storage and transportation. [130]

In the beginning of the century and for a medium period of time, fossil fuels were announced to produce and mainly participate to the hydrogen production, which has actually happened and continue to be the case so far. Biomass was not seen as a major part of the production quantity, neither today where its role is still not significant for hydrogen production. Indeed, biofuels for transport as well as power and heat generation represent the main uses of the biomass process. [38], [78]

Hydrogen gas and thus, its production, is an essential part for the petroleum refining application which started in the 20^{th} century and chemical industries (e.g. ammonia). But the main problem, especially regarding the climate crisis and environment issues, is the production process for pure hydrogen which is almost exclusively from fossil energy sources. For example, coal gasification produces syngas which creates hydrogen with GHG and represents 23% of the annual production where electrolysis stands for hardly 2%.

The production is actually creating about 830 million tons of CO_2 annually and is due to the demand for hydrogen which tripled from 1975 to 2018. One possible solution to resolve this issue could be the rise of the low hydrogen production from electrolysis of water, where many efforts have been done by publishing several research papers lately. This method is more environmental-friendly regarding the small CO_2 emissions amount emitted in the atmosphere whether the source of electrical energy used does not directly emit carbon emissions such as renewable energies and nuclear power. In the past, hydroelectric power from a dam were providing a steady power source for the electrolysers. Today, more renewable intermittent energies are utilised, like wind power for the example of this thesis, and a problem is then instability and non-constant electricity source. [58],[130],

[57], [127], [69], [65], [47]

Electrolysis of water, principle and chemical reactions

Electrolysis process is known and perceived by people, researchers and companies as an encouraging opportunity to produce hydrogen gas from a green source of energy regarding CO_2 emissions, i.e. nuclear and renewable energies such as offshore wind turbines in this thesis. In that case, the mechanical energy delivered from the wind is first converted to an electric source of energy, that last one is well known today after using it for several years. This includes a loss coefficient due to the good but imperfect conversion and is then either sent to the electricity grid to power houses, industries and cities or transformed with electrolysers to chemical energy for hydrogen production. The system needs "an input of energy of 1.23 eV ($\Delta Go298K$, 1 bar) or 1.48 eV (ΔHo)" [56] to basically split both elements of water, oxygen and hydrogen, by extracting the power from electricity. Indeed, this transformation can be easily described by the chemical reaction (24) below which stipulates the disintegration of water into ions, then into gases from the atoms of the initial water, in other words into hydrogen and oxygen respectively from H_2 and O in the water molecule H_2O. The Figure 1, from [113], allows clearly to see the whole system and atom/molecule organisation happening during the transition in an electrolyser. [83]

Furthermore, a fuel cell strategy in Taiwan for 2025 with electrolysers and their integration into a large-scale wind farm has been analysed in [22].

The results showed that an increase of the available energy can be obtained and up to 7% thanks to this system.

$$\begin{gathered} H_2O \rightarrow H_2 + \frac{1}{2}O_2 \\ \text{OR} \\ 2 \times H_2O \rightarrow 2 \times H_2 + O_2 \end{gathered} \tag{24}$$

Non-disconnected molecules constitutes mainly water and there is no significant charge in the water due to the weak concentration of those ions, as a consequence of auto-ionisation of water. Thus, there is an obligation to use an electrolyte, dispersed in water. Such substances are for examples: $NaOH$, $NaSO_4$, or H_2SO_4 which makes the water conductive enough where, in the electrolytic liquid, two electrodes are immersed with an outer electric source of power. Electrolyte is somewhat important because the half reactions expressed in equations (25), (26), and (27) depend directly on it.

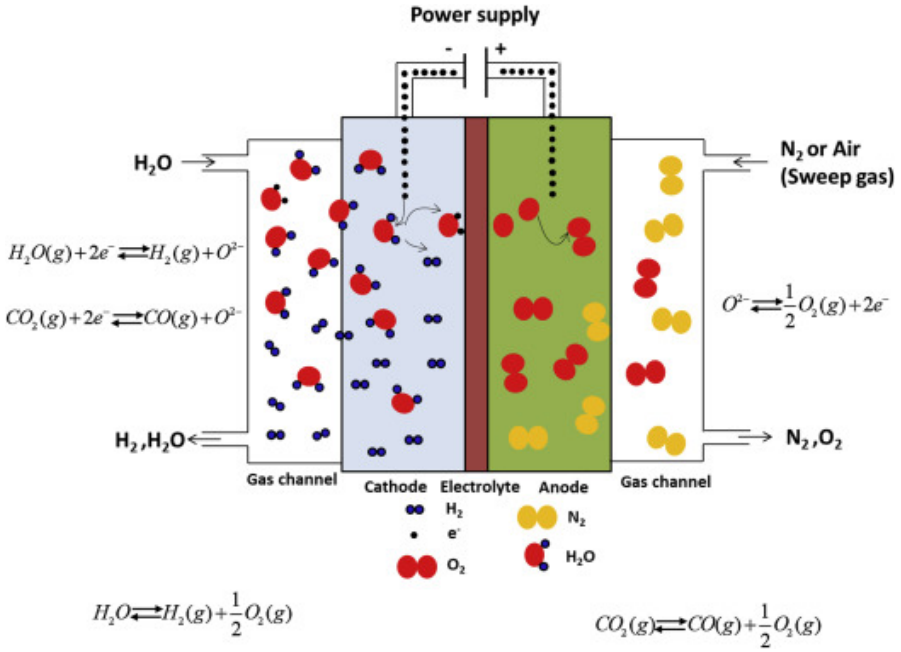

Figure 1: Reaction system occurring in an electrolyser unit cell
Source: Bengt Sundén, [113],
`https://doi.org/10.1016/B978-0-12-816950-6.00003-8`

Half reaction with the following substance as electrolyte = $NaSO_4$

$$\begin{aligned} \textbf{Cathode:}\quad & 4H_2O + 4e^- \rightarrow 2H_2 + 4HO^- \\ \textbf{Anode:}\quad & 2H_2O \rightarrow O_2 + 4H^+ + 4e^- \end{aligned} \tag{25}$$

When the reaction occurs, the movement of the electric charges begins where, on one side, the cathode is charged negatively and the positive ions, Na^+ if $NaSO_4$ is used and existing in the solution beforehand, migrate towards this cathode. Regarding the anode, the opposite situation happens. The anodic electrode is charged positively and the negative ions, SO_4^- if still $NaSO_4$ is used and existing in the solution beforehand, migrate there. This reaction is described by the half reactions in (25). [83]

A second example would be whether the electrolyte selected is $NaOH$. In that situation, the ions HO^- and Na^+ would be found to the anode (charged positively) and cathode (charged negatively), respectively. The reactions (26) occur instead of reactions (25), where only the anodic reaction changes. [113]

Half reaction with the following substance as electrolyte = NaOH

$$\begin{aligned} \textbf{Cathode:}\ & 4H_2O + 4e^- \rightarrow 2H_2 + 4HO^- \\ \textbf{Anode:}\ & 4HO^- \rightarrow O_2 + 2H_2O + 4e^- \end{aligned} \tag{26}$$

Another last case is to pick H_2SO_4 which is then separated in the positive and negative ions, H_3O^+ and SO_4^-, respectively migrating to the cathode (charged negatively) and to the anode (charged positively). It finally gives the half reactions written in equations (27). [113]

Half reaction with the following substance as electrolyte = H_2SO_4

$$\begin{aligned} \textbf{Anode:}\ & 2H_2O \rightarrow O_2 + 4H^+ + 4e^- \\ \textbf{Cathode:}\ & 4H^+ + 4e^- \rightarrow 2H_2 \end{aligned} \tag{27}$$

Inside a PEM electrolyser, it is either a solid polymer or a plastic which constitutes the electrolyte. Polymer Electrolyte Membrane (PEM) electrolysers are of great interest due to the environmental crisis and the need to find other cleaner ways to produce hydrogen for use or storage. At the anode, oxygen as well as positive hydrogen ions and negative electrons are formed with the split of water; at the cathode, hydrogen gas is created thanks to the union between, first, the electrons from the external electric circuit and, second, the hydrogen ions which migrated over the proton exchange membrane. Both anode and cathode reactions are given by, respectively, the anodic half reaction from (25) and the cathodic one from (27). All of the system is running at a temperature between 70 to 90°C. However, this temperature range is slightly higher for alkaline electrolysers which operate between 100 and 150°C. Those electrolysers are still producing hydrogen from the cathode but will transport, from cathode to anode, the hydroxide ions, HO^-, by handling a potassium hydroxide or a liquid alkaline solution of sodium. [113] [24] [83]

The last type of unit is using a solid ceramic material for the electrolyte and is called solid oxide electrolysers. The negative oxygen ions, O_2^-, are then conducted at such a higher operating temperature, ranging between 700 and 800°C to allow the appropriate membrane or electrolyte functioning. The principle stays somewhat similar by forming the hydrogen gas at the cathode with the reaction of the electrons. The heat source can be provided from some different sources producing enough residual heat but this system is simply introduced in this document since no commercialised products have been put into the market yet. [20]

When hydrogen is produced, there is a choice to store it, transport it and use it as a gaseous form or liquefied form. For both situations, a compression step is

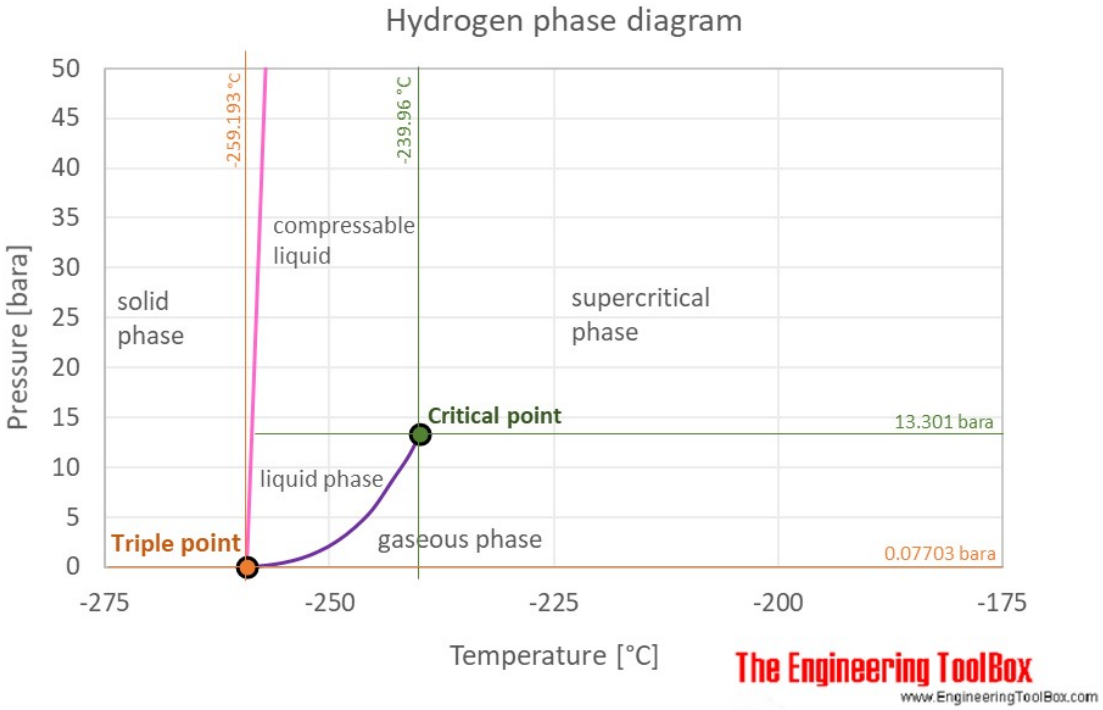

Figure 2: H_2 at 25°C (77°F, 298°K) and atmospheric pressure
Source: The Engineering Toolbox, [117]
`https://www.engineeringtoolbox.com/hydrogen-d_1419.html`

required. Energy is needed for producing hydrogen. Indeed, the need is [10 ; 15]% of the hydrogen energy content, and up to 30% with high pressure compression, for having gaseous hydrogen. Concerning liquefaction of hydrogen, it is [30 ; 40]% of the hydrogen energy content which is absorbed by the process.

As an example, on one hand, a hydrogen compression of about 5MPa (50 bar), from 2 to 7MPa (20 to 70 bar), will require an energy amount of 0.66kWh·kg^{-1} which represent a conversion of 2.4MJ·kg^{-1}. The power for the liquefaction, on the other hand, is between [15 ; 17.5]kWh·kg^{-1} that represents, after conversion, [54 ; 63]MJ·kg^{-1} and that is a considerable amount of energy to transform the state of hydrogen into a liquid. Furthermore and according to Figure 2, liquid hydrogen needs to be kept under -252.87°C if the pressure is 0.1013MPa (1.013 bar) or else the critical point for hydrogen is represented by a temperature of -240°C for a pressure of 1.3MPa (13 bar). The liquefied phase of hydrogen will be, thus, not regarded as a viable large scale solution in this thesis. The huge energy loss related to this phase transformation is a parameter too much crucial, especially today and in a close future, when the energy consumption is and will be a main factor with the ongoing or soon decrease of fossil energy production. [130], [44], [23], [7], [117],

[18], [61]

Electrolysis system powered by offshore wind farm

It is common to see the term *Power-to-Gas* resulting from the generation of gas as an energy storage from electricity. There are three principal technologies to produce H_2 with electrolysis:

- The first, oldest and most commercially developed one is **alkaline water electrolysis (AWE)**, where anodes and cathodes are separated by a membrane. Hydroxide ions are the only ions to penetrate it, thus no protons H^+ which contributes to the separation between the gas evolution and the ions.

  An additional information is that, from a general point of view, a hydrogen production demand of $[1\ ;\ 1000]\mathrm{Nm}^3\cdot\mathrm{h}^{-1}$ can be provided by the commercial alkaline electrolysis; and this which includes the efficiency from electricity to hydrogen in the order of [62 ; 82]%. [129] [130]

- The second one, **polymer electrolyte membrane electrolysis (PEMEC)**, is available on the market but is still on development and considered as a new technology comparing with AWE. [26]

  They receive a high interest these years thanks to their flexibility. Indeed, a fluctuation for the incoming current can be handle by this type of electrolyser which will then create unstable rates of hydrogen based on the power provided. This characteristics makes their utilisation combined to intermittent sources of energy, such as wind power, promising. [24]

- The third one, **solid oxide electrolysis (SOEC)**, has the best efficiency of all thanks to high temperatures. However, it has not been commercialised yet, therefore will not be considered in this part of the paper. [20]

Relevant results for this document regarding electrolysis offshore production of hydrogen are going to be introduced below. Indeed, the performance of an offshore wind farm in Netherland providing a 1-GW power to an electrolyser, based on the ISPT HydroHub project, have been incorporated in [26]. [59]

In total, there were three power profile. The first one, which also represents the reference, is providing a constant power supply named Eq. FLH for equivalent full load hours. A wind power profile based on a theoretical 1GW plant in the Netherlands constitutes the second type obtained from the website [95].

The last profile is the same as the second one except that it takes a period of a quarter hour instead of an hour for the data points and is then considered as

an accelerated wind profil. Thus, this considers the whole time period accurately, with a full load hours of 3983 hours. Combinations of the two commercialised electrolysers introduced above, AWE and PEMEC, are examined at atmospheric pressure conditions, LP for Low Pressure, and at the delivery pressure of the hydrogen gas at 30 bar, HP for High Pressure.

Results from the framework

The framework obtained results by using several parameters where the main ones are listed in Table 22 in Appendix B. Regarding the design for blocks, the number of megawatts of stacks in a block is affected neither by the type of technology nor by the pressure. In addition, the stack size does not influence the hydrogen production rate because the efficiency is independent on the stack dimension. Nevertheless, a higher pressure will make the efficiency of the stack lower and restrain the reaction, that is why a higher hydrogen production rate is related to a low pressure design. For a similar given load, alkaline electrolyser stack, AWE designs, have a lower hydrogen production rate than PEM electrolysers. For the balance of plant, PEM designs use more power than AWE which is explained by the higher H_2 production for the same loading level implying an increase for the flow rate, thus for the balance of plant power usage. It is important to notice, yet, that the number of stack has no impact on the balance of plan power consumption balance and simply increase the water or hydrogen (and oxygen) flow rate. For the balance of plan components, this is different because the power consumption will go up from the moment that the flow rates go up as well. The Table 2 summarises the data for the specific hydrogen production rate in 10^{-3}kg·s^{-1}(MW stack)$^{-1}$ and for the specific Balance of Plan, BoP, power use in 10^{-3}MW(BoP)(MW stack)$^{-1}$ for each technology at high or low pressure. The tendency described above is seen from the values in this table.

Electrolyser technology	H_2 Production rate (10^{-3}kg·s^{-1} (MWstack)$^{-1}$)	BoP Electricity usage (10^{-3}MW(BoP) (MWstack)$^{-1}$)
AWE HP // AWE LP	5.08 // 5.24	8.7 // 58.4
PEM HP // **PEM LP**	5.56 // **5.72**	9.5 // **63.8**

HP = High Pressure ; LP = Low Pressure

Table 2: Specific H_2 production rate and Balance of Plan Power Usage for each electrolyser technology

Source: Cooper, N. [26]
https://doi.org/10.1016/j.ijhydene.2021.12.225

As a summary, it can be stated that the lowest hydrogen production rate per MW of the stack as well as the lowest balance of plant power consumption is

achieved with the high pressure AWE designs. In the same way, the highest of both characteristics is obtained with the low pressure PEM designs. For further information, PEM designs can support a current density of 2A.cm^{-2} which is the double of the value for alkaline designs with a current density of 1A.cm^{-}2 and those two values are respectively their operational point. [26]

Regarding the design of the system, the three power profiles, responding to various load conditions, differ from the uses between AWE and PEM. From a defined input power, PEM are more quickly adaptable regarding changing loads in addition to produce more hydrogen by being more efficient at high current densities but they also cost more to manufacture; thus, it impacts the cost of the hydrogen created by them, see section *Economy for electrolysis system powered by offshore wind farm* III on the economic details of this type of hydrogen production with the exact same configuration.

Load Condition	Design configuration (all are High Pressure: HP)
Eq. FLH (ref.)	AWE 10 MW, 10 Stacks – 7 blocks PEM 10 MW, 10 Stacks – 3 blocks
Wind	AWE 10 MW, 10 Stacks – 9 blocks AWE 10 MW, 5 Stacks – 2 blocks
Wind Quarter	AWE 10 MW, 10 Stacks – 1 block AWE 10 MW, 5 Stacks – 1 block PEM 10 MW, 10 Stacks – 8 blocks PEM 10 MW, 5 Stacks – 1 block

Table 3: Design configuration of the three different load conditions
Source: Cooper, N. [26]
https://doi.org/10.1016/j.ijhydene.2021.12.225

Load condition	Hydrogen production (10^6kg/yr)	System Energy Use (10^9Wh)	Utilisation Factor
Eq.FLH (ref.)	84.4 (ref. value)	3920 (ref. value)	1.0 (ref. value)
Wind	79.6	**3920**	**1.0**
Wind Quarter	**83.2**	3900	0.995

ref. value = reference value (due to the constant power supply)

Table 4: Technical characteristics of the three load conditions
Source: Cooper, N. [26]
https://doi.org/10.1016/j.ijhydene.2021.12.225

According to the design configuration chosen and listed in Table 3, the first condition, equivalent full load hours, has an optimal design combining mainly AWE blocks with still a few PEM blocks. The reason behind it is that PEM blocks are able to carry much more current density, having a higher efficiency and then, they produce hydrogen at a high rate. The largest part of the load is handled by those PEM blocks and the rest is distributed to the remaining AWE blocks. However, the price of the whole system gets higher with the PEM blocks but larger are the blocks and cheaper is the price per Megawatt. The comparison made in the framework included the stack sizes of 1, 5, and 10MW stacks from industrial systems with the number of 1, 5, and 10 stacks per block. [19]

About the energy efficiency of the configurations, on one hand both the Wind and Equivalent Full Load Hours requested the same amount of energy and used it fully by having a Utilisation Factor of 1 from Table 4. On the other hand, the last configuration, Wind Quarter, has a slightly lower utilisation factor which keeps still the use of 99.5% of the whole energy. Furthermore, regarding the production, this last condition creates a non negligible amount of Hydrogen compared to the Wind scenario producing 3600 additional tons of hydrogen.

Finally, from the framework comparing all these scenarios, from the technical results, it is the constant power supply condition which produced the more hydrogen with 84.4 million kg and Wind condition the least. PEM technologies, even though highly expensive, are the best for the adaptability due to changes in loading level and for the efficiency. The framework still decided to opt for a mix in the blocks to extract the benefits of a technology mix and to not yield a disproportionate price for the economic side with more detailed in section *Economy for electrolysis system powered by offshore wind farm* III. [26]

Electrical energy consumption for the electrolysis process

Electrolysis of water is a tempting way to produce H_2 when the electricity price of the country is low but more especially when the electric grid is delivering a low carbon electricity, e.g. in Europe: Norway, Sweden, France mainly due to the nuclear and hydro power of those countries. [24], [110], [34], [111] [112]

Electrolysers are also especially attractive when the production of relatively small quantities is required. There is a minimum of electricity amount of 39 kWh in order to produce about 1 kg of hydrogen. This value is the ideal amount of electricity required for 1 kg of hydrogen while the actual values are around 50 to 60 kWh$\cdot kg_{H_2}^{-1}$, the higher value will be taken for the calculation below. To quickly be able to seize the meaning of this number, the following comparison with the electrical consumption per person is done below with the calculation (28)-(30). Data as population (order of magnitude) and world electricity net consumption

are taken in order to determine the consumption per inhabitants worldwide. Then, dividing the electric consumption for 1 kg of hydrogen by the electrical consumption per inhabitant allows to obtain the average period of time that one person uses for the daily electricity consumption. [24]

- **Original Data:**

$$\begin{aligned}
\text{Electricity Consumption Hydrogen}_{(\text{ideal})} &= ECH_2(i) = 39kWh \cdot (kg_{H_2})^{-1} \\
\text{Electricity Consumption Hydrogen}_{(\text{real})} &= ECH_2(r) = 60kWh \cdot (kg_{H_2})^{-1} \\
\text{Population}_{(2019)} &= (POP) = 7\ 683\ 437\ 980 \text{ persons} \\
\text{Annual World Electricity Net Consumption}_{(2019)} &= (AWENC) \\
&= 23\ 787 \text{ billion } kWh \\
&= 23\ 787 \cdot 10^9 kWh
\end{aligned} \tag{28}$$

- **Annual electric consumption per inhabitant worldwide:**

$$\begin{aligned}
\text{Electricity Consumption}_{(2019)}\text{: } ECi \text{ in } &\left(kWh \cdot (\text{persons} \cdot \text{year})^{-1}\right) \\
ECi = \frac{(AWENC)}{(POP)} &\cdot \left(kWh \cdot (\text{persons} \cdot 365 \text{ days})^{-1}\right) \\
\implies ECi = \frac{(AWENC)}{365 \times (POP)} &\cdot \left(kWh \cdot (\text{person} \cdot \text{days})^{-1}\right)
\end{aligned} \tag{29}$$

- **Amount of time corresponding to the electric consumption to produce 1 kilogram of hydrogen with electrolysis**

$$\begin{aligned}
\text{Time}_{(\text{ideal case})} &= \frac{ECH_2(i)}{ECi} \approx 5(\text{days} \cdot \text{persons}) \cdot (kg_{H_2})^{-1} \\
\text{Time}_{(\text{real case})} &= \frac{ECH_2(r)}{ECi} \approx \boxed{7(\text{days} \cdot \text{persons}) \cdot (kg_{H_2})^{-1}}
\end{aligned} \tag{30}$$

Finally, the results state that about a week of electrical consumption for one person represents the same amount of electrical energy for 1 kg of H_2. The results can also simply be interpreted as the consumption of 7 persons in a day, 2 persons in 3.5 days and so on... The same calculation states a result for Norway approximately equal to 1 $(\text{days} \cdot \text{persons}) \cdot (kg_{H_2})^{-1}$ stipulating that 1 kg of hydrogen needs the same amount of electrical energy as a Norwegian inhabitant during a day. A European/Norwegian inhabitant consumes generally more than an average person on Earth related to the level of development for the country and spending power

per inhabitant, both significant in Norway. Moreover, the electricity-to-hydrogen efficiency is assumed to be [62 ; 82]% and high temperature or high pressure might reduce the electrolysis energy use for the production process but could create corrosion challenges.[130], [55], [33]

Composite materials for hydrogen use in pipelines

Characteristics of the composite materials

Overview of composite

Composite materials have invaded our everyday life from tools and simple objects to the high engineering pieces of an airplane for example. The basic definition of a composite material is that it is formed by using a minimum of two other different materials. For example, concrete is a very good example of composite material since it is produced by mixing rocks and cement. Therefore, it can be easily seen that the creation and use of composite materials is not recent at all and some of them have been used for centuries.

The recent increase of interest for this category of material mainly comes from the industrial period during the last two centuries when there were needs in many industrial sectors. A huge part of composite materials includes plastic materials which were invented at the beginning of the twentieth century concerning the synthetic polymer. Obviously, the plastics alone cannot be satisfying for many applications which require high amount of strength. That is why, e.g. for structural applications, the needs of composite materials are strongly expressed since plastics are not sufficient in many situations. The purpose was then to use another type of material in order to fortify the plastic ones and to have a new material which would be lighter than metals and stronger than plastics. In aviation, saving weight is even more critical than the cost it will imply. In order to do so, the utilisation of composite materials is of relevance for aircraft. It allowed the aviation sector to save weight, compared to aluminium, thus to reduce fuel consumption so diminishing the cost by increasing the efficiency of a plane trip. The life cycle and phenomenon as corrosion are also improved when metals are changed for composite, the cost for maintenance and during operations has then also been reduced. Industries that use carbon fibre composites and dependent on the mass parameter, such as transports, make a wise choice by avoiding steel which represents the double in density. To be in phase with the carbon emission reduction plan for the next years until 2050, one of the solution proposed is to reduce the weight, thus the fuel consumption, of transportation modes like cars. This last proposition is particularly relevant for countries having an electricity system mainly based on

high carbon emission such as coal, thus where the electric cars would have a bad, even worse, CO_2 footprint. As an example, Volkswagen proposed a model called *XL1* which only consumes about 0,9 litre per 100km by improving a lot the weight of the car using the fifth of the vehicle body for polymer composites. [15], [77], [104], [21], [92]

The different types of composite materials

As stated above, composite are different as other materials since it is a mix of several of them. Thus, the choices of the materials which will constitute the composite depend on the properties of the individual materials themselves and what the combination can give. Their function in the composite will also play a different and important role regarding their characteristics compared to the properties alone.

In general, the composite material for Fibre Reinforced Polymer is formed of two elements. One is the matrix of the composite; it will then contribute to the final shape, protect the reinforcement materials inside and distribute better the stress and forces acting on the composite. The other one is called reinforcement; it helps to strengthen the matrix and the global material by changing the mechanical properties. It exists mainly three types of matrix: Polymer, Metal and Ceramic Matrix Composites called respectively PMC, MMC and CMC. Since the MMC is usually for engine components dealing with heat and CMC for blades in high temperature of gas turbines, brake disks or space applications, the next sections will focus more on the polymer type (PMC). In order to fortify the PMC, fibres are used from mainly three materials: aramid (AF), carbon (CF) and glass fibre (GF). The two last are improving the strength and stiffness-to-weight ratios significantly which explains partly why the typical material is produced with glass reinforcement within a plastic matrix, which is called GFRP for Glass Fibre Reinforced Polymers while CFRP is defining Carbon Fibre Reinforced Polymers. The fibres provide a direction in the composite materials and, thus, modify the mechanical properties in a polymer composite by making them much better depending on the orientation. [104], [80], [114]

Machining of composite materials

To make Fibre Reinforced Polymers (FRP) for composite pipelines, the machining process is called *laying-up techniques*. Regarding the fabrication of metal matrix composites, the method used to make this composite component is called *casting techniques*. Even though there are many reasons to switch from metals to composite materials, the machining of composite materials appears to still include difficulties, especially for cutting aramid fibres, and it is one of the parameters that

explains the higher price than usual plastics. Although this machining process is not an easy task, many operations were developed to be able to cut both parts of the composite, i.e. the fibrous and particulate materials, when a slice is performed through the whole material. In addition, the ceramic type of composite has the most difficult machining and thus require more efforts to perform the desire operation. [103], [80], [32], [30], [21]

Composite reinforced for pipelines

As stated above, the composites which have a reinforcement thanks to fibres for their polymer matrix are named as FRP. By regrouping the fibres within the polymer matrix, these composites have remarkable characteristics like an advanced strength and modulus-to-weight with better fatigue performance as well as exceptional magnetic and corrosion resistance. Also, the properties acquired would not be obtained from exclusively one of the material component alone. This creates interest for this combination including the composites with reinforced fibres where several types exist, e.g. glass, carbon, aramid, boron and so on... Nevertheless, concerning the resin matrix, there are mainly two types called thermoset and thermoplastic that are going to be expressed below in this chapter at section *Thermoset and thermoplastic resin II*. Many applications use composite materials starting from the basic sport goods or phones to the most sophisticated spacial and military structures.

The fibres and their characteristics

The resin matrix is not the strongest material constituting the composite but it has such an important role which is to maintain the fibres in the orientation desired. Indeed, the main purpose is to act like a load transfer through the matrix between the fibres which are, then, protected from potential external damages coming from the environment. That is why one of the component is not more important than the other one in a composite structure since they have both different functions in the material. Nevertheless, it appears obvious that parameters as the ratio between length and diameter together with the volume of the fibres highly affects the properties of the reinforcement within the resin matrix. It will be stronger for a larger volume as well as with a high fibre length-to-diameter ratio. [125]

Glass fibres, where properties are summarised in Table 5, represent the most usual type of reinforcing fibres in composites. They are made by using a very high temperature to achieve melting and are produced from materials such as borocalcite, limestone, pyrophyllite, camsellite, dolomite and quartz sand. To form it, the molten mixture of SiO_2, called silica, with other oxides as well will be

Glass fibre	
Technical values (Glass fibre: E-type)	- Density = 2.54 g/cm^3 - Tensile strength = 3.45 GPa - Tensile modulus = 72.4 GPa
Mechanical properties	- Low stiffness - High strength but decrease with elevated temperature - Brittle
Interaction with heat, electromagnetism and electricity	- Good insulation so it implies a strong thermal endurance
Surface alteration	- High corrosion resistance - High chemical and biological resistance - Sensitive to surface damage - Low abrasion resistance
Other information	- Type of fibre = Isotropic - Fibre diameter value between 10 and 20μm - Lowest cost (for the E-type, cost is increased for S-shape)

Table 5: Characteristics properties of the glass fibre
Source: Mallick, P.-K. (Technical values) [74]; Wang, B. [125]
https://doi.org/10.1201/9781420005981
https://doi.org/10.1007/978-3-030-71438-3_2

quenched either by air or through a spray of water. Then, the binding behaviour is enhanced by the coating applied on the surface of all the fibres to protect them. The glass fibre has the property to be isotropic because there is not any preferential orientation in its microstructure. Considering the machining stage, glass is very challenging to produce because the structure is highly abrasive. However, the cost of the E-type glass fibre remains the lowest one among the commercially available. There is also another type, called S-shaped glass fibre, and it has a greater tensile strength but the manufacture process of this type of glass fibre is more expensive. [132], [103], [104], [125], [6], [123], [64]

Carbon fibres, where properties are summarised in Table 6, are produced by carbonisation and graphitising of organic fibres in pile, which gives at the end a microlite graphite material. However, this type constitutes an inorganic polymer fibre with a carbon content generally above 90%. Graphite is the name given to the same fibre but, this time, by exceeding a content of 99%. Unlike glass, the carbon

Carbon fibre	
Technical values (Carbon fibre: T300)	- Density = 1.76 g/cm^3 - Tensile strength = 3.65 GPa - Tensile modulus = 231 GPa
Mechanical properties	- High axial strength & modulus - Low density - Good fatigue durability - Highest tensile strength - Low strain-to-failure - Low impact resistance
Interaction with heat, electromagnetism and electricity	- Low coefficient of thermal expansion - Good X-ray permeability - Intermediate specific heat & conductivity - Electromagnetic shielding satisfactory - Low electrical conductivity
Surface alteration	- Excellent corrosion resistance
Other information	- Type of fibre = Anisotropic - Fibre diameter value between 5 and 8 μm

Table 6: Characteristics properties of the carbon fibre
Source: Mallick, P.-K. (Technical values) [74]; Wang, B. [125]
https://doi.org/10.1201/9781420005981
https://doi.org/10.1007/978-3-030-71438-3_2

fibres are anisotropic therefore, the properties change according to the direction of the fibres. They also have very different values for the tensile modulus according to performance of the fibres, this is usually comprised between 207 and 1035 GPa for, respectively, the low and high side.
Usually, if the low modulus fibres are chosen, they will have a low density, low cost and higher tensile than the high-modulus ones. The carbon fibres remain to be an excellent material which combines good properties such as low density, high strength and stiffness with an intermediate cost. All of this explains why the carbon fibre is usually the second choice for a reinforced fibre, after the glass one. There is a broad use of carbon fibres in the aeronautic industry where the weight is among the first priorities for obvious reasons such as fuel consumption and flight efficiency. [74], [103], [104], [125], [6], [64]

Aramid fibres, where properties are summarised in Table 7, are defined by their crystalline fibres which are in addition aromatic and polyamide. The common commercial category called *Kevlar* by the company *DuPont* is usually renowned

for famous features and fonctions. Although it has been said that the carbon fibres above are usually chosen thanks to their low density among other important particularities, the aramid type is the one with the lowest density as well as the highest tensile strength-to-weight ratio. Furthermore, they possess exceptional corrosion, resistance to high temperature, and are ones of the lightest fibres. Plus, the tensile strength and resistance to impact is remarkable. That is why, they are widely used in ballistic applications like body/vehicle armour, military helmet, fireproof suits for firemen protection or simply in ropes, e.g. climbing ropes. However, their difficult machining, especially for the cutting stage, makes them less interesting for other general purposes. Despite this drawback, the exceptional properties for the specific usages listed above are still of great interest in those sectors. [31], [70], [10], [76]

Aramid fibre

Technical values (Aramid fibre: Kevlar 49)	- Density = 1.45 g/cm^3 - Tensile strength = 3.62 GPa - Tensile modulus = 131 GPa
Mechanical properties	- High stiffness (superior than glass) but time dependent - Exceptional toughness (which creates problem in machining because it is difficult to cut) - High strength (superior than glass too) in transverse direction but also time dependent - Low compressive strength in transverse direction - The lowest density
Interaction with heat, electromagnetism and electricity	- High insulation so it implies a low heat conductivity - Low coefficient of thermal expansion
Surface alteration	- Good damage tolerance
Other information	

Table 7: Characteristics properties of the aramid fibre
Sources: Mallick, P.-K. (Technical values) [74]; Vasiliev, V.-V. [122]; Wang, B. [125]
https://doi.org/10.1201/9781420005981
https://doi.org/10.1016/C2016-0-04497-2
https://doi.org/10.1007/978-3-030-71438-3_2

Boron fibre is the last type of fibre introduced in this document. The method of Chemical Vapour Deposition (CVD) is used to manufacture the boron fibres on

a tungsten wire as the base, or sometimes on a carbon monofilament. The diameter is notably larger for this fibre and values are comprised between a hundred and two hundred micrometres, i.e. $[100; 200]\mu m$. This specificity implies an extraordinary good resistance to buckling, including a high compressive strength. However, above a temperature of 500°C, both the tensile and compressive strength decrease considerably in air atmosphere. This fibre represents less interest than the previous ones stated above because it has only limited applications. [73] [122]

Thermoset & thermoplastic resins and sustainable recycling process

Regarding the thin area between the laminae, the shear strength in this region is also a parameter to consider and the matrix has an important impact on this shear strength. Therefore, in addition to diffuse the stress and loads through the matrix to the fibres and to act as a protection for them against the external environmental hazards, the resin is then a part to highly consider as much as the fibres even though its main goal is not to reinforce the final composite.

One of the major characteristic of the **thermosetting resin** composites is the inability to be melted and moulded again. This occurs because of the property of the thermosetting resin composites to have a three dimensional cross-linking structure. The basic principle behind recycling a material is to separate and make the components individual in order to treat them correctly. Thus, it makes the reuse of this type of composite material more difficult and elaborated. Since thermosetting composites are broadly employed by industries, this specificity might need a better recycling process with perhaps a higher efficiency. [21], [6]

The challenge for recycling composite materials can easily be understood because it consists of a mix of different materials putting together. It has been showed that the chemical recycling gives the highest-strength fibres by taking into account the three main composite recycling processes which are using either chemical or mechanical or thermal technologies. The most interesting way for composite materials is to finally be recycled, or reused, as composite structures rather than only to composite constituents such as fibres, reinforcement and so on. This contributes to transform the recycled materials to new high-technology products for several other industries like automobile, construction, electronic, transportation etc and potentially helping to reduce the overall cost. Moreover, it also needs less labour, natural resources and energy to produce them. In consequence, new potentialities will appear from the direct structural recycling of composite materials for sustainable composite products and fibres. [11]

Either a heating and pressurisation process or, a curing agent and an ultraviolet light process is used to produce the chemical reaction for the thermosetting resin. The usual attributes regarding this type of resin are expressed in Table 8. It has a

Thermosetting resin	
Advantages	- High rigidity - High hardness - Inflammability
Disadvantages	- High brittleness - Low mechanical features
Main types of thermosetting resins	- Phenolic aldehyde - Epoxy - Amino - Unsaturated polyester - Silicon ether

Table 8: Characteristics properties of the thermosetting resin
Source: Wang, B. [125], Campbell, F. C. [21], Ahmad, J. [6]
https://doi.org/10.1007/978-3-030-71438-3_2
Ebook ISBN = 9781615031405
https://doi.org/10.1007/978-0-387-68619-6_1

low molecular weight but when the resin is cured, there is no way to have it softer even though pressure or heat are applied.

Regarding the **Thermoplastic resin**, where main features are found in Table 9, the situation is opposite since it has a high molecular weight. In addition, there is no inter-molecular cross-linking but being exposed to high temperature during a long time can damage or even disintegrate the resin.

FRP composites

Historically, the development of Reinforced Thermoplastic Pipes (RTP) started in the early 1990s because of a high demand in the sector of non-corrosive conduits. Hence, for applications in oil and gas (onshore) industry and especially in the Middle East, they replaced the medium pressure steel pipes. Synthetic fibres composed the first pipes developed. Also, many names and accronyms are given to this type of pipe and the reader can find all the following names regarding this product: "Flexible Flowline", "Flexible Linepipe", "Flexible Reinforced Pipe", "Reinforced Line Pipe", "Spoolable Composites" or "Spoolable Reinforced Plastic Linepipe" in general and "Flexible Umbilical Risers" or "Offshore Flexibles" for offshore use. [107], [106]

A typical FRP pipeline includes a non-porous barrier with a tubular shape inside the pipe. This layer conveys the fluid (defined as a gas or liquid) and there are several other protective surfaces over the barrier tube which are listed by order

Thermoplastic resin	
Advantages	- Simple shaping - High mechanical energy
Disadvantages	- Low heat resistance, thus low insulation - Low rigidity
Main types of thermoplastic resins	- Polyamide (PA) - Polycarbonate (PC) - Polyethene (PE) - Polyformaldehyde (POM) - Polyphenyl ether - Polypropylene (PP) - Polystyrene (PS) - Polysulfone - Polyvinyl chloride (PVC) - Rubber

Table 9: Characteristics properties of the thermoplastic resin
Source: Wang, B. [125],, Campbell, F. C. [21], Ahmad, J. [6]
https://doi.org/10.1007/978-3-030-71438-3_2
Ebook ISBN = 9781615031405
https://doi.org/10.1007/978-0-387-68619-6_1

from inside to outside the pipe as follow: protective layer, interface layer, fibre composite layers, barrier layer for outer pressure, external protective layer. The Figure 4 is representing a basic FRP pipeline, and the layers inside, from the company *Strohm* for a product called *TCP Flowline*. [105]

In general, FRP composites are simple and low cost to manufacture because it does not need sophisticated machines and equipment. There are not two many production procedures which also simplify the operation. Regarding the composites with carbon or aramid fibres the heat stability is remarkably good. In addition, properties such as strength and modulus to weight are highly advantageous with the FRP composites. The carbon fibres especially deliver impressive characteristics regarding these points. Finally, the design is quite interesting in order to use few materials for still amazing performances. [125]

Nevertheless, even though the manufacture process is low cost, at the end, this type of material is expensive especially with boron or carbon fibres while using glass stays the cheapest option. The anisotropy of composites can also be a problem depending on the situation. The orientation of fibres give exceptional qualities along their direction but the mechanical performance for loads applied

perpendicularly of them is low. Last of all, the technologies for detecting structure irregularities and fissures is not optimal yet but will surely be improved in a close future. [123]

From Table 10, the density, tensile strength and modulus values are expressed for the following three types of composite pipes. CFRP, GFRP and AFRP mean respectively Carbon, Glass and Aramid Fibre Reinforced Polymer. High strength-to-weight, relatively high for CFRPs, characterises GFRPs and AFRPs but unfortunately also with a high modulus-to-weight. GFRPs are now intensively used because of their corrosion resistance, quite easy manufacturing and their low cost. AFRPs turns into a popular material, though they have a higher costs. The highest cost is from CFRPs which possess anti-fatigue performance, high temperature resistance and great thermostability. [123]

Type of FRP	Density (g/cm^3)	Tensile strength (GPa)	Tensile modulus (GPa)
CFRP (unidirectional)	1.55	1550	137.8
GFRP (unidirectional)	1.85	965	39.3
AFRP (unidirectional)	1.38	1378	75.8

Table 10: Values of the properties for the three main FRP composites
Source: Mallick, P.-K. [74]
`https://doi.org/10.1201/9781420005981`

Overview and comparison of the energy and carbon footprint of composite pipes

A study comparing the carbon dioxide emissions of composite pipes and the difference with a carbon steel pipe has been published recently for applications in the oil and gas sector, in 2021. It has been shown, on Figure 3, that the conventional carbon steel pipes produce higher carbon and energy footprint compared to the non-metallic pipes. Among them, it appears that the glass reinforced epoxy and glass fibre-RTP are the ones with the least CO2 emissions and it can reach a global reduction of 60%. Those emissions usually come from the materials themselves which represent half percent of the total emission of the carbon steel pipe and up to 90% in the case of the non-metallic types with the reinforcement layer accounting for most of it. A solution that has been studied to even reduce more the carbon footprint of the composite pipes was to enhance the weight efficiency of the pipe. By replacing the glass fibres to carbon fibres, a total of 35% of weight saving is done but unfortunately this is not a solution that actually reduce the CO2

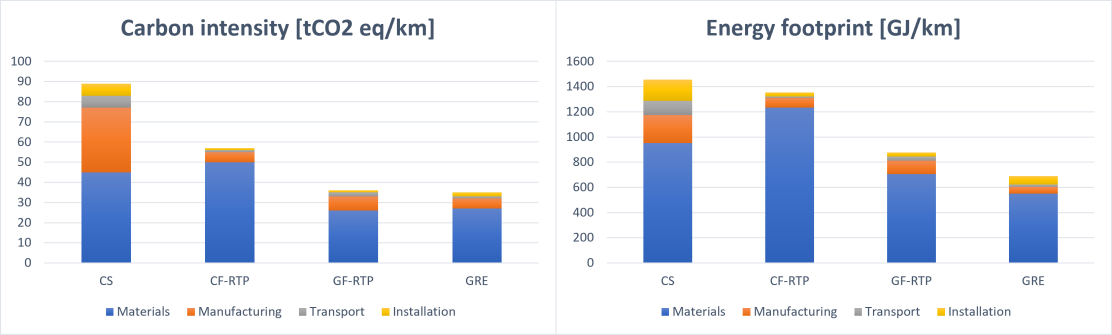

CS = Carbon Steel ; CF = Carbon Fibre ; GF = Glass fibre ;
GRE = Glass Reinforced Epoxy

Figure 3: Carbon and energy footprint for pipes in composite materials and carbon steel

Source: A.Zubail, [131]
https://doi.org/10.1016/j.jclepro.2021.127150

footprint because of the high intensity of the carbon fibre material itself. This explains why glass fibre composite pipes produce the least carbon emissions. Even though this study is a computational analysis and would need to be checked with actual data from production, this study gives a tendency and allows to have an overview of the carbon and energy footprint for each composite pipe by comparing them between each other and with a basic carbon steel type. The data were based on the technical information listed on Table 11. [131]

Specifications	CS	CF-RTP	GF-RTP	GRE
Product type	Rigid	Spoolable	Spoolable	Rigid
Internal diameter (mm)	146.3	142.2	142.2	150.6
HDPE liner thickness (mm)	-	5.38	5.38	-
Structural layer thickness (mm)	-	4.4	6.7	9.6
HDPE cover thickness (mm)	-	3.58	3.58	-
Fibre content (volume %)	-	60	60	58
Fibre orientation	-	$[40,55_3]_s$	$[55]_s$	$[55]_s$

Table 11: Technical specifications for the composite products analysed in [ref]
Source: A.Zubail, [131]
https://doi.org/10.1016/j.jclepro.2021.127150

Technical analysis of pipelines produced by companies

In this section, the goal is to describe deeper and further the specificity of the current composite pipelines developed and sometimes also produced by some companies. The global aspects and specific characteristics are first expressed for each composite FRP. Then, extra information and specific properties to each product are detailed in order to better compare them and analyse which composite pipe from these companies could be the best for hydrogen regarding the topic of this paper. Those specific details have been obtained by contacting engineers from the companies directly by email, by having a Teams-meeting in addition for some of them and also by consulting the information available on the websites.

Pipes from *NOV Completion and Production Solutions*

Bondstrand Fibreglass pipe

This first composite pipe from *NOV*, Brondstrand^{TM}, is using the technology of glass fibres with a matrix composed of epoxy, thermosetting resin. It is included in the GRE category for Glassfibre Reinforced Epoxy pipe systems. Therefore, as described earlier it combines several good parameters like needing small amount of maintenance as well as being lightweight, resistant to corrosion and harsh environment which makes it favourable for marine and offshore applications. It is been 65 years that those corrosion-resistant and non-metallic composite solutions represent a good option for several projects in mining, chemical or marine and offshore industries. This type of pipeline symbolises a potential and *NOV* thinks, through the emails exchanged during this thesis work, that it can be used for H_2 transportation in the future. There are different series which has been elaborated from this type of pipeline, including different parameters and characteristics. The purpose here is not to detail deeply one type but more to analyse all of the potential ones which could fit for hydrogen transportation and in order to detect a tendency when parameters are modified.

Firstly, the *Bondstrand 2000 Series* is recommended mainly for hot water services. However, it can also carry industrial waste whereas *Bondstrand 2400* can, in addition, ensure the transport of several types of water (brackish, salt, potable water and sewage) as well as mild chemicals or crude oil transmission.

Secondly, *Bondstrand 3000, 3200* and *3300* are types of pipes for generally water and waste water utilisation. Nevertheless, the *Bondstrand 4000* are more resistant and designed specifically for aggressive chemical service like solvents,

alkalis and non-oxidizing acids.

Finally, *Bondstrand 5000* and *7000* are respectively the best choice for the most chlorinated/acidic mixtures and for situations which need high-strength conductive filaments for jet fuel as an example of non-conductive fluid which may need to dissipate electrical charge.

Some characteristics are similar to these different products and can be grouped together. For example, the aromatic amine cured epoxy gives high toughness and also a good temperature performance for types *2000* and *4000*. In addition, the dual-angle construction method from the products *3000*, *3200* and *3300* provides to the pipelines high stiffness and stability. Concerning the lock systems, they utilise different systems corresponding to different characteristics and needs. The *key-lock* mechanical joint is used on *2400* type for fast assembly but the *quick-lock* joining system gives a finer close tolerance fabrication of system and is thus preferred for types *4000*, *5000* and *7000*. The resins in *5000* are also of interest with a vinylester resin matrix which is employed for oxidizing acid and purification systems of water. In addition, this product can reach a maximum temperature of 93°C. [81], [2], [1], [89]

Fiberspar Spoolable Fibreglass Pipe

The *Fiberspar* model is a thermoplastic pipe, also reinforced by glass fibres where the matrix is made of epoxy, therefore it is described as a glass reinforced epoxy pipelines. The design is made to mainly handle corrosive and sour applications for liquids and gases. The maximum performances for hydrocarbon applications are about 17.2MPa ($\approx$ 172bar) and 82°C.

One of the main advantage of this thermoplastic pipe concerning the offshore transportation of hydrogen is the ability to be rolled on reels which increases considerably the installation time per distance of pipe. The continuous length is of 2740 metres before needing to be joined, this represents a very long distance for a composite pipe stocked on reels. The connectors can be from different systems and all the configurations can be chosen such as flanged, threaded, weld-end and so on... By reducing the time, it is the installation costs that are also strongly reduced. Below is Table 12 regrouping the main properties of these two pipes produced by *NOV*. The goal of comparing those two pipes is to easily see the main differences between a pipe developed for liquid transportation, Bondstrand type, and the Fiberspar one which can handle gas in addition. It is especially different regarding the possible diameter size and pressure range. Very large diameter, up to 1 metre are manufacture for the liquid pipe *Bondstrand 2400* while it "barely" reaches 0.15 metre for the liquid and gas *Fiberspar Spoolable* pipe. About the pressure, this last one also made for gas can resist to a maximum pressure which is almost 5 times than the maximum pressure of the *Bondstrand 2400*. Obviously,

this pressure is possible for the smallest diameters of the Fiberspar type, until 3 inches $\approx$ **76.2mm**, then it drops to 1500 psi $\approx$ **10.3MPa** = 103*bar* for the diameter size until 10 inches $\approx$ **254mm**.[82], [115], [25], [1], [2]

Pipe types	*Bondstrand 2400* (for liquids)	*Fiberspar Spoolable* (liquids & gas)
Diameter	2 to 40 inches $\approx$ [**50** ; **1000**] **mm**	2 to 6 inches $\approx$ [**50** ; **150**] **mm**
Inner corrosion barrier	0.5mm of a resin-rich reinforced liner	HDPE or HTP neat resin
Pressure range	10 to 50 bar = **[1 ; 5] MPa**	until 3,500 psi = until **24.1 MPa**
Pipe construction	Filament wound and Aromatic Amine cured epoxy	Filament wound and Anhydride cured epoxy
Temperature allowed	**[-40 ; 93] °C**	**[-34 ; 60, 82 or 95] °C** according to the different types
Joint system	- "Taper/Taper adhesive bonded" - "Key-Lock Mechanical joint"	"Mechanical-flanged, threaded"
Fittings	- "Filament wound with integral Taper Bell ends" - "Single-piece or Van Stone Flanges" (dependent on size).	"Not applicable/corrosion resistant metallic as needed"
Chemical service	Water	Usual services but excluding aromatics and solvents

Table 12: Main differences between the two main possible pipelines of *NOV* for H_2 transportation
Source: Product Data of the Bondstrand 2400 Series pipe systems and Fiberspar Spoolable pipe [2], [81], [82]
`https://www.nov.com/products/bondstrand-fiberglass-pipe`
`https://www.nov.com/products/fiberspar-spoolable-fiberglass-pipe`

Conclusion regarding the composite pipes from *NOV*

Ultimately, the *Fiberspar Spoolable* pipe is able to endure higher pressures which will make the size diameter smaller than a classic liquid pipe which can possibly handle higher temperatures in some circumstances. In addition, all of the fittings are manufactured by the company using the filament winding method of fabrication.

Also, after having discussed by email with an engineer from the company, who provided additional information and data about those types of composite pipes,

he explained that they actually expect the thermoset piping to perform better than the HDPE lined flexible for the future hydrogen permeation. More in details, contacting the company was very useful in order to receive typical properties of their *Brondstrand Fibreglass* pipe and also some links to the relevant products described above that they feel aligned with the standard ASME B31.12 for the hydrogen transmission in pipelines, see section IV in Appendix C.

NOV has surely good reasons to believe that this type of pipe could handle hydrogen transportation for the pipes described above. They unfortunately could not have shared any diffusion rate for hydrogen because the company is going to run permeability testing within the year.

Pipes from *Future Pipe*

High pressure spoolable pipe: Flexstrong

The company *Future Pipe Industries* has developed one product being a thermoplastic composite pipe called *Flexstrong* where the properties are summarised in the Table 13. It is enough flexible to be able to wrap it around a reel, and sometimes the term "spoolable" can be used to describe this property; it is also fully resistant to corrosion and very robust as many composite pipes.

The pipe combines different materials for the layer components. The outer is protecting the inner ones and consists of a coating made of thermoplastic. The reinforcement is composed of a tape which contained a uni-directional fibre in a HDPE (High-density polyethylene) matrix and that is wrapped with a helical movement. Inside, a liner of thermoplastic HDPE is used. Then, to obtain a perfect bond, those layers are melt-fused together.

For now, this specific type of pipe is mainly recommended for applications with a high corrosion potential in the Oil & Gas sector. This includes multiphase fluids and liquids like water or brine but also gases. Among them, natural gas and CO_2 are able to be used. [88], [41] [115]

Conclusion regarding the properties of the *Flexstrong* pipe

According to Table 13, this *Flexstrong* flexible pipe is very interesting for many reasons. First, it can handle high pressures in addition of being corrosion free. Second, it is fully bonded and has a length which can reach more than a kilometre, 1 100 metres to be precised. This allows then to reduce time for the installation. Finally, the thermoplastic structure and material gives the lightweight characteristic, which is of concern for the transport of the pipe as well as the installation, and it finally provides a good durability. [41]

Pipe type	Flexstrong (D = 3 inches)	Flexstrong (D = 6 inches)
Diameter	3 inches ≈ [**76.2**] **mm**	6 inches ≈ [**152**] **mm**
Inner corrosion barrier	Pipe liner HDPE	Pipe liner HDPE
Pressure range	[750 ; 1500] psi ≈ [**5.17 ; 10.34**] **MPa**	[750 ; 1500] psi ≈ [**5.17 ; 10.34**] **MPa**
-> Inner diameter (constant with pressure) -> Outside diameter (changing with pressure values)	-> [2.60] inches = [**66.0**] **mm** -> [3.74 ; 3.79] inches = [**95.0 ; 96.2**] **mm**	-> [5.67] inches = [**144.0**] **mm** -> [7.14 ; 7.29] inches = [**181.4 ; 185.2**] **mm**
Pipe construction	fibres in a HDPE matrix wrapped with a helical angle	
Maximum temperature	up to [**65 ; 85**]° **C**	
Joint system	flanged connector / coupler connector / weld-neck connector	
Chemical service	Ideal for Oil & Gas: general and sour products, H_2O	

Table 13: Summary of characteristics for the thermoplastic pipe *Flexstrong* from *Future Pipe*

Source: Flyer and webpage of the Flexstrong product [41], [88]
`https://flexstrong.com/`
`https://futurepipe.com/wp-content/uploads/2021/07/FlexstrongFlyer.pdf`

Pipes from *Soluforce*

Description of the company

The company *Soluforce* is a technological leader of Flexible Composite / Reinforced Thermoplastic Pipe (FCP / RTP) for high pressure applications. They do the distribution, manufacturing and also development of the FCP systems onshore as well as offshore. They believe it is the 21st century solution in the pipeline sector because it is suitable for many applications without any corrosion or maintenance for their pipes. Since the beginning of the century, in 2000, they have installed 3 500 kilometres of FCP. The environmental sustainability is also taking into account seriously and the company follows the certification ISO 14001, see

section IV in Appendix C. It encompasses the environmental management system that can be used to enhance environmental performance regardless the size and purpose of the company itself. Furthermore, and according to the company, their pipes are producing four times less carbon dioxide emission than the equivalent other alternatives and are reusable. [106] [107],

The hydrogen *Soluforce* pipe: H2T

Soluforce is one of the only companies producing Fibre Reinforced Polymers which has already developed a product able to carry hydrogen transportation. They have developed this product recently in 2019 and the main properties are going to be described below in Table 14. This will be the only case studied in this paper which has already certified a hydrogen pipeline according to national standards of a country, in the Netherlands here. Thus, this is the world first pipe to be certified for transporting hydrogen. Indeed, after having a Teams meeting with two members of the engineering board, they explained that *Soluforce* is still working with the national organisation which certified the hydrogen pipeline utilisation in the Netherlands. They are now also trying to extend this certification at a broader scale, at the European level for example. Regarding transport of gas with *Soluforce*'s pipelines such as *Light* or *Classic*, the certification ISO TS 18226 *Reinforced Thermoplastic Piping Systems for Gaseous Fuels* is used.

About the hydrogen composite reinforced pipe itself, it can carry an intermediate range of operating pressure up to 4.2 MPa (42 bar = 609 psi) with a maximal temperature of 65°C and also no permeation. Moreover, this pipe is running its first application, at Groningen Seaports in Delfzijl, in the Netherlands from 2020. At the end, it will represent four kilometres of pipeline system installed in order to transport and convey hydrogen at a pressure of 32barg ($\approx$ 33 bar = 3.3 MPa) which will be produced by the wind power infrastructures installed in the North Sea. This hydrogen will be produced and distributed for the companies near by for the industrial and chemical sectors. [107], [101]

Pipe type	Hydrogen Tight (H2T)	Classic Gas Tight (GT) (Models M480 GT & M570 GT)
Diameter	[4 ; 6] inches ≈ [**102** ; **152**] **mm** *	[4 ; 6] inches ≈ [**102** ; **152**] **mm**
Pressure range	Until 42 bar (= 609 psi) ≈ **4.2 MPa**	until [113 or 90] bar (=1639 or 1305 psi) ≈ **[11.3 or 9] MPa** (depending on the inner diameter)
Pipe construction	- Smooth bore - Manufactured with a unique bonded aluminum layer (preventing H2 permeation) - Reinforcement with aramid (synthetic) fibre. - Non-corrosive HDPE used for inside and outside layers	- Smooth bore - Manufactured with a unique bonded aluminium layer (preventing permeation of gases) - Reinforcement with (synthetic) fibre tape. - No venting of permeated gases - HDPE liner (Darcy Weisbach surface roughness = 1.5μm) needed.
Maximum temperature	up to **65°C**	up to **85°C**
Maximum depth for offshore applications	**80m** ≈ 260 feet (unfilled) * > **80m** * (filled)	**80m** ≈ 260 feet (unfilled) **1000m** ≈ 3280 feet, reached during a test (filled)
Chemical service	Shaped, designed, produced and certified for the specific hydrogen transport.	- H_2S - CO_2 - Strong inorganic acids like HCl and H_2SO_4 - Strong alkaline materials, including $NaOH$, KOH and NH_2 solutions - Anti-corrosion additives - Mineral salts
Lifetime	**[20 ; 50] years**	

Table 14: Characteristics summary for the *H2T* and *Classic* pipe from *SoluForce*
Approximations are indicated by *
Source: Hydrogen Tight H2T and General Brochures [106], [108]

The *H2T* pipe has the same features as another family of pipes produced by *Soluforce* called *SoluForce Classic*. An analogy is then made below between these two pipes and their main characteristics summarised in a table. There are not a lot of information available that can be shared publicly on the *H2T* pipe of interest in this document. Therefore, a mix of the properties for this pipe and also geometry parameters from the *Classic Gas Tight* (GT) pipe are combined. Here, it is assumed that the combination of both could give a good approximation of all the main properties for the *H2T* though without having those information. Approximations will be announced by the symbol *****, in the Table 14.

Regarding both hydrogen, *H2T*, and gas, *GT*, pipes from *Soluforce*, the safety, health and environmental problems are removed by having no permeation which is avoided thanks to a manufactured bonded aluminium layer. The flow resistance is low while the flow capacity is improved thanks to the smooth bore. A very important component of the pipe is the HDPE liner because it prevents erosion. Additionally, the pipes from *Soluforce* are all verified for requirements about natural disaster such as earthquakes or landslides.

In addition, those pipes are showing an interest regarding sustainability because reusable. The benefits are various for using composite pipelines and the main advantages of having a non-metallic structure are, among other things:

- 4 times less CO2 footprint
- No hydrogen embrittlement and no corrosion
- Entirely flexible
- Easy and fast to install

One example of an offshore application regarding the classic GT pipe was to assemble it onshore and then transport it. The pipe was located at 40 metres under the sea level and then stabilised on the seabed by placing concrete blocks along the pipe. The general lifetime expected for all the pipes of *Soluforce* is a minimum of 20 years and it can reach 50 years maximum for buried pipes as an example. [106], [107], [108]

Installation and maintenance costs are lower for this type of pipes because, as explained earlier, neither special treatment nor venting of permeated gases are needed. Transportation and installation are also reduced by the way of producing pipes of a length of 400 metres rolled up around a reel.

Also, for the specific hydrogen pipeline, it includes a non-corrosive HDPE placed as an inner and outer layer where the reinforcement of the composite material contains aramid (synthetic) fibres. Moreover, this *H2T* pipe for hydrogen

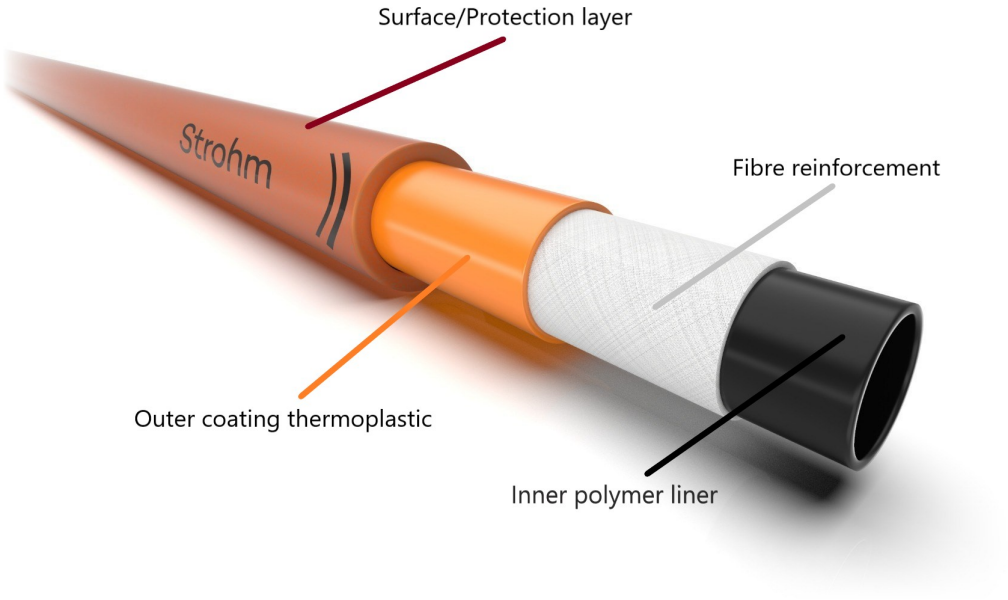

Figure 4: TCP flowline from *Strohm* and its different layers
Source: Company *Strohm* (website) [4]
`https://strohm.eu/tcp-flowlines`

resisting to up 4.2 MPa (42 bar) suits perfectly a production of hydrogen created by electrolysers which usually create hydrogen at a pressure of about 3.0 MPa (30 bar). Regarding the work of this thesis, it seems technically suitable for an offshore production of hydrogen by electrolysers integrated with the wind turbines. [98], [106], [108]

Pipes from *Strohm*

Description of the company

The company *Strohm* is providing pipelines for many applications such as chemical, water or methanol injections, hydrocarbon production as well as gas transport with carbon dioxyde CO_2 and hydrogen H_2. Concerning the *Flowline* pipe that is going to be described below, they make the designing and manufacturing stage of this TCP (Thermoplastic Composite Pipe) product themselves. They have been developing TCP products from the beginning of the company's creation, when its name was still Airborn Oil & Gas from 2007 until 2020. They are and can be very proud to affirm that no ruptures or failures happened to the TCP products from the first day they have been used in operations.

The *Flowline* pipe developed by *Strohm*

The last example among the composite pipes developed and produced by engineering companies, contacted for this thesis, is the composite pipe named *Flowline* from the company *Strohm*.

Pipe type	TCP flowline (D_{in} = 4 inches) at 5.0 MPa (50 bar)
Internal diameter	4 inches ≈ [**102**] **mm**
Outer diameter	6.9 inches ≈ [**175.6**] **mm**
Inner corrosion barrier	smooth bore polymer and fully bonded liner
Mass empty pipe [in air ; in seawater]	**[32.3 ; 7.5] kg/m**
Specific gravity of empty pipe in seawater	**1.30**
Design pressure	725 psi = 50 bar ≈ **5.0 MPa**
Pipe construction	E-Glass Fibre / Polyethylene Thermoplastic Composite Pipe (EGF/PE TCP)
Temperature range	[-4 ; 140]°F = **[-20 ; 60]° C** (for design and also storage)
Design life	**20 years** (which can be extended)
Maximum water depth	50 metres
Tension load for installation	25 kN
Minimum radius [storage ; installation ; subsea bending]	[1.9 ; 3.3 ; 3.4] m
Chemical service	hydrocarbon production, gas lift, water, chemicals and methanol, hydrogen and CO2.

Table 15: Summary of the main data for a TCP flowline from *Strohm*
Source: *Strohm* Preliminary data sheet [3]

As for the previous composite pipe manufacturers, there is no corrosion anymore with this type of material. This point is always of importance. Indeed, it allows manufacturers and users of the pipes to have materials which have almost no operation cost at all in addition to the amazing performance in corrosive conditions. The company also affirms that the cost in total after installation for greenfield, brownfield and hydrogen applications is the lowest. The last application mentioned is particularly relevant for the project of this thesis. It will be

detailed further below after the general description of this type of pipe by using a hydrogen permeation experiment. The term greenfield refers to a site where nothing has been built yet and brownfield for an area that has already been used for industry previously. Inside the pipe, there is a smooth liner made of polymer which is entirely bonded. It is important to notify that the pigging of the pipe is still allowed with this liner. In addition, the high performance of the TCP under heating, which can reach up to 121°C (under certain other conditions), is also a non negligible point. This pipeline can be used and put on the seabed because it stays stable with the integrated weight coating. Depending on the diameter and pressure, the pipeline can have a continuous length of several thousand metres, from 3000 to 6000 m, wrapped on a reel. As stated earlier in this chapter, there is a significant reduction of cost for the installation process when composite pipes are used and rolled. The company estimates a reduction of installation cost of 0.3, in other words 30%. This is estimated without taking into account the additional reduction of cost related to the maintenance due to corrosion in classic steel pipes. The company can manufacture the TCP flowline to resist pressure up to 68.9 MPa (689 bars) or also to have an internal diameter as large as 190 mm (7.5 inches) for specific conditions. But these extreme cases do not apply for the possible pipe used for hydrogen transport. Furthermore, the mechanical tests realised by *Strohm*, detailed below, and data obtained from it were done with the *TCP Flowline* at a diameter size of 120mm (4 inches). Thus, it has been chosen to describe the *TCP Flowline* with an internal diameter of 102mm (4 inches) in Table 15 in order to be in the same range as the H_2T pipe from *Soluforce* detailed above in Table 14. [4], [3]

Mechanical tests of the *TCP Flowline* pipe

Strohm analysed some parameters, from the same document shared by the company [3], by varying the temperature environment from 0°C to 60°C.

On the first experiment where results are reproduced on Figure 5, **axial stiffness EA** [kN] and **axial strain** ε [%] were plotted as functions of the **axial force** $\mathbf{F_{axial}}$ [kN].
For an increase of temperature with a constant value of $\mathbf{F_{axial}}$, the **EA** value decreases to reach, at 60°C, approximately the fifth of the value at 0°C.
The tendency is reversed for the strain ε when the maximum value is obtained for the maximum temperature. In addition, ε growths linearly with $\mathbf{F_{axial}}$ while **EA** has a constant value , so regardless $\mathbf{F_{axial}}$.

On the second experiment where curves can be seen on Figure 6, **bending stiffness EI** [kN.m^2] and **bending reaction moment BRM** [kN.m] were plotted

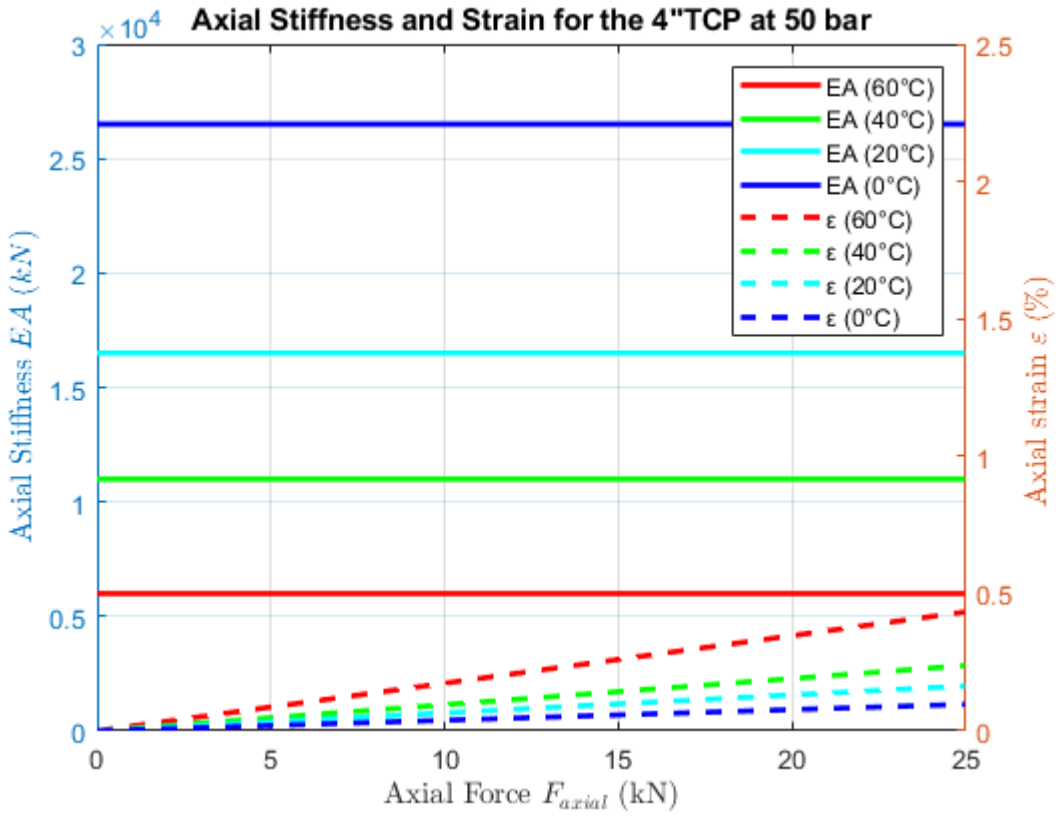

Figure 5: Reproduction of curves for Axial Stiffness (EA) and Axial Strain (ε) with the software Matlab

Source: *Strohm* Preliminary Data Sheet (shared by the company) [3]

as functions of the **curvature** κ [m^{-1}].
An increase in temperature makes decreasing both **EI** and **BRM** values. When κ has a higher value, **BRM** is also higher while **EI** is lower. An interesting point from these curves can be noticed. At a given κ, $0.2m^{-1}$, both **EI** and **BRM** have the same value which depends only on the temperature. And as detailed above, a higher temperature gives lower **EI**, thus lower **BRM** as well.

On the third and last experiment where the plot can be checked on Figure 7, **torsional stiffness GJ** [kN.m^2] and **torsional reaction moment T** [kN.m] were plotted as functions of the torsional angle per length unit $\theta_{\mathbf{torsion}}$ [°/m].
The values $\theta_{\mathbf{torsion}}$ were comprised only from 0°/m to 2°/m. And it induces no change in **GJ**, which stays constant, but implies a linear increase of **T** with, then, a maximum values obtained for bigger angles. However, **GJ** constant value and **T** depend both on the increase of temperature which makes their values decreasing.

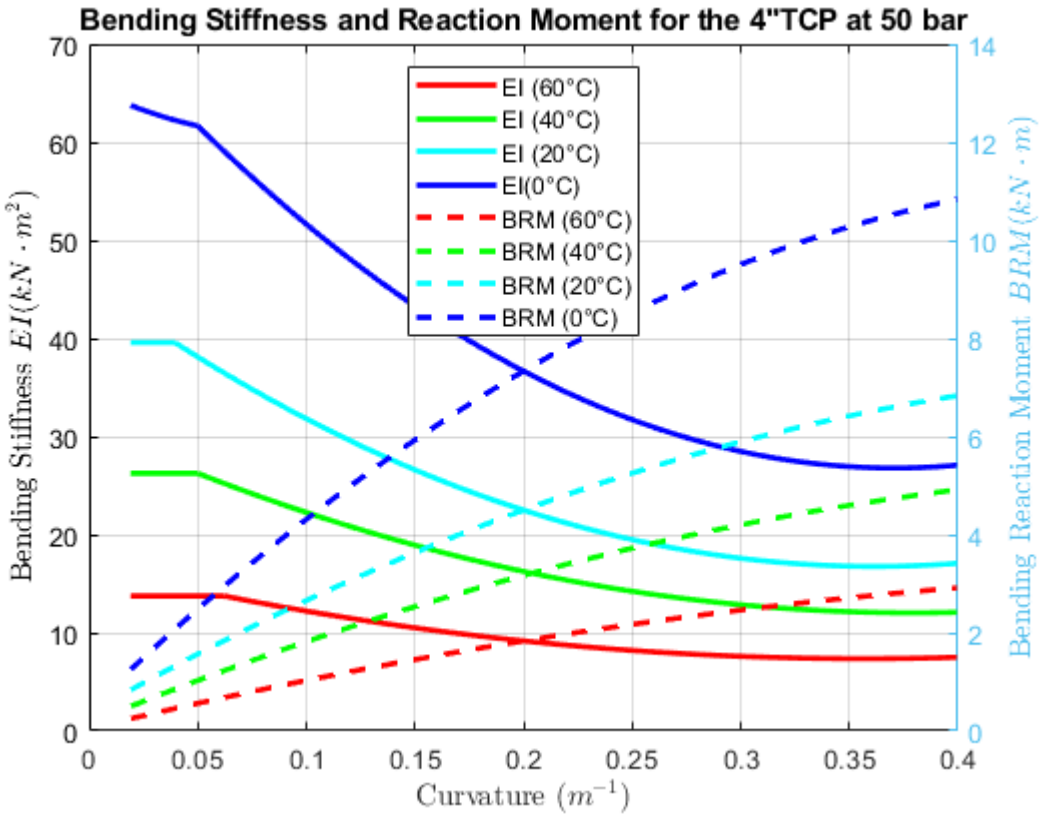

Figure 6: Reproduction of curves for Bending Stiffness (EI) and Bending Reaction Moment (BRM) with the software Matlab

Source: *Strohm* Preliminary Data Sheet (shared by the company) [3]

Hydrogen permeability prediction of a technical note from *Strohm*

The company *Strohm* has done a hydrogen permeation prediction last year on the E-Glass Fibre / Polyethylene Thermoplastic Composite Pipe (EGF/PE TCP) described above with the specific *Flowline* pipe. They chose to follow the CheFEM model to perform this prediction of hydrogen permeation. The objective of the analysis was to use different conditions and situations by varying the pressure, temperature and design of the pipe. They also utilised two different safety classes which modify the laminate thickness. The choice made for the different designs regarding the laminate, liner and coating layer thickness was based on the design safety class. In order to treat as best as possible the results, only the maximum safety class from the tests is going to be considered here, thus inducing a thicker laminae. [84]

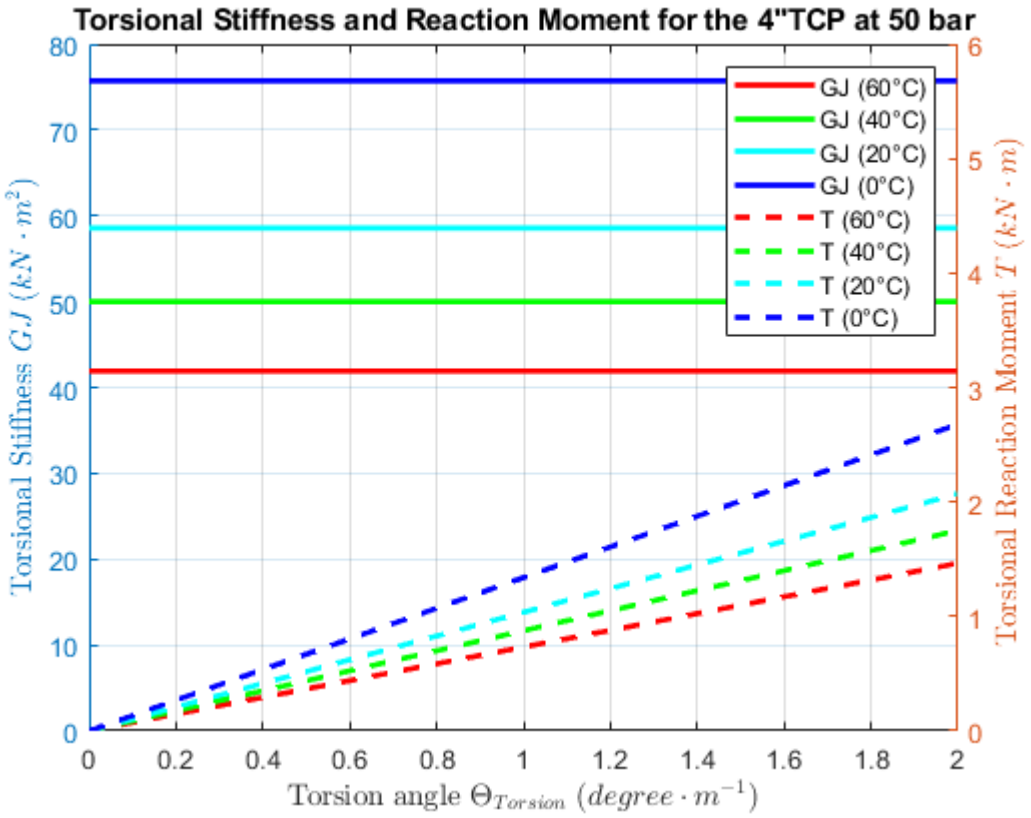

Figure 7: Reproduction of curves for Torsional Stiffness (GJ) and Torsional Reaction Moment (T) with the software Matlab

Source: *Strohm* Preliminary Data Sheet (shared by the company) [3]

Regarding the parameters, pressure was applied between 50 and 200 bar (5 to 20 MPa) and temperature between 20 and 60 °C where internal and external values were the same, an important assumption which remove any possible temperature gradient. The composition of hydrogen for this technical note was a pure amount of hydrogen gas, so 100% of H_2. There were three sizes for the internal diameter: 4, 5 and 6 inches giving in the international system respectively 102, 127 and 152 millimetres. For the first type, so with an internal diameter of 102 mm, the thickness for the liner and coating was the same and equal to 7 mm. The two last, so with an internal diameter of 127 and 152 mm, had a higher liner thickness equal to 9 mm by keeping the same coating thickness, 7 mm.

The results for hydrogen permeability, measured in g/(m·day) are obtained with half-hundred of load cases. From them, the maximum and minimum values can be extracted.

The lowest hydrogen permeability rate for the EGF/PE TCP is obtained at the

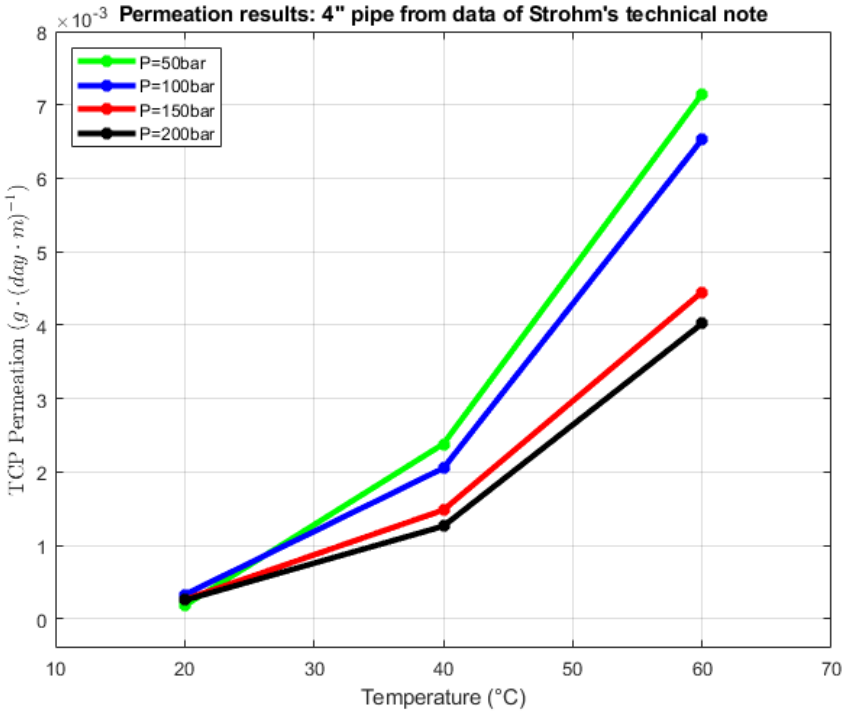

Figure 8: Reproduction of curves for permeation values of the 4" (102mm) pipe with the software Matlab
Source: *Strohm* Technical Note TN741: Hydrogen Permeation of EGF/PE TCP (shared by the company) [84]

lowest temperature or else at the highest pressure for a given temperature. It also corresponds to the maximum laminate thickness applied to the largest internal diameter pipe. However, highest hydrogen permeability rate is obviously found for the opposite situation which means thinnest laminate when pressure is the lowest and temperature the highest.

According to graphs plotted in Figure 8 and Figure 9, for the 4" (102mm) and 6" (152mm) pipe respectively, from the company's data shared, a tendency from the effect of temperature and pressure can be deduced. Indeed, when the temperature is low, around 20°C, the pressure difference is minor in the TCP permeation. Nevertheless, this divergence increases significantly and nonlinearly during the temperature growth. This means that the difference of pressure has a more important role in the hydrogen permeability when temperature is higher.

It is also important to remember that one of the main lack from this technical note is to not have considered any temperature gradient between the inside and outside of the pipe. The initial approximation is to keep both temperatures equal

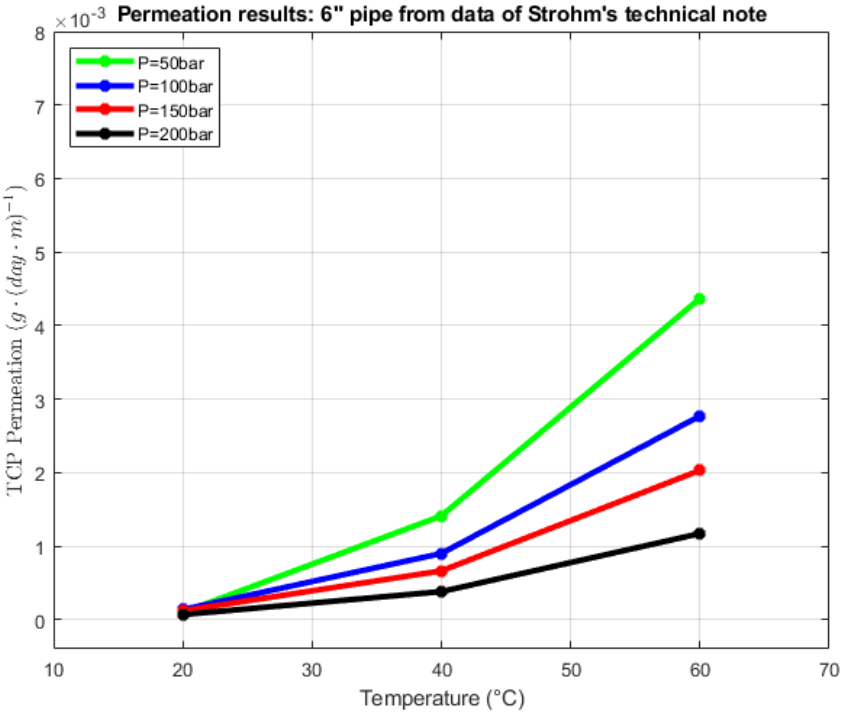

Figure 9: Reproduction of curves for permeation values of the 6" (152mm) pipe with the software Matlab
Source: *Strohm* Technical Note TN741: Hydrogen Permeation of EGF/PE TCP (shared by the company) [84]

even though in actual offshore applications, this will surely never be the case. This point is very important when considering to use an offshore pipeline to transport gas, hydrogen in this case. The material properties vary when there is a difference in temperature and so the temperature gradient in the pipe influences also the hydrogen permeation through the material. But, by stating this hypothesis, the results obtained depend only on a couple of parameters. Furthermore, it allows to show clearly the behaviour of the hydrogen permeation from the main variables acting on the pipe which are: internal diameter size (including a change in liner and laminate thickness), pressure and temperature of the pipe. [84]

As a partial technical conclusion, one of the ideal configuration to use an offshore composite pipe in order to transport hydrogen from a renewable production of offshore wind farms can be described as follow.

The pipe size should be large, therefore it can be recommended to use an internal diameter equal to minimum 6 inches (152mm) which would induce a thicker

liner reaching for example 9mm.

Regarding the layers, the recommendation is to use a pipe with a laminate layer as thick as possible because it has a direct and important effect on the hydrogen permeability rate. And this is one of the few parameters that can be changed in the design phase, unlike the temperature which mainly depends on the environmental conditions.

The last recommendation relates pressure which is actually a contingent parameter regarding the possible future production and distribution of hydrogen. Nevertheless, the pressure should be as high as possible especially in a high temperature environment. [84]

Summary and comparison

As it has been seen, hydrogen is surely going to play an important industrial role in addition to the already ongoing uses (refinery of oil by the hydrogenation process and production of Ammonia mainly) combined with other secondary applications like transport for example. Its use should be, ideally, kept as an energy storage for surplus of renewable, so intermittent, energy production.

Regarding the fibres and the different types produced today, it would be privileged to choose glass or carbon materials. On one hand, carbon (anisotropic) fibres owns outstanding properties, depending on their orientation, and combine in addition low weight and small diameter. However, the costs of this type of fibre might make it less competitive. On the other hand, glass fibres (isotropic) still have very good properties with a higher density and allows to have the lowest cost among the different types in this document. Thus, it is recommended to chose carbon fibres when maximum and exceptional properties, like weight gain, are required regardless the price but to keep using glass fibres in the most general case.

Soluforce has developed a pipe which is already operational for hydrogen transport in the Netherlands using aramid fibres for this project. The characteristics for future pipes may be inspired from the technical data in Table 14. The information collected from the hydrogen permeation test done by *Strohm* should also be taken into account. This means that a low temperature is preferably chosen for transporting the gas, but a high pressure would be the best option, if the temperature is still relatively high, in order to minimise the permeation rate of hydrogen. About the pipe, the possible largest laminate and liner (order of magnitude around 9mm) thicknesses together with the feasible highest internal diameter value (order of magnitude around 152mm, 6 inches) should be of concern regarding the design phase.

Part III
Production, demand and transportation costs of hydrogen gas and pipelines

Hydrogen production costs of electrolysis

The production of hydrogen, as technically described in section *Production of Hydrogen* II, can be done by a few different processes. Each of them has their own advantages and costs. For example, the cost for producing hydrogen through electrolytic process in association with wind, hydro and solar energy is still very expensive, though under important consideration to exploit surplus of energy during the night for example. [130]

Production processes, efficiencies and their costs

To obtain hydrogen gas, it is possible to utilise either electrolysis of water, fossil fuel and industrial operation (Chloralkali). China produced the double amount of hydrogen, about 8 million tonnes, than the United States, about 4.3 million, in 2018 and is aiming mostly to develop the last two process of production stated above. Indeed, China deploys fossil fuel intensively and especially coal synthesis to hydrogen combined with hydrogen byproducts from chemical industry (ethane cracking, palladium hybride, Chloralkali, and oil refining). This allows china's hydrogen production to reach a low cost in the order of $2.6\$\cdot kg^{-1}$ while electrolysis, mainly employed in Japan, cost double at around $5.2\$\cdot kg^{-1}$. Nevertheless, the last process overcome the others by providing the purest product. The greenest method is called *renewable-to-gas* and its cost ranges between $[5\ ;\ 5.9]\$\cdot kg^{-1}$. Although, the fossil fuel produces a hydrogen gas with a high carbon intensity and less pure than by electrolysis, it keeps having the best economical option right now. [126]

Natural gas steam reforming is already an advanced technology utilised for many years with large industrial production sites. The efficiency of this commercial product ranges between 70 and 85% and can be increased if other sources supply the steam.

The efficiency decreases to [50 ; 70]% regarding the coal gasification technique which is in addition less used.

Between 62 and 82% is the efficiency range from the electricity to hydrogen for the commercial alkaline electrolysis which can satisfy a hydrogen demand range of

[1 ; 1000]$Nm^3 \cdot h^{-1}$. Nevertheless, the efficiency obtained with water electrolysis is between 60 and 75%. A high pressure or temperature makes the energy utilisation more efficient by the system. However, the compression of the gas requires [10 ; 15]% and up to 30% for large pressure compression of the hydrogen energy content. Liquefaction, obviously, needs even more power and will take [30 ; 40]% of the hydrogen energy. The cost for this compression stage is comprised between 0.9 and 1.75€$\cdot kg^{-1}$.

To determine the overall energy efficiency, it is necessary to also take into account the power generation efficiency. Then, both are multiplied together to obtain the overall efficiency. Multiplying this result by the efficiency of hydrogen to utilisation would state the global efficiency from generation to use. For example, if heat is used as primary source and by taking usual thermo-electrical efficiency of the power system between 30 and 55% (basic values for combined or Rankine cycles powered by heat with temperature above 400°C), then the efficiency goes down quickly to reach 18 to 41%.

The cost ratio between natural gas steam reforming or coal gasification and electrolysis is in the order of 3. Although the prices are highly dependent on the electricity costs, it gives a clear advantage for a large scale production based on fossil fuels. The high difference of costs also guides industries and economic decisions to add a carbon capture storage system to the fossil fuel production of hydrogen instead of changing for a viable and cleaner but more expensive option. [130], [45]

Example of electrolysis in British Columbia, Canada

For estimating the cost of hydrogen through the electrolysis process, the electricity represents a main factor. Canada can be taken as an example from [51] where the industrial electricity cost reaches 60\$$\cdot$(MWh)$^{-1}$, the hydrogen price would be in the range [5 ; 7]\$$\cdot$kg^{-1}. The estimation showed that for the Canadian case, the electricity cost has to not exceed 40\$$\cdot$(MWh)$^{-1}$ in order to keep electrolysis as a competitive production way for hydrogen, otherwise other processes would appear costly advantageous. In this amount, 80% of the total hydrogen price is actually from the operational cost powered by electricity. However, when the utilisation equals hardly 40% instead of running all the time, the costs change drastically regarding the capital expenses being multiplied by a factor 2.5 while the operational ones is slightly raising. This brings the global price of hydrogen between 8 and 9\$$\cdot$kg^{-1} Moreover, as detailed in sections "Economy for electrolysis system powered by offshore wind farm" III and "Electrolysis system powered by offshore wind farms" II, the plant size is of importance with the economy of scale effect. Indeed, a change from 10 to 100MW would reduce the cost by about 30%, a non negligible decrease, whereas increasing it from 100 to 500MW would produce

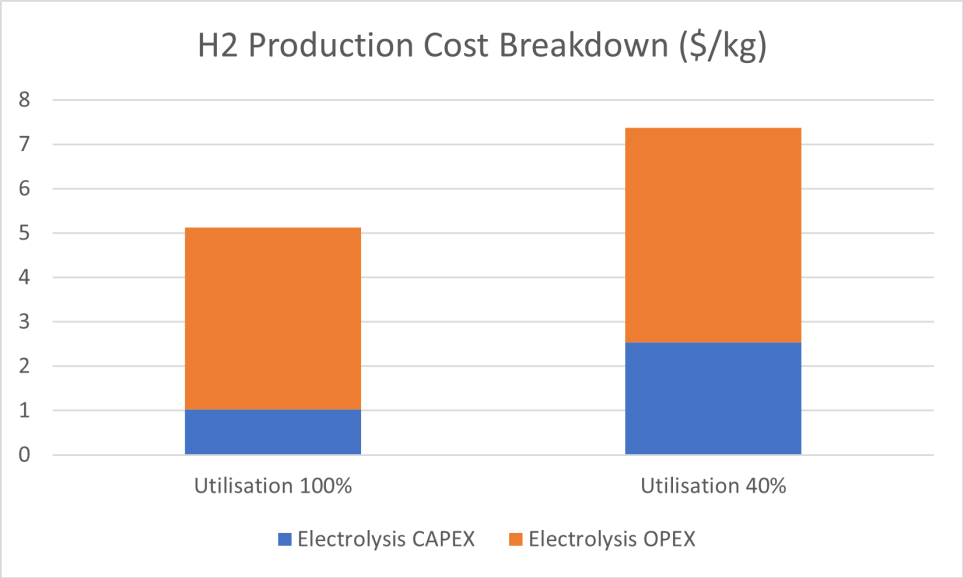

Figure 10: Canada costs for electrolysis regarding capital and operational expenses
Source: ZEN & British Columbia [51]
`https://www2.gov.bc.ca/assets/gov/government/ministries-organizations/zen-bcbn-hydrogen-study-final-v6.pdf`

an insignificant slop on the price line. [24]

Challenges, storage costs of electrolysis and "colours" of hydrogen

The document [130] grouped important general data regarding the four main technologies to produce hydrogen. Some of the data can be found here in the Table 16. This table contains assumptions on energy source costs which are: 0.8€·MWh^{-1} for electricity, 0.7€·Nm^{-3} for natural gas and 250€·$tonne^{-1}$ for coal. According to the characteristics listed in the Table 16, it seems that Steam Methane Reforming (SMR) has the highest energy efficiency, size, market part and production cost. All of this makes that production system as the most competitive technology which still represent almost half of the whole market share. Electrolysis, which is of interest in this document, has the highest production cost reaching about three times the cost required for SMR or Gasification of coal in addition to having a lower efficiency than using natural gas. This implies that electrolysis is by far the lowest production technology utilised today with barely 5% of the market share.

Technologies	SMR	POX	Electrolysis	Gasification
Energy source	Natural gas + electricity	Hydrocarbons + electricity	Electricity	Hydrocarbons + electricity
Energy efficiency	**[70 ; 85]**	[60 ; 78]	[62 ; 82]	[50 ; 70]
Typical size ($Nm^3 \cdot h^{-1}$)	**[10 ; 20]·10³**	**[10 ; 20]·10³**	[0.5 ; 10]	**[10 ; 20]·10³**
Technical lifetime	[2 ; 5] years	[2 ; 5] years	**40 000 h**	[2 ; 5] years
Market share⁺ (%)	**48%**	30%	4%	18%
Production cost* (€·Nm^{-3} H_2)	**[0.05 ; 0.1]**	[0.07 ; 0.15]	[0.16 ; 0.30]	**[0.05 ; 0.1]**
Cost breakdown*: material (%)	30%	30%	50%	30%
process (%)	40%	40%	30%	40%
labour (%)	30%	30%	20%	30%

⁺ From 2012 ; * From 2011 ;
SMR = Steam Methane Reforming; POX = Partial Oxydation

Table 16: Hydrogen production data
Source: Zoulias, M. [130]
`https://iea-etsap.org/E-TechDS/PDF/P12_H2_Feb2014_FINAL%203_CRES-2a-GS%20Mz%20GSOK.pdf`

Fossil fuels produce hydrogen by using large scale facilities and CO_2 emissions in the same time but their low production cost guides the investment decisions which results of the current situation. Yet, electrolysis is a flexible and adaptable technology enabling to create a pure hydrogen emitting negligible CO_2 emissions and other substances for small and medium quantity of H_2. Electrolysers have to operate at a temperature below the water boiling point and under the pressure of 50 bar in order to avoid corrosion.

By the way, all the estimations referring to future cost and expections are not taken into account in this thesis. This choice is mainly motivated by an unprecedented world energy crisis situation in a close future for the next years (see J.M. Jancovici [61], [62]). The consequences associated to this decline in fossil fuels (oil and gas) and in particular the economic ones, are mainly due to an economic system based on growth, together with the inaccuracy of economic

projections made in the past about hydrogen market and technologies for today implying that most of the data projections are unrealistic and irrelevant for this thesis. Other random consequences with natural origins will happen due to the environmental problem/climate change and will probably destabilise the system, e.g. food production, water availability raw materials availability for metals and other components and so on... [130] [18], [61] [62]

Hydrogen storage aspects

To introduce briefly the storage of hydrogen, there exists three different processes: Compression with high pressure, liquefaction by reaching the cryogenic temperature which is both a liquid and gaseous storage and, storage in solid materials. The two first ones are the common techniques while the last one, even though presenting several advantages for energy consumption, handling and compactness, is still under development and thus, it will not be ready for use in a close future period of time due to commercial and technical difficulties. As stated above, compression and liquefaction energy amounts require respectively about [10 ; 15]% and [30 ; 40]% of the hydrogen energy content. It appears clear that the total costs of liquefaction is highly related to electricity due to the huge amount of energy needed for the phase changing of hydrogen. Nevertheless, running the compressor makes the compression process also dependent on the electricity costs as well as on the costs of the machine itself ranging between 45 000€ and 90 000€ for a 300-bar compressor reaching a capacity of $20 Nm^3 \cdot h^{-1}$. This is converted to $[0.63 ; 1.3] €\cdot kg^{-1}$ as a hydrogen cost. Finally, the electricity used by compression is assumed to cost $[0.3 ; 0.45] €\cdot kg^{-1}$ applied to commercial pressures at about [300 ; 350] bar. Thus, the combination of the electricity and capital costs together states a price range of $[0.9 ; 1.75] €\cdot kg^{-1}$. In comparison, liquefiers, with a small/medium scale, would cost $[0.5 ; 1.1] €\cdot kg^{-1}$. The interest of liquefaction, despite the large amount of additional energy needed compared to compression, is to produce a density by around 800 times higher than the gaseous form of hydrogen at atmospheric pressure. Another good point for this type of storage is the low pressure required whereas the gaseous storage needs much more compression for containing the same energy amount. An additional information to take into account in those price ranges is the moment when the economy of scale will be large enough to affect and allow a potential lower compressor's prices. [130]

Costs depending on the hydrogen "colours"

As a way of differentiating the different production systems and create a difference in their sustainability characteristic by including for example the GHG emissions created, colours have been adopted to classify them. Costs are related

to the different colours from the work done by the European Parliamentary Research Service EPRS from [37].

Hydrogen "colour"	CO_2 emissions ($kg_{CO_2} \cdot (kg_{H_2})^{-1}$)	Cost (€·kg^{-1})
Green hydrogen	0	[2.5 ; 5.5]
Grey hydrogen	9.3	1.5
Blue hydrogen	0.93*	2
Turquoise hydrogen	0	-

*supposing a 90% efficiency for the CCS system from [9]

Table 17: CO_2 emissions and cost for the common colours of hydrogen
Source: G. Erbach [37]
`https://www.europarl.europa.eu/RegData/etudes/BRIE/2021/689332/EPRS_BRI(2021)689332_EN.pdf`

A "*clean hydrogen*", also characterised as "*renewable hydrogen*" or "*green hydrogen*", describes one of the most sustainable way to produce hydrogen regarding the GHG emissions. It uses the electrolysis of water which is powered by renewable energies. The cost range is [2.5 ; 5.5]€·kg^{-1} and is dependent on the cost of electricity. It is expressed that no GHG are emitted during the process but this does not mean that no GHG are emitted at all if the production and transport of the materials to have the renewable energy sources and the electrolysers are included in the evaluation.

By contrast, "*grey hydrogen*" represents the major way of producing hydrogen today, which is by using natural gas by Steam Methane Reforming (SMR). This process costs around 1.5€·kg^{-1}, depends mainly on the price of gas and carbon emissions and the amount of GHG emissions reaches about 9.3 kilograms of CO_2 per kilogram of hydrogen (kgCO_2·(kgH_2)$^{-1}$).

This production process will have a cost of 2€·kg^{-1} when using a Carbon capture and storage (CCS) system and thus the colour classification *blue hydrogen* is attributed to it. Thus, that is more expensive than the *grey hydrogen* but still more economically attractive than *green hydrogen*. The tendency to reduce the investment would be then to install a CCS system to an already existing facility producing *grey hydrogen* to transform it into *blue hydrogen* whether the CO_2 storage capacity is available. The last colour which is mentioned here is *turquoise hydrogen* which is produced by pyrolysis of natural gas. It represents still an insignificant part of hydrogen produced right now because it is at an early stage of the development. Nevertheless, it has the property to be a cost-efficient system without emitting any CO_2 gas emissions during the process since pure carbon would be transformed which could be sold on the market.

Although the classification, with costs grouped in Table 17, is slightly simplified and somewhat not comprehensive, it makes discussion around hydrogen more attractive and allow media as well as people to understand quickly by using this visual reference in order to distinguish clearly a difference between green or grey hydrogen for example. [37] [9]

Economy for electrolysis system powered by offshore wind farm

By taking the similar analysis made in the previous chapter at section *Electrolysis system powered by offshore wind farm* II, the economic point of view is summarised regarding electrolysis systems used offshore and powered by wind farm.

As stated in the technical analysis section for the similar case, fossil fuel sources are completely dominant in the annual hydrogen production and they create about 830 million tonnes of CO_2. This huge production replies to a demand of 70 Megatonnes (=Million tonnes), in 2018, that tripled since 1975.

AWE stands for Alkaline Water Electrolysis; PEMEC stands for Polymer Electrolyte Membrane Electrolysis which is a new technology and available commercially in smaller units than in AWE. SOEC stands for Solid Oxide Electrolysis and has the highest efficiency but is unfortunately not commercially available. [58], [57], [127], [20]

Several research papers have been published on the economy of electrolysers powered by wind turbines. Taking advantage of the excess wind power has been analysed and costs are found to be very expensive at around $[20 ; 30]\$\cdot kg^{-1}$, though increasing the viability of the wind power plants. [118]

However, using the surplus of electricity from the wind farms with electrolysers to make hydrogen would still be cheaper than taking electricity from the electrical grid. [128]

In the way to have a combination with hydrogen and offshore wind farm, limiting the number of possible final uses for the hydrogen in addition to fuel few energy products would be the key for a viable economy. [72]

The scale of the technology is also a key factor to obtain a better cost for the hydrogen production. [67]

Also, an interesting fact is that cheapest hydrogen would be produced when electrolysers take advantage of the off-peak electricity instead of running under continuous operations. [90]

This section below concerns exclusively the operation and design by focusing on the cost aspects from [26]. As already detailed, the first profile tested is a constant power supply, the second is a wind profile from actual data and the third

one is the same but with a more detail period of time: The full load hours of the system is 3983 hours. An assumption of the analysis is that 10% of the whole block cost is dedicated to operation, maintenance, and stack replacement costs: OpMainRep.

Results from the framework

About the cost for the block design, in all cases the PEM designs, which are a new technology and use rare and costly metals, are thus more expensive than the AWE ones. The price would also increase with a higher number of stacks for each block and with a bigger size for the individual stacks. For example, the most expensive system to build is composed of ten stacks. In addition, a design including the 10MW stack types will also be more expensive to build, reaching millions of euros more for one block. Furthermore, high pressure designs are usually cheaper than the low pressure. Hence, the cheapest design block includes one single 1MW stack running at high pressure being AWE type while a system with ten stacks of 10MW each running at low pressure and being PEM type represents the most expensive block. Finally, this comparison is somewhat too simplistic due to the absence of technical efficiency of the system itself. In order to be more precise and correct in the investigation, the relative values, or ratios, corresponding to the price per MW of blocks should be the major preoccupation.

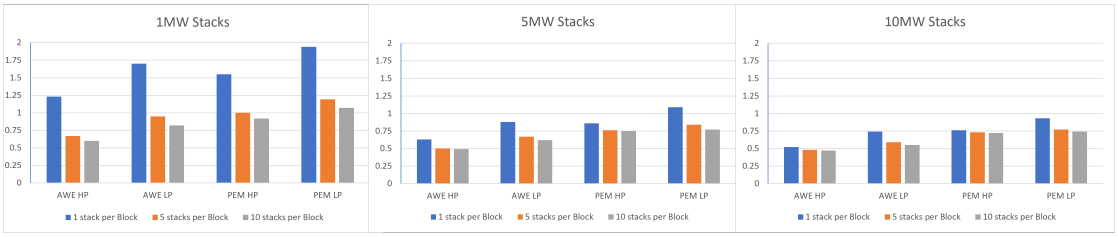

Figure 11: Cost per Megawatt in (M€·(MW)$^{-1}$) for three different types of Stacks
Source: Cooper, N. [26]
https://doi.org/10.1016/j.ijhydene.2021.12.225

The situation changes when the costs per MW of blocks are compared together because it appears that an increase in the size of the stack will reduce the cost of blocks, see Figure 11. Then, using 10 MW stacks per block becomes the cheapest option because more efficient than the other cheap one using absolute values. The logic is the same concerning the number of stacks which should be increased ideally to 10 for the purpose of lowering the cost. However, since the technology type as well as the pressure do not influence the amount of megawatts of stacks in a block, the cost per MW still stays more expensive for both PEM designs and low pressure.

In Table 18, the final technical and economic data are summarised. The lowest Levelised Cost Of Hydrogen (LCOH) is reached for the first condition delivering a constant power because it produces the most quantity of H_2, the equivalent full load hours loading *Eq. FLH*, at 4.73€·kg^{-1}. However, the lowest annual cost is obtained with the regular wind condition, at 383.8 ·10^6€·year^{-1}, which has the second lowest LCOH even though it produces the least production quantity of H_2. Another detail to notice with this second loading condition is the lowest Capital Expense over time, at 1462 million €. On the other hand, the lowest Operating expenses is obtained with the Wind Qtr loading profile. Nevertheless, the annual cost is the highest for this last condition but it is important to notice the close value of hydrogen production compared to the first profile with full load hours. But this is not enough to produce a significant decrease in the LCOH value.

As explained in the technical analysis of these results, the differences between the three conditions is mainly driven by the number and specific characteristics of AWE or PME. The cost of hydrogen produced is impacted by the type used. For example, by installing PME systems, the efficiency will be better but since it is more expensive to build as well, the cost of hydrogen will also increase. In order to design the configuration of the system, the whole price of the system is important and depends mainly on the choice between having a majority of AWE blocks or of more expensive PEM blocks.

Load condition	*Eq. FLH*	*Wind*	*Wind Qtr*
Design configuration	- AWE HP 10MW 10 stacks, 7 blocks - PEM HP 10MW 10 stacks, 3 blocks	- AWE HP 10MW 10 stacks, 9 blocks - AWE HP 10MW 5 stacks, 2 blocks	- AWE HP 10MW 10 stacks, 1 block AWE HP 10MW 5 stacks, 1 block PEM HP 10MW 10 stacks, 8 blocks PEM HP 10MW 5 stacks, 1 block
H_2 Production (10^6 kg·year^{-1})	**84.4**	79.6	83.2
LCOH* (€·kg^{-1})	**4.73**	4.82	5.15
Cost (annual) (10^6 €·year^{-1})	399.6	**383.8**	428.3
Utilisation factor / System energy use (GWh)	**1.0** / **3920**	**1.0** / **3920**	0.995 / 3900
CapEx** (10^6€)	1535	**1462**	1671
OpEx*** (10^6€·year^{-1})	166.7	166.7	**165.9**

Table 18: Final technical and economic data from Cooper, N. [26]
Source: `https://doi.org/10.1016/j.ijhydene.2021.12.225`
* Levelised Cost of Hydrogen
** Capital Expense of the system annualised over time (Million €)
*** Operating expenses of each time period (Thousands €)

Those results show different technical, already mentioned in section *Electrolysis system powered by offshore wind farm* II, and economical aspects expressed above. To summarise, the cost comparison included the design and other technical differences, the cost for operation according to the power supply scenarios and capital of the systems together with the Levelised Cost Of Hydrogen. For the situation presented, and originally from [26], the AWE designs are found cheaper than the corresponding PEM designs for the optimisation presented. In addition, smaller blocks are more expensive than bigger ones. For the same amount of loading hours, the first condition with the constant power supply condition showed the best ideal results regarding the quantity of hydrogen produced with 84.4 million kg and the

cheapest levelised hydrogen cost as well by reaching $4.73€\cdot kg^{-1}$. The power production profile *wind* corresponding to a theoretical 1 GW plant by the coast of the Netherlands obtained the lowest annual cost and capital expense as well as a good Levelised Cost of Hydrogen which is 2% above the constant power supply *Eq. FLH*. The last profile, *Wind Qtr*, is globally the worst economic solution except regarding the operating expenses. However, only looking at the technical aspect of this accelerated wind profile, it is by far more interesting than the classic wind profile and produces about 4000 additional tons of hydrogen over a year. Moreover, it is composed of a technology mix which represents a high potential benefit knowing that PEM technology designs adapt faster to any changes of loading level but still keeping some AWE.

As a main conclusion of the both technical and economical parts for this framework, all profiles have mainly their own characteristics which make hard to chose only one in particular. Despite this difficulty, it is expressed that on a pure economic view, the design configuration of the wind profile is the cheapest option to opt for while the accelerated wind profile is technically better, and closer to the constant power profile, with a larger hydrogen production and a satisfying utilisation factor. [26]

Hydrogen transportation and H2 pipe costs

Volume and capacity

The modes of hydrogen transportation depends mainly on the quantity and distance that are required which makes the feasibility and cost changing according to which option is chosen. Regarding the costs mentioned by IEA-ETSAP in 2014 [130], liquid tankers would create a transport cost at $0.13€\cdot kg^{-1}$ which is the same order of magnitude as the estimation done by the US-DOE at around $0.15€\cdot kg^{-1}$. The physical characteristics for the tube trailers are a pressure of 200 bar (20MPa) for 300kg of gas stored which explains its interest only for small quantities and over short distances to reduce the high cost implied by carrying small amounts of H_2 gas. Nevertheless, the flexibility is an important criterion regarding this way of transportation like when delivering to new places and customers, unlike pipelines which are fixed for years. The costs for hydrogen transportation by tube trailers over 100 kilometres without and with the gas compression are respectively, $0.6€\cdot kg^{-1}$ and $2.2€\cdot kg^{-1}$. As expected, pipelines are the most effective solution economically and technically to deliver gas with a high capacity but will require additional energy to compress and pump the gas as well as efforts to deploy them in a smart and sustainable way. It is important to be aware of the assumption on a minimum quantity of 5 billion m^3 per year made by IEA-ETSAP in order

to specify the values for the pipeline transport. The values mentionned in this part are summarised in the Table 19 and the conversion for the specific volume $12.1m^3 \cdot kg^{-1}$ of hydrogen from [117] can be used if needed. The graph in Figure 12 shows the cost behaviour decreasing in the same time as the increase of the mass quantity of hydrogen transported by pipeline. [130]

Modes of transport	Mass/Volume transported	Costs	Additional information
Liquid tankers	[400 ; 4000]kg	[0.13 ; 0.15]€/kg	
Tube trailers	[300]kg	[0.6 ; 2.2] €/(kg·100km)	20 MPa (200 bar)
Pipelines*	$5{\cdot}10^9 m^3$/year	0.261€/kg	23.47€/($10^3 m^3$)
Pipelines*	$10{\cdot}10^9 m^3$/year	0.185€/kg	16.62€/($10^3 m^3$)
Pipelines*	$20{\cdot}10^9 m^3$/year	0.152€/kg	13.64€/($10^3 m^3$)
Pipelines*	$30{\cdot}10^9 m^3$/year	0.139€/kg	12.47€/($10^3 m^3$)

*valid only for a quantity above $5{\cdot}10^9 m^3$/year

Table 19: Data results from the capacity and cost analysis
Source: Zoulias, M. [130]
`https://iea-etsap.org/E-TechDS/PDF/P12_H2_Feb2014_FINAL%203_CRES-2a-GS%20Mz%20GSOK.pdf`

To conclude, liquid hydrogen is still representing a lost of energy non-negligible in addition to the already existing low ratio of energy conversion into hydrogen, especially regarding the use of electrolysis of water. Moreover, as stated in section II from Figure 2, they have to be kept at an extreme low temperature of -240°C, at a pressure of 1.3MPa (13 bar), or colder if the pressure is decreased (-252.87°C at amospheric pressure, 1.013 bar). That is why, despite the attractive cost per kg transported, liquid tankers should be kept for exceptional projects requiring this physical form of H_2. Tube trailers are transporting small amount of hydrogen gas for small needs but are quite expensive over hundred kilometres when the cost of gas compression is taken into account. Pipelines can then be a solution for transporting hydrogen but needs a higher demand implying huge volume transported within the year to be fully employed at a potential medium to low cost.

Needs and demand for hydrogen FRP pipelines

The demand estimated by [105] in their analysis is half a kilogram, i.e. 0.5kg, of hydrogen per capita based on some technical targets and already existing transportation data. The distance from the plant has been chosen fixed at 200 miles and starting pressure at 1000psi with an allowable drop of 300psi, which gives in

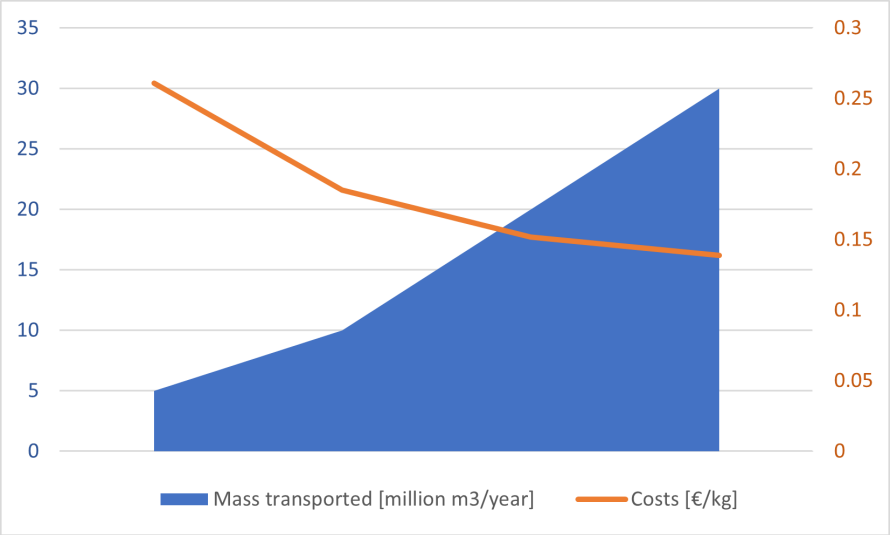

Figure 12: Cost behaviour with the mass transported by pipelines
Source: Zoulias, M. [130]
`https://iea-etsap.org/E-TechDS/PDF/P12_H2_Feb2014_FINAL%203_CRES-2a-GS%20Mz%20GSOK.pdf`

international units 322 kilometres and around 6.9Mpa with a drop of 2.07Mpa (69 bar / 20.7 bar). Three scenarios for the population are taken: 100 000, 1 and 10 million persons. The interesting fact regarding this study is the inclusion of the spoolable composite pipes (FRP) simplifying installation and manufacturing process, thus small diameters for the pipes are considered from 4 to 12 inches (102mm to 305mm). Similarly as electricity supply, a peak demand has to be taken into account and was set at 1.5 times the average demand of 0.5kg/(day·capita) which gives 0.75kg/(day·capita). Thus, the following calculation details briefly the ratio multiplied by the number of persons in order to find the Peak Demand PD per hour for the given population in each situation:

$$\mathrm{PD}_{/\mathrm{capita}} = 0.75\ \mathrm{kg}_{/(\mathrm{day})} = 0.75 * (24)^{-1}\ \mathrm{kg}_{/(\mathrm{hour})} = 0.03125\ \mathrm{kg}_{/(\mathrm{hour})} \tag{31}$$

Then, for the peak demand of a population with a hundred thousands persons, it gives: $0.03125 \times 10^5 = 3125kg \approx 3000kg$.
The Table 20 is thus obtained with the results by varying the population size.

From the data combined in the table it is clearly seen that by increasing the pressure, the number of pipes to meet the required demand decreases significantly. This is due to a higher density for a stated mass flow rate. The specific energy loss is unchanged after the pressure change.

In order to illustrate the results of this report [105] , the demand is going to be calculated for Stavanger city area on the west coast of Norway counting 229 911

Population (million)	0.1	1	10
Peak demand [kg·h^{-1}]	3 125	31 250	312 500
Pressure at 6.9MPa (1500psi) and with a drop of 2.07MPa			
No. 4-inch pipes	**5**	**50**	**500**
No. 8-inch pipes	1	9	90
No. 12-inch pipes	/	3	30
Diameter for a single pipe	8	18	44
Pressure at 24.8MPa (3600psi) and still with a drop of 2.07MPa			
No. 4-inch pipes	**3**	**30**	**300**
No. 6-inch pipes	**1**	**10**	**100**
No. 8-inch pipes	/	5	46
No. 12-inch pipes	/	2	16
Diameter for a single pipe	6	15	36

Table 20: Number of pipelines needed for different peak demand from population size
Source: Smith, B. (Oak Ridge National Laboratory) and Paster, M. (DOE) [105]
`https://www.hydrogen.energy.gov/pdfs/progress05/v_a_2_smith.pdf`

inhabitants. [102]

The population and thus the peak demand, for the case of Stavanger city area, are both multiplied by the factor 2.29911 and this gives:

- Population = $0.1 \cdot 10^6 \times 2.29911$ inhabitants= 229 911 inhabitants
- Peak demand = 3125×2.29911 kg·h^{-1} $\approx$ 7185 kg·h^{-1}
- Number of 4-inch pipes$_{(6.9\text{MPa})}$ = $5 \times 2.29911 \approx \boxed{12}$ pipes
- Number of 8-inch pipes$_{(6.9\text{MPa})}$ = $1 \times 2.29911 \approx \boxed{3}$ pipes
- Number of 4-inch pipes$_{(24.8\text{MPa})}$ = $3 \times 2.29911 \approx \boxed{7}$ pipes
- Number of 6-inch pipes$_{(24.8\text{MPa})}$ = $1 \times 2.29911 \approx \boxed{3}$ pipes
- Number of 8-inch pipes$_{(24.8\text{MPa})}$ = $\frac{5}{10} \times 2.29911 \approx \boxed{1}$ pipe

Related to the technical analysis done in the previous part of this work related to companies working with FRP pipeline II, only the first two numbers of pipes are relevant so far because they are running at pressure (about 6.9MPa = 69 bar) and diameters (4 or 8 inches) close to the ones that has been approved for the Hydrogen Tight product from SoluForce (4.2 MPa = 42 bar ; [4-6]inches)

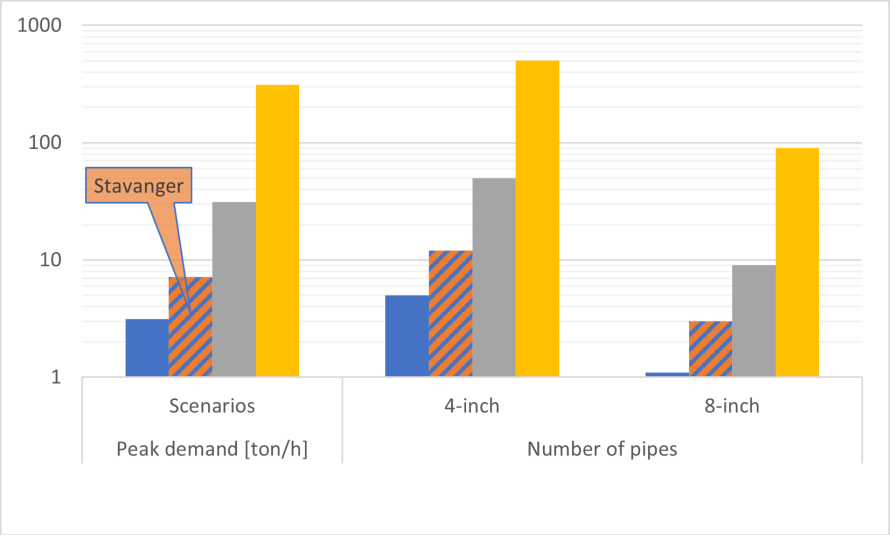

Figure 13: Number of pipes depending on the initial peak demand at 6.9MPa
Source: Smith, B. (Oak Ridge National Laboratory) and Paster, M. (DOE) [105]
`https://www.hydrogen.energy.gov/pdfs/progress05/v_a_2_smith.pdf`

Small changes in the parameters such as pressure, allowable drop and capacity must be taken into account in order to have an accurate economical system close to the reality. A few changes of them can modify drastically the results obtained as it was the case for changing the pressure value in the second part of the Table 20 for example.

To conclude, increasing pressure allows to reduce the number of hydrogen pipes thanks to a higher density for a given mass flow rate. For example a pressure increase of about 3 would reduce by a factor 2 the number of pipes required to meet the demand.

Costs of hydrogen FRP pipelines

From the same report [105], the cost of a spoolable FRP 4-inch at 6.9MPa for hydrogen has been estimated at about $10\$_{/\text{foot}} = \boxed{32.79\$_{/\text{m}}}$ and this analysis matches most of the technical criteria required for this thesis. Although, it has been conducted in 2005, the order of magnitude is assumed to be very close to what is expected today especially since there is still no actual economic market regarding hydrogen spoolable FRP yet which will put the prices significantly down. So far, there is no known pipes developped to transport hydrogen gas at a pressure above or equal to 20.68MPa (3000psi = 206.8 bar). However, according to the same simulation, the cost for that hypothetical pipe would be multiplied by a factor 1.4

giving a cost of $14\$_{/\text{foot}} = \boxed{45.90\$_{/\text{m}}}$. For complex installation with location for example in mountain or urban area, the maximum installation cost of the same type of pipe could arise up to $20\$_{/foot} = \boxed{65.57\$_{/m}}$.

If in the future, larger diameter pipes for hydrogen are manufactured, it would be a good idea to maybe not rush on that option. Indeed, a number of a few small FRP pipes allows a reducing in capacity without serious damages to one pipe. Also, the consumption usually increases with time, so the economy can adapt with the previous market needs. Thus, starting with perhaps smaller diameter pipes and then modifying the configuration in the future by adding a few more pipes proportionally to the increase in demand instead than a large diameter pipe immediately would be judicious. This logic economic strategy is more in favor to deploy spoolable FRP pipe thanks to their low installation cost combined with a short diameter size, less than 10 inches (254mm) so far.

Although not included in this document, the transport of the pipe itself is also a characteristic to take into account in a project analysis. Regarding the offshore transport of the spoolable pipe itself, more space are available to move it, unlike by road or highway, and the size can reach a diameter of 12 inches (305mm) or even more. [105]

To conclude, the costs for a FRP pipeline would be included between about 32$ and 46$ per meter and that could peak at about 66$ per meter for demanding installation conditions.

Cost reduction with retrofit and difference with electricity lines

The electricity transmission lines are usually more expensive than hydrogen pipelines but it obviously depends on the need. Regarding the situation as a transfer of energy between two different locations, hydrogen pipelines appear more relevant and interesting for specific applications. Indeed, for $1/8^{th}$ of the electricity transmission lines cost, hydrogen pipelines would transport about 10 times more energy and they, in addition, last longer. Therefore, when the need is to use hydrogen gas or to store it as an energy storage instead of obtaining electricity for the final product, considering hydrogen pipelines would probably be an accurate option instead of electricity lines. Nevertheless, it is important to remember that there is a non-negligible loss factor to convert electricity to hydrogen during the production process, see section *Production processes, efficiencies and their costs* III , that is why this fact above concerns strictly the transport of electricity or hydrogen gas and not the entire analysis.

Besides, a pipeline allows long distance travel from 500 and up to 5000 kilometres for a low cost compared to other transportation options. McKinsey, [28],

insists especially on the cost reduction of the pipelines when retrofit is possible which can allow a cost saving of 60 to 90% of greenfield pipeline development. To give an example, capital expenditures (capex) costs would reach [2.2-4.5]million $\$_{/km}$ for a new built onshore transmission including the compression while it would cost approximately the fourth, [0.6-1.2] million $\$_{/km}$ by using retrofit.

More specifically related to the topic of this thesis, a factor between 1.3 and 2.3 higher is usually giving the costs for offshore/subsea pipelines. This can be explained because of the additional challenges and conditions required in this type of environment. Thus, it would give a minimum of [2.86-5.85]million $\$_{/km}$ and a maximum of [5.06-10.35]million $\$_{/km}$ cost range, depending on the multiplicative factor used, for a newly built offshore transmission including the compression systems. Nevertheless, retrofit of the pipes would contribute to a minimum and maximum cost of [0.78-1.56]million $\$_{/km}$ and [1.38-2.76]million $\$_{/km}$ respectively. Those results are summarised in the Figure 14. [28]

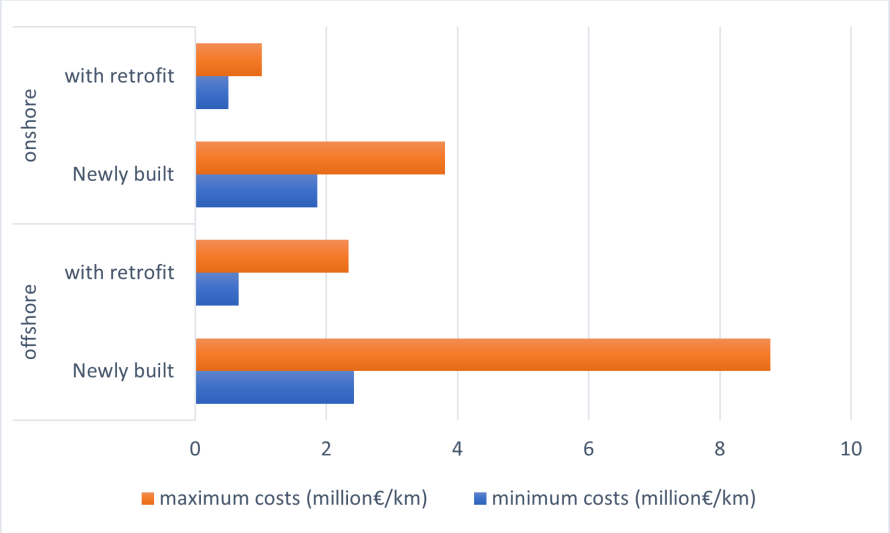

Figure 14: Differences in costs using retrofit for hydrogen pipelines
Source: Hydrogen Council and Mc Kinsey Company [28]
`https://hydrogencouncil.com/wp-content/uploads/2021/02/Hydrogen-Insights-2021.pdf`

To conclude and regarding the strict transport of energy, hydrogen pipelines are more relevant than electricity lines. They are able to move 10 times more energy for the eighth of the cost and by lasting longer in time. As expected, the costs for installation of offshore pipelines are higher than onshore, then, retrofit of these pipes could be a solution to reduce the expenses.

A short price comparison with the two main global energies

In order to understand the more or less expensive production and overall price of hydrogen gas as an energy carrier, a comparison is made with the natural gas price as well as crude oil. This comparison is especially useful for showing that, first, hydrogen keeps to be highly expensive and, second, it is nonsense to have the ambition of replacing natural gas or oil by hydrogen since hydrogen is not an energy, thus, will not solve any energy crisis but could help for energy storage.

Crude oil price

Currently, in Mai 2022, crude oil price is at about **110 USD/Bbl** where Bbl designates the unit *Barrel*. Since the order of magnitude is interesting in this short calculation and also that the price of crude oil is highly unstable, the value ≈ 100 USD/Bbl is chosen. [29]

The unit barrel is defined as follow: [35]

$$\begin{aligned} 1\text{barrel} &= 42 \text{ gallons and,} \\ 1 \text{ gallon}_{\text{crude oil}} &= 3.79 \cdot 10^{-3} m^3 \text{ so,} \\ \implies 1 \text{ barrel} &\approx 0.159 m^3 = 159 l \end{aligned} \tag{32}$$

In order to understand better how to interpret this value, the purpose is to modify it to obtain a volumetric price with the following equations:

$$\begin{aligned} \text{Crude oil} &\approx 100\$ \cdot \text{barrel}^{-1} \text{ (or 110 on the day of calculation)} \\ &= 100 \times (0.159)^{-1} \$ \cdot m^{-3} \\ \implies \text{Crude oil} &\approx \boxed{629\$ \cdot m^{-3}} \text{ (or 692)} = \boxed{0.629\$ \cdot l^{-1}} \text{ (or 0.692)} \end{aligned} \tag{33}$$

The price of crude oil is then in the order of 629\$/m^3 (0.629\$/l).

Natural gas price

The price of natural gas is expressed in another unit which is in USD per million of British Thermal Unit: USD·MMBtu^{-1}. First, changes are required to express the price with the international units which can be a volumetric price as before stated for crude oil. And the value of 10^3Btu·ft^{-3} from [ref] is used for the conversion. [115] [42]

$$
\begin{aligned}
1\text{ft} &= 0.305m \\
10^3\ \text{Btu} \cdot \text{ft}^{-3}_{Nat.gas} &= 10^3\ \text{Btu} \cdot (0.305)^{-3} \cdot m^{-3} \\
&= \left(\frac{10}{0.305}\right)^3 \text{Btu} \cdot m^{-3} \\
1\ \text{MMBtu}_{\text{ Nat.gas}} &= 10^6\ \text{Btu}_{\text{ Nat.gas}} \\
&= 10^6\ \text{Btu} \times \left[\left(\frac{10}{0.305}\right)^3\ \text{Btu} \cdot m^{-3}\right]^{-1} \\
\implies \quad \text{MMBtu}_{\text{Nat.gas}} &= \boxed{3.05^3 m^3}
\end{aligned}
\tag{34}
$$

The price of natural gas in Mai 2022 is around 7.8 USD·MMBtu^{-1} and it is usually under 10 USD·MMBtu^{-1}, thus this last value is the order of magnitudes for the next calculations. And in order to change the volumetric cost (per cubic metre) to a mass cost (per kilogram), the density of natural gas is used with the approximate value $\rho_{\text{ Nat.gas}} \approx 0.8kg \cdot m^{-3}$: [79] [43]

$$
\begin{aligned}
\text{Natural gas} &\approx 10\$ \cdot (\text{MMBtu})^{-1} \\
&= 10\$ \times (3.05^3 m^3)^{-1} \\
\implies \quad \text{Nat.gas} &\approx \boxed{0.3525\$ \cdot m^{-3}} \\
&= 10 \cdot 3.05^{-3}\$ \cdot m^{-3} \times \left(0.8kg \cdot m^{-3}\right)^{-1} \\
\implies \quad \text{Nat.gas} &\approx \boxed{0.44\$ \cdot kg^{-1}}
\end{aligned}
\tag{35}
$$

The price of natural gas is, then, in the order of 0.3525\$/m^3 giving $0.44\$ \cdot kg^{-1}$.

Recent projection on hydrogen price by pipeline transportation

Ultimately, the most recent report (April 2022) used in this thesis, regarding hydrogen and including transportation, estimated a global investment needed in Europe ranging between 80 and 143 billions of euros for 2040. This investment and strategy proposed integrates onshore but also subsea pipelines as well as interconnectors which will connect the different places to offshore energy hubs and possible export areas. This report expressed a range of price for both onshore and offshore applications. Regarding the purpose of the thesis, the following prices for hydrogen transport by offshore pipelines is concluded to reach [0.17 ; 0.32]€·(kg·1000km)$^{-1}$. By comparison, the prices regarding H_2 transport onshore were estimated at [0.11

; 0.21]€·(kg·1000km)$^{-1}$ which corresponds to a difference of about 35% between both situations. By including projections in a close future, 28000 kilometres of pipeline are assumed by 2030 and 53000 kilometres for 2040. As stated above, projections in the future, especially regarding costs, are often unstable but can give a tendency. Here, the study appeared during the writing period of this thesis and it is shown that the number of pipeline would increase fast. Also, it states that this option would be the most cost-effective option regarding large scale applications implying long distance for the transport. [96]

Part IV
Conclusion

Hydrogen is an interesting atom because it represents the lightest element on Mendeleev table and concentrate an important amount of energy. Nevertheless, its production and transportation are very challenging in many ways. The complication is even intensified for liquid hydrogen which needs to be kept under the critical point at a temperature of -240°C and a pressure of 1.3MPa and, that process loses between 30 and 40% of the hydrogen energy content when produced. Therefore, the choice for producing and transporting hydrogen gas is more relevant.

Firstly, for the production of hydrogen via renewable energy sources offshore, using electrolysers is a viable technical way to perform this project. Globally, 2 main technologies called AWE and PEM exist commercially to perform the production of H_2. PEM is more efficient, adaptable and flexible than AWE but the cost is in favour of this last one. And this is basically the same logic when talking about a whole system containing several electrolysers with different configurations: when the technical efficiency and production is clearly improved, the cost is increased. Nevertheless, regardless the cost, it seems that the configuration detailed in Table 3 presents technical characteristics for hydrogen production from an unstable source of wind power very close to a system with a constant power supply.

Secondly, the utilisation of composite pipelines for the hydrogen transportation can definitely solve some problems and should be developed further for future projects. Indeed, hydrogen embrittlement occurring in steel is not of concern anymore and using pipe in composite materials instead of carbon steel will notably reduce both the carbon and energy footprint, especially for GFRP and GRE, see Figure 3. The analysis of the pipes manufactured by the companies introduced as well as the properties of components have been detailed in this thesis. It appears relevant to choose a thermoplastic pipe and wrap it around a reel to minimise the costs and accelerate its installation. Also, the reinforcement of a FRP pipe is usually done by glass fibres but other fibres such as carbon or aramid fibres, integrated in the hydrogen pipe H2T, can also be used creating a different manufacturing costs. The size for the actual H2T pipe and the others few ongoing hydrogen transportation projects intend to utilise a diameter of around 6", so 152mm and they usually last from 20 to 50 years. In addition, they generally resist to pressure between 40 and 80 bars and temperature around 80 °C.

The hydrogen permeability prediction made and shared by the company Strohm, see Figure 8 and 9, allows to draw a conclusion about how to orient parameters for a low permeability rate. Therefore, a thick laminate layer, a thicker liner by increasing the diameter of the pipe, a high pressure and a low temperature are the

main points to reduce the hydrogen permeation.

Thirdly, the production costs are reaching double to triple price from fossil fuel H_2 production, e.g. steam methane reforming (SMR) or coal gasification, to electrolysis of water. Moreover, the production efficiency is higher for SMR than electrolysis. That mainly explains why approximately 95%, including about half for SMR percentage, of the whole H_2 production is done with fossil energies creating 830 million tons of CO_2 emissions each year. To detail further the costs, compression stage reaches from 0.9 to 1.75€·kg^{-1} and a 300-bar compressor costs between 45 000€ to 90 000€. The operational costs represents about 80% of the total hydrogen price. Also, the running utilisation of the system is of importance because an under-use reaching 40% would multiply the capital expenses by a factor 2.5 and slightly increase the operational ones. The plant size should also be designed big enough since a change from 10 to 100MW would decrease the cost by about 30% per MW due to the economy of scale as already explained for the size cost per MW of the stacks, in Figure 11. Finally, all those points clarify why *green hydrogen* is so costly with a range of [2.5 ; 5.5]€·kg^{-1} compared to *blue/grey hydrogen* made from fossil fuel energies at [1.5 ; 2]€·kg^{-1}.

Fourth, the transport of hydrogen by pipeline is also a part of the cost and reach between 0.139 to 0.261€·kg^{-1} (for a demand equal or above $5{\cdot}10^9$m^3·year^{-1}). In comparison, tube trailers transport, mainly for small quantities, costs between [0.6 ; 2.2]·kg^{-1} over 100 kilometres, therefore, pipelines appear highly suitable economically on condition that a minimum demand is assured. The demand has been estimated by a number of 9 or 50 pipelines for 1 million persons with a diameter of 8 (203mm) or 4 (102mm) inches respectively when the pressure is set at 6.9 MPa (69 bars). For example, the calculations for the city of Stavanger, in Norway, estimated the need for 3 or 12 pipes, respectively. This number can be lowered by increasing the pressure allowed. Beside those H_2 transport costs, the price of a FRP pipeline is globally comprised between 32$ and 46$ per meter and up to 66$ per meter for difficult conditions for the installation phase.

Ultimately, the strategy of establishing a hydrogen project, network or even society has to really take into account all the characteristics linked to a hydrogen production and transportation. For example, it has been shown that the electricity consumption to produce 1 kilogram of hydrogen is equivalent to a weekly electrical consumption for an average inhabitant worldwide. That brings the important question whether the electricity is better to be used for hydrogen production or for electricity uses directly. To finish, the most important points to remember for deciding a hydrogen strategy are:

- Hydrogen is not an energy source, it is an energy carrier.

- Before thinking about new possible ways of using *green hydrogen*, it would be more efficient to try replacing the already existing 95% of hydrogen produced each year for industries via fossil fuel; also, producing *green hydrogen* for steel industry seems highly relevant, feasible and efficient to cut CO_2 emissions, see [71].
- Production and transport of *green hydrogen* is the ideal solution regarding technical data and the environmental problem, however, the economic system makes it 2 to 3 times more expensive than the one produced by emitting GHG emissions.
- Regarding only energy transport, hydrogen pipelines move 10 times more energy for eighth of the electricity lines costs; the offshore H_2 transport costs by pipe would range $[0.17\ ;\ 0.32]€\cdot(kg\cdot 1000km)^{-1}$.
- Thus, when a project is required and hydrogen needs to be transported, FRP pipelines constitute the best option by reducing the carbon and energy footprint, the costs, the travel time and by increasing the efficiency and quantity transported.

Recommendations for further future work

- Based on the information expressed and presented in this thesis, analysing an actual ongoing project of reinforced pipeline to transport hydrogen with design simulation and/or economic estimation and calculation for the project costs. Then, comparing the results with the information and ranges from this master's thesis.

- Analysing in detail the future hydrogen standards and performing simulations or experiences with these hydrogen regulations regarding FRP pipes.

- It could be interesting as well to perform a detailed paper analysing different strategies and ways to perform a reduction in GHG by using H_2 and then concluding by suggesting with order of priority which option would be the most efficient to decrease CO_2 emissions for example.

References

[1] NOV (company). *Bondstrand 2400 Series Product Data: Glassfiber Reinforced Epoxy (GRE) pipe systems for Marine and Offshore services*. Sept. 2014. URL: https://www.nov.com/-/media/nov/files/misc/bondstrand-composite-solutions/bondstrand-2400-series-product-data-sheet.pdf.

[2] NOV (company). *Bondstrand 2400 Series: Product Data - Glassfiber Reinforced Epoxy (GRE) pipe systems (document shared by the company)*. Apr. 2019.

[3] Strohm (Company). *Preliminary Data Sheet: 4.0" TCP Flowline with Weight Coating - 50 bar*. Document shared by the company by email. 2021.

[4] Strohm (Company). *TCP Flowlines*. Strohm. 2021. URL: https://strohm.eu/tcp-flowlines.

[5] Z. Abdin, C. J. Webb, and E. MacA. Gray. "Modelling and simulation of a proton exchange membrane (PEM) electrolyser cell". In: *International Journal of Hydrogen Energy* 40.39 (Oct. 19, 2015), pp. 13243–13257. ISSN: 0360-3199. DOI: 10.1016/j.ijhydene.2015.07.129. URL: https://doi.org/10.1016/j.ijhydene.2015.07.129.

[6] Jamal Ahmad. *Machining of Polymer Composites*. 1st ed. Springer New York, NY, 2009. 315 pp. ISBN: 978-0-387-68619-6. URL: https://doi.org/10.1007/978-0-387-68619-6.

[7] AirLiquide. *How is hydrogen stored ?* Air Liquide Energies. June 16, 2017. URL: https://energies.airliquide.com/resources-planet-hydrogen/how-hydrogen-stored.

[8] Fatima Ghassan Alabtah, Elsadig Mahdi, and Faysal Fayez Eliyan. "The use of fiber reinforced polymeric composites in pipelines: A review". In: *Composite Structures* 276 (Nov. 15, 2021), p. 114595. ISSN: 0263-8223. DOI: 10.1016/j.compstruct.2021.114595. URL: https://doi.org/10.1016/j.compstruct.2021.114595.

[9] Muhammad Haider Ali Khan et al. "A framework for assessing economics of blue hydrogen production from steam methane reforming using carbon capture storage & utilisation". In: *International Journal of Hydrogen Energy* 46.44 (June 28, 2021), pp. 22685–22706. ISSN: 0360-3199. DOI: 10.1016/j.ijhydene.2021.04.104. URL: https://doi.org/10.1016/j.ijhydene.2021.04.104.

[10] R. A. Ash. “9 - Vehicle armor”. In: *Lightweight Ballistic Composites (Second Edition): Military and Law-Enforcement Applications*. Ed. by Ashok Bhatnagar. Woodhead Publishing Series in Composites Science and Engineering. Woodhead Publishing, 2016, pp. 285–309. ISBN: 978-0-08-100406-7. DOI: 10.1016/B978-0-08-100406-7.00009-X. URL: https://doi.org/10.1016/B978-0-08-100406-7.00009-X.

[11] Eylem Asmatulu, Janet Twomey, and Michael Overcash. “Recycling of fiber-reinforced composites and direct structural composite recycling concept”. In: *Journal of Composite Materials* 48.5 (Mar. 1, 2014). Publisher: SAGE Publications Ltd STM, pp. 593–608. ISSN: 0021-9983. DOI: 10.1177/0021998313476325. URL: https://doi.org/10.1177/0021998313476325.

[12] ASME. *B31.12 - Hydrogen Piping & Pipelines*. ASME: The American Society of Mechanical Engineers, 2020, p. 280. URL: https://www.asme.org/codes-standards/find-codes-standards/b31-12-hydrogen-piping-pipelines.

[13] ASME. *B31.3 - Process Piping*. ISBN: 9780791873663. 2021, p. 544. URL: https://www.asme.org/codes-standards/find-codes-standards/b31-3-process-piping.

[14] W. R. Aykroyd. “CHAPTER VIII - THE HONOURABLE HENRY CAVENDISH”. In: *Three Philosophers*. Ed. by W. R. Aykroyd. Butterworth-Heinemann, 2014, pp. 71–78. ISBN: 978-1-4831-6697-1. DOI: 10.1016/B978-1-4831-6697-1.50014-4. URL: https://doi.org/10.1016/B978-1-4831-6697-1.50014-4.

[15] Alan A. Baker and Murray L. Scott. *Composite Materials for Aircraft Structures*. 3rd ed. AIAA Education Series. American Institute of Aeronautics and Astronautics, Inc., Sept. 30, 2016. 700 pp. ISBN: 978-1-62410-629-3. DOI: 10.2514/5.9781624103261.0000.0000. URL: https://doi.org/10.2514/4.103261.

[16] B. Bensmann et al. “Energetic evaluation of high pressure PEM electrolyzer systems for intermediate storage of renewable energies”. In: *Electrochimica Acta*. ELECTROCHEMISTRY FOR ADVANCED MATERIALS, TECHNOLOGIES AND INSTRUMENTATION 110 (Nov. 2013), pp. 570–580. ISSN: 0013-4686. DOI: 10.1016/j.electacta.2013.05.102. URL: https://doi.org/10.1016/j.electacta.2013.05.102.

[17] Arthur P. Boresi. “Chapter 4: Three-Dimensional Equations of Elasticity”. In: *Elasticity in engineering mechanics*. In collab. with K. P. Chong and J.D. Lee. 3rd ed. New York: John Wiley & Sons, Inc., 2011, pp. 226–364. ISBN: 978-0-470-40255-9. DOI: 10.1002/9780470950005. URL: https://onlinelibrary.wiley.com/doi/book/10.1002/9780470950005.

[18] BP. *BP Statistical Review of World Energy*. 2015. URL: http://large.stanford.edu/courses/2015/ph240/zerkalov1/docs/bp2015.pdf.

[19] Alexander Buttler and Hartmut Spliethoff. "Current status of water electrolysis for energy storage, grid balancing and sector coupling via power-to-gas and power-to-liquids: A review". In: *Renewable and Sustainable Energy Reviews* 82 (Part 3 Feb. 2018), pp. 2440–2454. ISSN: 1364-0321. DOI: 10.1016/j.rser.2017.09.003. URL: https://doi.org/10.1016/j.rser.2017.09.003.

[20] Q. Cai et al. "The Effects of Operating Conditions on the Performance of a Solid Oxide Steam Electrolyser: A Model-Based Study". In: *Fuel Cells* 10.6 (Nov. 2010). Publisher: John Wiley & Sons, Ltd, pp. 1114–1128. ISSN: 1615-6846. DOI: 10.1002/fuce.200900211. URL: https://doi-org.ezproxy.uis.no/10.1002/fuce.200900211.

[21] F. C. Campbell. *Structural composite materials*. Ed. by ASM International. 1st ed. A S M International, 2010. 621 pp. ISBN: 978-1-61503-140-5.

[22] P. L. Chang, C. W. Hsu, and C. M. Hsiung. "Functional assessment for large-scale wind-hydrogen energy integration electricity supply system in Taiwan". In: *2013 IEEE International Conference on Industrial Engineering and Engineering Management*. 2013 IEEE International Conference on Industrial Engineering and Engineering Management. ISSN: 2157-362X. Bangkok, Thailand: IEEE, Dec. 2013, pp. 1283–1287. ISBN: 978-1-4799-0986-5. DOI: 10.1109/IEEM.2013.6962617. URL: https://ieeexplore.ieee.org/document/6962617.

[23] Tan-Ping Chen. *Final Report - Hydrogen Delivery Infrastructure Options Analysis*. DOE Award Number: DE-FG36-05GO15032 Consortium/teaming Partners: Air Liquide, Chevron Technology Venture, Gas Technology Institute, NREL, Tiax, ANL. Nexant The Power of Experience, 2006, p. 349. URL: https://www.energy.gov/sites/prod/files/2014/03/f11/delivery_infrastructure_analysis.pdf.

[24] British Columbia. *Hydrogen study, Final report*. June 2019. URL: https://www2.gov.bc.ca/assets/gov/government/ministries-organizations/zen-bcbn-hydrogen-study-final-v6.pdf.

[25] Fiber Glass Systems NOV Completion and Production Solutions. *High Pressure Fiberglass Line Pipe Product Guide: For Oil & Gas Applications*. June 2016. URL: https://www.nov.com/-/media/nov/files/products/caps/fiber-glass-systems/star-fiberglass-pipe/high-pressure-fiberglass-line-pipe-product-guide-brochure.pdf.

[26] Nathanial Cooper et al. “A framework for the design & operation of a large-scale wind-powered hydrogen electrolyzer hub”. In: *International Journal of Hydrogen Energy* 47.14 (Feb. 15, 2022), pp. 8671–8686. ISSN: 0360-3199. DOI: 10.1016/j.ijhydene.2021.12.225. URL: https://doi.org/10.1016/j.ijhydene.2021.12.225.

[27] Hydrogen Council. “Hydrogen Council highlights investment”. In: *Fuel Cells Bulletin* 2021.3 (Mar. 1, 2021). Publisher: Elsevier, pp. 8–8. ISSN: 1464-2859. DOI: 10.1016/S1464-2859(21)00140-1. URL: https://doi.org/10.1016/S1464-2859(21)00140-1.

[28] Hydrogen Council and Mc Kinsey Company. *Hydrogen Insights: A perspective on hydrogen investment, market development and cost competitiveness*. URL of the blog post: https://hydrogencouncil.com/en/hydrogen-insights-2021/. Feb. 2021. URL: https://hydrogencouncil.com/wp-content/uploads/2021/02/Hydrogen-Insights-2021.pdf.

[29] *Crude oil - 2022 Data - 1983-2021 Historical*. Trading Economics. 2022. URL: https://tradingeconomics.com/commodity/crude-oil.

[30] Deborah D.L. Chung. *Composite Materials _ Science and Applications*. 2nd ed. Engineering Materials and Processes. Springer London, 2010. 371 pp. ISBN: 978-1-84882-831-5. URL: https://doi.org/10.1007/978-1-84882-831-5.

[31] D. Dixit et al. “6 - Lightweight composite materials processing”. In: *Lightweight Ballistic Composites (Second Edition)*. Ed. by Ashok Bhatnagar. Woodhead Publishing Series in Composites Science and Engineering. Woodhead Publishing, 2016, pp. 157–216. ISBN: 978-0-08-100406-7. DOI: 10.1016/B978-0-08-100406-7.00006-4. URL: https://doi.org/10.1016/B978-0-08-100406-7.00006-4.

[32] Aleksendric Dragan and Carlone Pierpaolo. *Soft Computing in the Design and Manufacturing of Composite Materials _ Applications to Brake Friction and Thermoset Matrix Composites*. Elsevier Science & Technology, Feb. 17, 2015. 319 pp. ISBN: 978-1-78242-180-1. URL: https://ebookcentral-proquest-com.ezproxy.uis.no/lib/uisbib/detail.action?docID=4003154.

[33] EIA. *International - U.S. Energy Information Administration*. Indepedent Statistics and Analysis - U.S. Energy Information Administration. 2019. URL: https://www.eia.gov/international/data/world/electricity/electricity-consumption?pd=2&p=0000002&u=0&f=A&v=mapbubble&a=-&i=none&vo=value&t=C&g=00000000000000000000000000000000000000000000000001&l=249-ruvvvvvfvtvnvv1vrvvvvfvvvvvvfvvvou20evvvvvvvvvvnvvvs0008&s=315532800000&e=1546300800000&vb=33&ev=true.

[34] ElectricityMap. *Live 24/7 CO_2 emissions of electricity consumption*. URL: http://electricitymap.tmrow.co.

[35] *Energy Content in common Energy Sources*. The Engineering Toolbox. 2005. URL: https://www.engineeringtoolbox.com/energy-content-d_868.html.

[36] National Research Council {and} National Academy of Engineering. *The Hydrogen Economy: Opportunities, Costs, Barriers, and R&D Needs*. Washington, DC: The National Academies Press, 2004. 256 pp. ISBN: 978-0-309-09163-3. DOI: 10.17226/10922. URL: https://doi.org/10.17226/10922.

[37] Gregor Erbach and Liselotte Jensen. "EU hydrogen policy: Hydrogen as an energy carrier for a climate-neutral economy". In: *European Parliament*. EU Hydrogen policy (Apr. 2021), pp. 1–8. URL: https://www.europarl.europa.eu/RegData/etudes/BRIE/2021/689332/EPRS_BRI(2021)689332_EN.pdf.

[38] HFP europe. *European Hydrogen & Fuel Cell Technology Platform: Stractegic Research Agenda*. July 2005. URL: https://www.fch.europa.eu/sites/default/files/documents/hfp-sra004_v9-2004_sra-report-final_22jul2005.pdf.

[39] European Commission - Directorate - General for Energy and Transport et al. *European energy and transport: trends to 2030*. In collab. with ESAP SA et al. OCLC: 630827053. Office for Official Publications of the European Communities, Apr. 2008. ISBN: 978-92-79-07620-6. URL: https://ec.europa.eu/energy/sites/ener/files/documents/trends_to_2030_update_2007.pdf.

[40] *Exports of Norwegian oil and gas*. Norwegian Petroleum. Mar. 24, 2021. URL: https://www.norskpetroleum.no/en/production-and-exports/exports-of-oil-and-gas/.

[41] Future Pipe Industries FPI. *High Pressure Spoolable Pipe: Flexstrong*. FX-CD-001 v6.0. URL: https://futurepipe.com/wp-content/uploads/2021/07/FlexstrongFlyer.pdf.

[42] *Fuel Gases - Heating Values*. The Engineering Toolbox. 2005. URL: https://www.engineeringtoolbox.com/heating-values-fuel-gases-d_823.html.

[43] *Gases - Densities*. The Engineering Toolbox. 2003. URL: https://www.engineeringtoolbox.com/gas-density-d_158.html.

[44] R. Gerboni. "11 - Introduction to hydrogen transportation". In: *Compendium of Hydrogen Energy*. Ed. by Ram B. Gupta, Angelo Basile, and T. Nejat Veziroğlu. Vol. 2. Hydrogen Storage, Transportation and Infrastructure vols. Woodhead Publishing Series in Energy. Woodhead Publishing, 2016, pp. 283–299. ISBN: 978-1-78242-362-1. DOI: 10.1016/B978-1-78242-362-1.00011-0. URL: https://doi.org/10.1016/B978-1-78242-362-1.00011-0.

[45] A. Giaconia. "10 - Thermochemical production of hydrogen". In: *Advances in Hydrogen Production, Storage and Distribution*. Ed. by Angelo Basile and Adolfo Iulianelli. Woodhead Publishing, 2014, pp. 263–280. ISBN: 978-0-85709-768-2. DOI: 10.1533/9780857097736.2.263. URL: https://doi.org/10.1533/9780857097736.2.263.

[46] Victor Giurgiutiu. "Chapter 2 - Fundamentals of Aerospace Composite Materials". In: *Structural Health Monitoring of Aerospace Composites*. Ed. by Victor Giurgiutiu. Oxford: Academic Press, Jan. 1, 2016, pp. 25–65. ISBN: 978-0-12-409605-9. DOI: 10.1016/B978-0-12-409605-9.00002-7. URL: https://www.sciencedirect.com/science/article/pii/B9780124096059000027.

[47] Syed Tauseef Hassan et al. "Is nuclear energy a better alternative for mitigating CO2 emissions in BRICS countries? An empirical analysis". In: *Nuclear Engineering and Technology* 52.12 (Dec. 2020), pp. 2969–2974. ISSN: 1738-5733. DOI: 10.1016/j.net.2020.05.016. URL: https://doi.org/10.1016/j.net.2020.05.016.

[48] Jan Fredrik Helgaker. *Transportation of hydrogen gas in offshore pipelines: H2Pipe*. DNV. URL: https://www.dnv.com/article/transportation-of-hydrogen-gas-in-offshore-pipelines-h2pipe-213006.

[49] Robin Findlay Hendry. "Elements". In: *Philosophy of Chemistry*. Ed. by Andrea I. Woody, Robin Findlay Hendry, and Paul Needham. Vol. 6. Handbook of the Philosophy of Science. Amsterdam: North-Holland, 2012, pp. 255–269. DOI: 10.1016/B978-0-444-51675-6.50020-7. URL: https://doi.org/10.1016/B978-0-444-51675-6.50020-7.

[50] Suong V. Hoa. *Principles of the Manufacturing of Composite Materials*. 2nd ed. DEStech Publications, Inc, 2017. 445 pp. ISBN: 978-1-60595-421-9. URL: https://www.destechpub.com/product/principles-manufacturing-composite-materials-second-edition/.

[51] BC Hydro. *General Service Business Rates*. BC Hydro Power Smart. 2021. URL: https://www.bchydro.com/accounts-billing/rates-energy-use/electricity-rates/business-rates.html.

[52] *Hydrogen element (NIST)*. NIST: National Institute of Standards and Technology; U.S. Department of Commerce. Publisher: National Institute of Standards and Technology. URL: https://webbook.nist.gov/cgi/cbook.cgi?ID=1333-74-0&Units=SI.

[53] *Hydrogen element from database ChemicalBook (element 1333-74-0)*. Chemical Book. URL: https://www.chemicalbook.com/ProductChemicalPropertiesCB7686195_EN.htm.

[54] *Hydrogen properties from database ChemicalBook (element 1333-74-0)*. Chemical Book. URL: https://www.chemicalbook.com/CASEN_1333-74-0.htm.

[55] The World Bank IBRD - IDA. *Population, total | Data*. The World Bank. 2019. URL: https://data.worldbank.org/indicator/SP.POP.TOTL?end=2019&start=1960.

[56] Hicham Idriss. "Hydrogen production from water: past and present". In: *Current Opinion in Chemical Engineering*. Reaction Engineering and Catalysis * Nanotechnology: Nanofluidics and Microfluidics 29 (Sept. 2020), pp. 74–82. ISSN: 2211-3398. DOI: 10.1016/j.coche.2020.05.009. URL: https://doi.org/10.1016/j.coche.2020.05.009.

[57] IEA. *Global Hydrogen Review 2021 – Analysis*. Technology report. IEA, Oct. 2021, p. 223. URL: https://www.iea.org/reports/global-hydrogen-review-2021.

[58] IEA. *The Future of Hydrogen Seizing today's opportunities*. International Energy Agency, 2019, p. 203. URL: https://www.iea.org/reports/the-future-of-hydrogen.

[59] ISPT. *Hydrohub GigaWatt scale electrolyser*. ISPT - Institute for Sustainable Process Technology. Nov. 1, 2018. URL: https://ispt.eu/projects/hydrohub-gigawatt/.

[60] *IUPAC Periodic Table of Elements*. IUPAC | International Union of Pure and Applied Chemistry. In collab. with Jan Reedijk et al. Dec. 1, 2018. URL: https://iupac.org/what-we-do/periodic-table-of-elements/.

[61] Jean-Marc Jancovici. *Peak oil? Did it already happen somewhere?* Dec. 1, 2015. URL: https://jancovici.com/en/energy-transition/oil/peak-oil-did-it-already-happen-somewhere/.

[62] Jean-Marc Jancovici. *Will technology save us from Climate Change ? MIT Media Lab*. MAHB. Apr. 5, 2021. URL: https://mahb.stanford.edu/library-item/jean-marc-jancovici-will-technology-save-us-from-climate-change-mit-media-lab/.

[63] Malte Jansen et al. “Offshore wind competitiveness in mature markets without subsidy”. In: *Nature Energy* 5.8 (Aug. 2020). Number: 8 Publisher: Nature Publishing Group, pp. 614–622. ISSN: 2058-7546. DOI: 10.1038/s41560-020-0661-2. URL: https://doi.org/10.1038/s41560-020-0661-2.

[64] Sankar Karuppannan Gopalraj and Timo Kärki. “A review on the recycling of waste carbon fibre/glass fibre-reinforced composites: fibre recovery, properties and life-cycle analysis”. In: *SN Applied Sciences* 2.3 (Feb. 18, 2020), p. 433. ISSN: 2523-3971. DOI: 10.1007/s42452-020-2195-4. URL: https://doi.org/10.1007/s42452-020-2195-4.

[65] Atsushi Kurosawa. “Long term nuclear power role under CO2 emission constraint”. In: *Progress in Nuclear Energy*. Global Environment and Nuclear Energy Systems-3 Proceedings of the Third International Symposium 37.1 (2000), pp. 101–106. ISSN: 0149-1970. DOI: 10.1016/S0149-1970(00)00032-9. URL: https://doi.org/10.1016/S0149-1970(00)00032-9.

[66] Stelios Kyriakides and Edmundo Corona. *Mechanics of Offshore Pipelines - Volume 1: Buckling and Collapse*. Ed. by Stelios Kyriakides and Edmundo Corona. Oxford: Elsevier Science Ltd, 2007. ISBN: 978-0-08-046732-0. DOI: 10.1016/B978-0-08-046732-0.X5000-4. URL: https://doi.org/10.1016/B978-0-08-046732-0.X5000-4.

[67] Boreum Lee et al. “Economic evaluation with sensitivity and profitability analysis for hydrogen production from water electrolysis in Korea”. In: *International Journal of Hydrogen Energy* 42.10 (Mar. 9, 2017), pp. 6462–6471. ISSN: 0360-3199. DOI: 10.1016/j.ijhydene.2016.12.153. URL: https://doi.org/10.1016/j.ijhydene.2016.12.153.

[68] Sergei Georgievich Lekhnitskii. *Theory of Elasticity of an Anisotropic Elastic Body*. Ed. by Julius J. Brandstatter. Holden-Day, 1963. 404 pp. URL: https://books.google.no/books?id=EcpEAAAAIAAJ.

[69] Binlin Li and Nils Haneklaus. “Reducing CO2 emissions in G7 countries: The role of clean energy consumption, trade openness and urbanization”. In: *Energy Reports*. 2021 International Conference on New Energy and Power Engineering 8 (July 2022), pp. 704–713. ISSN: 2352-4847. DOI: 10.1016/j.egyr.2022.01.238. URL: https://doi.org/10.1016/j.egyr.2022.01.238.

[70] Weihua Liu et al. “Chapter Two - Radiation Technology Application in High-Performance Fibers and Functional Textiles”. In: *Radiation Technology for Advanced Materials: From Basic to Modern Applications*. Ed. by Guozhong Wu, Maolin Zhai, and Mozhen Wang. Academic Press, 2019,

pp. 13–73. ISBN: 978-0-12-814017-8. DOI: 10.1016/B978-0-12-814017-8.00002-0. URL: https://doi.org/10.1016/B978-0-12-814017-8.00002-0.

[71] Wenguo Liu et al. "The production and application of hydrogen in steel industry". In: *International Journal of Hydrogen Energy* 46.17 (Mar. 8, 2021), pp. 10548–10569. ISSN: 0360-3199. DOI: 10.1016/j.ijhydene.2020.12.123. URL: https://doi.org/10.1016/j.ijhydene.2020.12.123.

[72] Rodica Loisel et al. "Economic evaluation of hybrid off-shore wind power and hydrogen storage system". In: *International Journal of Hydrogen Energy* 40.21 (June 8, 2015), pp. 6727–6739. ISSN: 0360-3199. DOI: 10.1016/j.ijhydene.2015.03.117. URL: https://doi.org/10.1016/j.ijhydene.2015.03.117.

[73] Jessica M. Maita et al. "Atomic arrangement and mechanical properties of chemical-vapor-deposited amorphous boron". In: *Materials & Design* 193 (Aug. 2020), p. 108856. ISSN: 0264-1275. DOI: 10.1016/j.matdes.2020.108856. URL: https://doi.org/10.1016/j.matdes.2020.108856.

[74] P. K. Mallick. *Fiber-Reinforced Composites: Materials, Manufacturing, and Design, Third Edition*. 3rd ed. Boca Raton: CRC Press, Nov. 19, 2007. 638 pp. ISBN: 978-0-429-12206-4. DOI: 10.1201/9781420005981. URL: https://doi.org/10.1201/9781420005981.

[75] Shigenori Maruyama et al. "Nine requirements for the origin of Earth's life: Not at the hydrothermal vent, but in a nuclear geyser system". In: *Geoscience Frontiers* 10.4 (July 2019), pp. 1337–1357. ISSN: 1674-9871. DOI: 10.1016/j.gsf.2018.09.011. URL: https://www.sciencedirect.com/science/article/pii/S1674987118302123.

[76] Bethany Middleton. "3 - Composites: Manufacture and Application". In: *Design and Manufacture of Plastic Components for Multifunctionality: Structural Composites, Injection Molding, and 3D Printing*. Ed. by Vannessa Goodship, Bethany Middleton, and Ruth Cherrington. Oxford: William Andrew Publishing, 2016, pp. 53–101. ISBN: 978-0-323-34061-8. DOI: 10.1016/B978-0-323-34061-8.00003-X. URL: https://doi.org/10.1016/B978-0-323-34061-8.00003-X.

[77] Nigel Mills, Mike Jenkins, and Stephen Kukureka. "Chapter 1 - Introduction". In: *Plastics (Fourth Edition) - Microstructure and Engineering Applications*. Ed. by Nigel Mills, Mike Jenkins, and Stephen Kukureka. Butterworth-Heinemann, 2020, pp. 1–11. ISBN: 978-0-08-102499-7. DOI: 10.1016/B978-0-08-102499-7.00001-1. URL: https://doi.org/10.1016/B978-0-08-102499-7.00001-1.

[78] F. Mueller-Langer et al. “Techno-economic assessment of hydrogen production processes for the hydrogen economy for the short and medium term”. In: *International Journal of Hydrogen Energy*. TMS06: Symposium on Materials in Clean Power Systems 32.16 (Nov. 2007), pp. 3797–3810. ISSN: 0360-3199. DOI: 10.1016/j.ijhydene.2007.05.027. URL: https://doi.org/10.1016/j.ijhydene.2007.05.027.

[79] *Natural gas - 2022 Data - 1990-2021 Historical*. 2022. URL: https://tradingeconomics.com/commodity/natural-gas.

[80] Luigi Nicolais, Michele Meo, and Eva Milella, eds. *Composite Materials _ A Vision for the Future*. 1st ed. London: Springer, 2011. 218 pp. ISBN: 978-0-85729-166-0. DOI: 10.1007/978-0-85729-166-0. URL: https://doi-org.ezproxy.uis.no/10.1007/978-0-85729-166-0.

[81] NOV. *Bondstrand Fiberglass Pipe*. NOV. URL: https://www.nov.com/products/bondstrand-fiberglass-pipe.

[82] NOV. *Fiberspar Spoolable Fiberglass Pipe*. nov.com. URL: https://www.nov.com/products/fiberspar-spoolable-fiberglass-pipe.

[83] Hydrogen {and} Fuel Cell Technologies Office. *Hydrogen Production: Electrolysis*. U.S. Department of Energy: Office of Energy Efficiency & Renewable Energy. URL: https://www.energy.gov/eere/fuelcells/hydrogen-production-electrolysis.

[84] J Oliveira. *Technical Note TN741: Hydrogen permeation of EGF/PE TCP*. In collab. with A Paternoster and F Janssen. Document shared by the company by email. June 29, 2021.

[85] Gabriel David Oreggioni et al. “Climate change in a changing world: Socioeconomic and technological transitions, regulatory frameworks and trends on global greenhouse gas emissions from EDGAR v.5.0”. In: *Global Environmental Change* 70 (Sept. 2021), p. 102350. ISSN: 0959-3780. DOI: 10.1016/j.gloenvcha.2021.102350. URL: https://www.sciencedirect.com/science/article/pii/S0959378021001291.

[86] Michael P. Paidoussis. *FLuid-Structures and Axial Flow: Slender Structures and Axial Flow*. 2nd ed. Vol. 1. Academic Press, 2014. ISBN: 978-0-12-397312-2. URL: https://doi.org/10.1016/C2011-0-08057-2.

[87] Dimitrios G. Pavlou. *Composite Materials in Piping Applications: Design, Analysis and Optimization of Subsea and Onshore Pipelines from FRP Materials*. Lancaster, Pa: DEStech Publications, Inc, 2013. 416 pp. ISBN: 978-1-60595-029-7. URL: https://www.destechpub.com/product/composite-materials-in-piping-applications/.

[88] Future Pipe. *Flexstrong: An FPI Product*. URL: https://flexstrong.com/.

[89] *Pipe Data Sheet: Bondstrand 5000/5000C Product Data (Severly Corrosive Industrial Service and Oxidizing Acids)*. 2022. URL: https://www.nov.com/-/media/nov/files/products/caps/fiber-glass-systems/bondstrand-fiberglass-pipe/pipe-data-sheet-bondstrand-5000-5000c-product-data.pdf.

[90] Abdulla Rahil, Rupert Gammon, and Neil Brown. "Flexible operation of electrolyser at the garage forecourt to support grid balancing and exploitation of hydrogen as a clean fuel". In: *Research in Transportation Economics* 70 (Oct. 2018), pp. 125–138. ISSN: 0739-8859. DOI: 10.1016/j.retrec.2017.12.001.

[91] Hayder A. Rasheed and Spyros A. Karamanos. "Stability of tubes and pipelines". In: *Buckling and Postbuckling Structures*. Vol. Volume 1. Computational and Experimental Methods in Structures Volume 1. IMPERIAL COLLEGE PRESS AND DISTRIBUTED BY WORLD SCIENTIFIC PUBLISHING CO., 2008, pp. 259–307. ISBN: 978-1-86094-794-0. DOI: 10.1142/9781848162303_0008. URL: https://doi.org/10.1142/9781848162303_0008.

[92] Sumant (Sumant Shreechandra) Raykar. "Analysis of energy use and carbon emissions from automobile manufacturing". Accepted: 2015-12-03T20:53:19Z. Thesis. Massachusetts Institute of Technology, June 2015. 184 pp. URL: http://hdl.handle.net/1721.1/100098.

[93] J. N. Reddy. "Chapter 1: Equations of Anisotropic Elasticity, Virtual Work Principles, and Variational Methods". In: *Mechanics of Laminated Composite Plates and Shells: Theory and Analysis, Second Edition*. 2nd ed. CRC Press, 2003, pp. 1–80. ISBN: 978-0-8493-1592-3. URL: https://www.routledge.com/Mechanics-of-Laminated-Composite-Plates-and-Shells-Theory-and-Analysis/Reddy/p/book/9780849315923.

[94] J. N. Reddy. *Mechanics of Laminated Composite Plates and Shells: Theory and Analysis*. 2nd ed. Boca Raton: CRC Press, Nov. 24, 2003. 858 pp. ISBN: 978-0-429-21069-3. DOI: 10.1201/b12409. URL: https://doi.org/10.1201/b12409.

[95] *Renewables.ninja*. URL: https://www.renewables.ninja/.

[96] Rik van Rossum et al. *The European Hydrogen Backbone (EHB) initiative | report*. Additional URL: https://ehb.eu/. The Netherlands, Apr. 2022. URL: https://ehb.eu/files/downloads/ehb-report-220428-17h00-interactive-1.pdf.

[97] Svein Sævik and Naiquan Ye. *Aspects of Design and Analysis of Offshore Pipelines and Flexibles*. 1st ed. Southwest Jiaotong University Press, Jan. 1, 2016. 293 pp. ISBN: 978-7-5643-4466-5. URL: https://www.sintef.no/en/publications/publication/1338979/.

[98] Arash E. Samani et al. "Grid balancing with a large-scale electrolyser providing primary reserve". In: *IET Renewable Power Generation* 14.16 (Nov. 29, 2020). _eprint: https://onlinelibrary.wiley.com/doi/pdf/10.1049/iet-rpg.2020.0453, pp. 3070–3078. ISSN: 1752-1424. DOI: 10.1049/iet-rpg.2020.0453. URL: https://doi.org/10.1049/iet-rpg.2020.0453.

[99] O. Schmidt et al. "Future cost and performance of water electrolysis: An expert elicitation study". In: *International Journal of Hydrogen Energy* 42.52 (Dec. 28, 2017), pp. 30470–30492. ISSN: 0360-3199. DOI: 10.1016/j.ijhydene.2017.10.045. URL: https://doi.org/10.1016/j.ijhydene.2017.10.045.

[100] Derick Scott. *Advanced Materials for Water Handling: Composites and Thermoplastics*. Ed. by Derick Scott. Oxford: Elsevier Science, 2000. ISBN: 978-1-85617-350-6. DOI: 10.1016/B978-185617350-6/50000-1. URL: https://doi.org/10.1016/B978-1-85617-350-6.X5000-2.

[101] Groningen Seaports. *Nobian and GIG join forces to launch leading green hydrogen company HyCC*. Groningen Seaports. Dec. 16, 2021. URL: https://www.groningen-seaports.com/en/nieuws/nobian-and-gig-join-forces-to-launch-leading-green-hydrogen-company-hycc/.

[102] SSB: Statistisk sentralbyrå and Statbank. *Population and land area in urban settlements*. SSB. Oct. 26, 2021. URL: https://www.ssb.no/en/befolkning/folketall/statistikk/tettsteders-befolkning-og-areal.

[103] Islam Shyha and Dehong Huo, eds. *Advances in Machining of Composite Materials: Conventional and Non-conventional Processes*. 1st ed. Engineering Materials. Cham: Springer International Publishing, 2021. 552 pp. ISBN: 978-3-030-71438-3. DOI: 10.1007/978-3-030-71438-3. URL: https://doi-org.ezproxy.uis.no/10.1007/978-3-030-71438-3.

[104] Islam Shyha, Dehong Huo, and J. Paulo Davim. "Introduction". In: *Advances in Machining of Composite Materials: Conventional and Non-conventional Processes*. Ed. by Islam Shyha and Dehong Huo. Engineering Materials. Cham: Springer International Publishing, 2021, pp. 1–13. ISBN: 978-3-030-71438-3. DOI: 10.1007/978-3-030-71438-3_1. URL: https://doi.org/10.1007/978-3-030-71438-3_1.

[105] B Smith et al. “V.A.2 New Materials for Hydrogen Pipelines”. In: *DOE Hydrogen Program*. FY 2005 Progress Report (2005), p. 7. URL: https://www.hydrogen.energy.gov/pdfs/progress05/v_a_2_smith.pdf.

[106] SoluForce. *SoluForce General Brochure: Advanced flexible pipeline systems for oil, gas and water*. Oct. 2020. URL: https://www.soluforce.com/content/dam/pipelife/soluforce/marketing/general/brochures/soluforce-general-brochure.pdf.

[107] SoluForce. *SoluForce: High Pressure Flexible Composite Pipe Systems*. Soluforce. URL: https://www.soluforce.com.

[108] *SoluForceH2T (Hydrogen Tight): Unique in the world of hydrogen transport and a global first*. Sept. 2021. URL: https://www.soluforce.com/content/dam/pipelife/soluforce/marketing/general/brochures/soluforce-hydrogen-tight-h2t-brochure.pdf.

[109] George H. Staab. *Laminar Composites*. In collab. with Victoria Pearson. 2nd ed. Amsterdam, Netherlands: Butterworth-Heinemann, 2015. 466 pp. ISBN: 978-0-12-802619-9. URL: https://ebookcentral-proquest-com.ezproxy.uis.no/lib/uisbib/detail.action?docID=2146005.

[110] Statista. *Electricity production by source France 2019-2020*. Statista. Apr. 2021. URL: https://www.statista.com/statistics/768066/electricity-production-france-source/.

[111] Statista. *Norway: electricity production by source 2020*. Statista. URL: https://www.statista.com/statistics/1025497/distribution-of-electricity-production-in-norway-by-source/.

[112] Statista. *Sweden: power mix*. Statista. URL: https://www.statista.com/statistics/1013726/share-of-electricity-production-in-sweden-by-source/.

[113] Bengt Sundén. “Chapter 3 - Hydrogen”. In: *Hydrogen, Batteries and Fuel Cells*. Ed. by Bengt Sundén. Academic Press, 2019, pp. 37–55. ISBN: 978-0-12-816950-6. DOI: 10.1016/B978-0-12-816950-6.00003-8. URL: https://doi.org/10.1016/B978-0-12-816950-6.00003-8.

[114] Amit Kumar Tanwer. “Mechanical properties testing of unidirectional and bi-directional glass fibre reinforced epoxy based composites”. In: *International Journal of Research in Advent Technology* 2.11 (2014), pp. 34–39.

[115] *The Engineering ToolBox website*. URL: https://www.engineeringtoolbox.com/.

[116] Stephen P. Timoshenko. *Theory of elasticity*. In collab. with J. N Goodier. 3rd ed. New York: McGraw-Hill, 1970. 567 pp. ISBN: 0-07-085805-5. URL: https://bibsys-almaprimo.hosted.exlibrisgroup.com/permalink/f/1te4v12/BIBSYS_ILS71467465740002201.

[117] Engineering ToolBox. *Hydrogen - Thermophysical Properties*. 2008. URL: https://www.engineeringtoolbox.com/hydrogen-d_1419.html.

[118] E. Troncoso and M. Newborough. "Electrolysers for mitigating wind curtailment and producing 'green' merchant hydrogen". In: *International Journal of Hydrogen Energy*. 11th International Conference: "Hydrogen Materials Science & Chemistry of Carbon Nanomaterials" 36.1 (Jan. 2011), pp. 120–134. ISSN: 0360-3199. DOI: 10.1016/j.ijhydene.2010.10.047. URL: https://doi.org/10.1016/j.ijhydene.2010.10.047.

[119] Stephen W. Tsai and Edward M. Wu. *A General Theory of Strength for Anisotropic Materials*. 1972, p. 71. URL: https://apps.dtic.mil/sti/citations/ADA306350.

[120] John Turner et al. "Record low surface air temperature at Vostok station, Antarctica". In: *Journal of Geophysical Research: Atmospheres* 114 (D24 Dec. 27, 2009). _eprint: https://onlinelibrary.wiley.com/doi/pdf/10.1029/2009JD012104. ISSN: 2156-2202. DOI: 10.1029/2009JD012104. URL: https://onlinelibrary.wiley.com/doi/abs/10.1029/2009JD012104.

[121] Harold C. Urey. "On the Early Chemical History of the Earth and the Origin of Life". In: *Proceedings of the National Academy of Sciences* 38.4 (Apr. 1, 1952). Publisher: Proceedings of the National Academy of Sciences, pp. 351–363. DOI: 10.1073/pnas.38.4.351. URL: https://doi.org/10.1073/pnas.38.4.351.

[122] Valery V. Vasiliev and Evgeny V. Morozov, eds. *Advanced Mechanics of Composite Materials and Structures*. Elsevier, 2018. 856 pp. ISBN: 978-0-08-102209-2. DOI: 10.1016/B978-0-08-102209-2.00013-X. URL: https://doi.org/10.1016/C2016-0-04497-2.

[123] Phuong Anh Vo Dong, Catherine Azzaro-Pantel, and Anne-Laure Cadene. "Economic and environmental assessment of recovery and disposal pathways for CFRP waste management". In: *Resources, Conservation and Recycling* 133 (June 2018), pp. 63–75. ISSN: 0921-3449. DOI: 10.1016/j.resconrec.2018.01.024. URL: https://doi.org/10.1016/j.resconrec.2018.01.024.

[124] Michael W. Hyer. *Stress Analysis of Fiber-Reinforced Composite Materials*. In collab. with Scott White. DEStech Publications, Inc, 2009. 687 pp. ISBN: 978-1-932078-86-2. URL: https://www.destechpub.com/product/stress-analysis-of-fiber-reinforced-composite-materials/.

[125] Ben Wang and Hang Gao. "Fibre Reinforced Polymer Composites". In: *Advances in Machining of Composite Materials: Conventional and Non-conventional Processes*. Ed. by Islam Shyha and Dehong Huo. Engineering Materials. Cham: Springer International Publishing, 2021, pp. 15–43. ISBN: 978-3-030-71438-3. DOI: 10.1007/978-3-030-71438-3_2. URL: https://doi.org/10.1007/978-3-030-71438-3_2.

[126] Yuki. *China's Hydrogen Value Chain Compared to the World's Leading Practices*. Energy Iceberg. Aug. 25, 2019. URL: https://energyiceberg.com/china-hydrogen-industry-comparison/.

[127] Kai Zeng and Dongke Zhang. "Recent progress in alkaline water electrolysis for hydrogen production and applications". In: *Progress in Energy and Combustion Science* 36.3 (June 2010), pp. 307–326. ISSN: 0360-1285. DOI: 10.1016/j.pecs.2009.11.002. URL: https://doi.org/10.1016/j.pecs.2009.11.002.

[128] Guotao Zhang and Xinhua Wan. "A wind-hydrogen energy storage system model for massive wind energy curtailment". In: *International Journal of Hydrogen Energy* 39.3 (Jan. 16, 2014), pp. 1243–1252. ISSN: 0360-3199. DOI: 10.1016/j.ijhydene.2013.11.003. URL: https://doi.org/10.1016/j.ijhydene.2013.11.003.

[129] Xiongwen Zhang et al. "Towards a smart energy network: The roles of fuel/electrolysis cells and technological perspectives". In: *International Journal of Hydrogen Energy* 40.21 (June 8, 2015), pp. 6866–6919. ISSN: 0360-3199. DOI: 10.1016/j.ijhydene.2015.03.133. URL: https://www.sciencedirect.com/science/article/pii/S036031991500779X.

[130] M Zoulias. *Hydrogen Production & Distribution*. Technology Brief P12. Catalog URL: https://iea-etsap.org/index.php. IEA-ETSAP (Energy Technology System Analysis Programme, Feb. 2014, pp. 1–9. URL: https://iea-etsap.org/E-TechDS/PDF/P12_H2_Feb2014_FINAL%203_CRES-2a-GS%20Mz%20GSOK.pdf.

[131] A. Zubail et al. "Carbon and energy footprint of nonmetallic composite pipes in onshore oil and gas flowlines". In: *Journal of Cleaner Production* 305 (July 10, 2021), p. 127150. ISSN: 0959-6526. DOI: 10.1016/j.jclepro.2021.127150. URL: https://doi.org/10.1016/j.jclepro.2021.127150.

[132] C. H. Zweben. “Composites: Overview”. In: *Encyclopedia of Condensed Matter Physics*. Ed. by Franco Bassani, Gerald L. Liedl, and Peter Wyder. Oxford: Elsevier, 2005, pp. 192–208. ISBN: 978-0-12-369401-0. DOI: 10.1016/B0-12-369401-9/00545-3. URL: https://doi.org/10.1016/B0-12-369401-9/00545-3.

A - Expression of the parameters related to the design aspects of FRP

Parameters for stiffness and compliance matrices

E_i defines the modulus of elasticity in the directions x_i and $\nu_{ij} = -\frac{\varepsilon_j}{\varepsilon_i}$ defines the Poisson's ratios.

$$S_{11} = \frac{1}{E_1}; \quad S_{12} = -\frac{\nu_{21}}{E_2}; \quad S_{13} = -\frac{\nu_{31}}{E_3} \tag{36}$$

$$S_{21} = -\frac{\nu_{12}}{E_1} = S_{12}; \quad S_{22} = \frac{1}{E_2}; \quad S_{23} = -\frac{\nu_{32}}{E_3} \tag{37}$$

$$S_{31} = -\frac{\nu_{13}}{E_1} = S_{13}; \quad S_{32} = -\frac{\nu_{23}}{E_2} = S_{23}; \quad S_{33} = \frac{1}{E_3} \tag{38}$$

$$S_{44} = \frac{1}{G_{23}}; \quad S_{55} = \frac{1}{G_{13}}; \quad S_{66} = \frac{1}{G_{12}} \tag{39}$$

$$C_{11} = \frac{S_{22}S_{33} - S_{23}^2}{S}; \quad C_{12} = \frac{S_{13}S_{23} - S_{12}S_{33}}{S}; \quad C_{13} = \frac{S_{12}S_{23} - S_{13}S_{22}}{S} \tag{40}$$

$$C_{21} = C_{12}; \quad C_{22} = \frac{S_{33}S_{11} - S_{13}^2}{S}; \quad C_{23} = \frac{S_{12}S_{13} - S_{23}S_{11}}{S} \tag{41}$$

$$C_{31} = C_{13}; \quad C_{32} = C_{23}; \quad C_{33} = \frac{S_{11}S_{22} - S_{12}^2}{S} \tag{42}$$

$$C_{44} = \frac{1}{S_{44}}; \quad C_{55} = \frac{1}{S_{55}}; \quad C_{66} = \frac{1}{S_{66}} \tag{43}$$

with: $S = S_{11}S_{22}S_{33} - S_{11}S_{23}^2 - S_{22}S_{13^2} - S_{33}S_{12}^2 + 2S_{12}S_{23}S_{13}$

Source: Pavlou, D. [87]

Parameter for the reduced stiffness matrix

$$Q_{11} = C_{11} - \frac{C_{13}^2}{C_{33}} = \frac{E_1}{1 - \nu_{12}\nu_{21}}; \quad Q_{12} = C_{12} - \frac{C_{13}C_{23}}{C_{33}} = \frac{\nu_{12}E_2}{1 - \nu_{12}\nu_{21}} \tag{44}$$

$$Q_{22} = C_{22} - \frac{C_{23}^2}{C_{33}} = \frac{E_2}{1 - \nu_{12}\nu_{21}}; \quad Q_{66} = C_{66} = G_{12} \tag{45}$$

Source: Pavlou, D. [87]

Transformation matrix

$$[T] = \begin{bmatrix} \cos^2\theta & \sin^2\theta & 2\sin^2\theta\cos\theta \\ \sin^2\theta & \cos^2\theta & -2\sin\theta\cos\theta \\ -\sin\theta\cos\theta & \sin\theta\cos\theta & \cos^2\theta - \sin^2\theta \end{bmatrix} \tag{46}$$

Source: Pavlou, D. [87]

Parameters for the transformed reduced stiffness and compliance matrices

By defining $c = \cos\theta$ and $s = \sin\theta$

$$\overline{S}_{11} = S_{11}c^4 + (2S_{12} + S_{66})c^2s^2 + S_{22}s^4 \tag{47}$$

$$\overline{S}_{12} = (S_{11} + S_{22} - S_{66})c^2s^2 + S_{12}(c^4 + s^4) \tag{48}$$

$$\overline{S}_{16} = (2S_{11} - 2S_{12} - S_{66})c^3s - (2S_{22} - 2S_{12} - S_{66})cs^3) \tag{49}$$

$$\overline{S}_{22} = S_{11}s^4 + (2S_{12} + S_{66})c^2s^2 + S_{22}c^4 \tag{50}$$

$$\overline{S}_{26} = (2S_{11} - 2S_{12} - S_{66})cs^3 - (2S_{22} - 2S_{12} - S_{66})c^3s \tag{51}$$

$$\overline{S}_{66} = 2(2S_{11} + 2S_{22} - 4S_{12} - S_{66})c^2s^2 + S_{66}(c^4 + s^4) \tag{52}$$

$$\overline{Q}_{11} = Q_{11}c^4 + 2(Q_{12} + 2S_{66})c^2s^2 + Q_{22}s^4 \tag{53}$$

$$\overline{Q}_{12} = (Q_{11} + Q_{22} - 4Q_{66})c^2s^2 + Q_{12}(c^4 + s^4) \tag{54}$$

$$\overline{Q}_{16} = (Q_{11} - Q_{12} - 2Q_{66})c^3s + (Q_{12} - Q_{22} + 2Q_{66})cs^3) \tag{55}$$

$$\overline{Q}_{22} = Q_{11}s^4 + 2(Q_{12} + 2Q_{66})c^2s^2 + Q_{22}c^4 \tag{56}$$

$$\overline{Q}_{26} = (Q_{11} - Q_{12} - 2Q_{66})cs^3 + (Q_{12} - Q_{22} + 2Q_{66})c^3s \tag{57}$$

$$\overline{Q}_{66} = (Q_{11} + Q_{22} - 2Q_{12} - 2Q_{66})c^2s^2 + Q_{66}(c^4 + s^4) \tag{58}$$

Source: Pavlou, D. [87]

Strain-displacement relations

$$\varepsilon_x = \frac{\partial u}{\partial x} \quad ; \quad \varepsilon_y = \frac{\partial v}{\partial y} \quad ; \quad \varepsilon_z = \frac{\partial w}{\partial z} \tag{59}$$

$$\gamma_{xy} = \frac{\partial v}{\partial x} + \frac{\partial u}{\partial y} \quad ; \quad \gamma_{xz} = \frac{\partial w}{\partial x} + \frac{\partial u}{\partial z} \quad ; \quad \gamma_{yz} = \frac{\partial w}{\partial y} + \frac{\partial v}{\partial z} \tag{60}$$

Source: Timoshenko, S.P. [116]

Tsai-Wu failure criterion parameters

By defining σ_i^C and σ_i^T as the compressive and tensile failure stress in the x_i direction and also τ_{12}^F as the shear failure stress in the $x_1 - x_2$ plane, the parameters are written below:

$$F_1 = \left(\frac{1}{\sigma_1^T} + \frac{1}{\sigma_1^C}\right) \quad ; \quad F_{12} = \left(\frac{1}{\sigma_2^T} + \frac{1}{\sigma_2^C}\right) \tag{61}$$

$$F_{66} = \left(\frac{1}{\tau_{12}^F}\right)^2 \quad ; \quad F_{11} = -\left(\frac{1}{\sigma_1^T \sigma_1^C}\right) \quad ; \quad F_{22} = -\left(\frac{1}{\sigma_2^T \sigma_2^C}\right) \tag{62}$$

Source: Tsai, S.W. [119]

Parameters in the equation of the thermal effect (23)

$$\begin{aligned} \overline{S}_{11} &= \frac{\cos^4\theta}{E_1} + \left(-\frac{2\nu_{12}}{E_1} + \frac{1}{G_{12}}\right)\cos^2\theta\sin^2\theta + \frac{\sin^4\theta}{E_2} \\ \overline{S}_{12} &= \left(\frac{1}{E_1} + \frac{1}{E_2} - \frac{1}{G_{12}}\right)\cos^2\theta\sin^2\theta - \frac{\nu_{12}}{E_1}\left(\cos^4\theta + \sin^4\theta\right) \end{aligned} \tag{63}$$

Source: Pavlou, D. [87]

B - Thermodynamics and physical properties for hydrogen

Thermophysical properties of hydrogen from [117]

Molecular Weight	2.016
Specific Gravity, air = 1	0.070
Specific Volume (ft^3/lb, m^3/kg)	194, 12.1
Density of liquid at atmospheric pressure (lb/ft^3, kg/m^3)	4.43, 71.0
Absolute Viscosity ($lb_m/ft\ s$, *centipoises*)	$6.05\ 10^{-6}$, 0.009
Sound velocity in gas (*m/s*)	1315
Specific Heat - c_p - (Btu/lb^oF *or* cal/g^oC, *J/kgK*)	3.42, 14310
Specific Heat Ratio - c_p/c_v	1.405
Gas constant - *R* - ($ft\ lb/lb^oR$, J/kg^oC)	767, 4126
Thermal Conductivity ($Btu/hr\ ft\ ^oF$, W/m^oC)	0.105, 0.182
Boiling Point - saturation pressure 14.7 psia and 760 mm Hg - (^oF, ^oK)	-423, 20.4
Latent Heat of Evaporation at boiling point (*Btu/lb, J/kg*)	192, 447000
Freezing or Melting Point at 1 atm (^oF, ^oC)	-434.6, -259.1
Latent Heat of Fusion (*Btu/lb, J/kg*)	25.0, 58000
Critical Temperature (^oF, ^oC)	-399.8, -240.0
Critical Pressure (*psia*, MN/m^2)	189, 1.30
Critical Volume (ft^3/lb, m^3/kg)	0.53, 0.033
Flammable	yes
Heat of combustion (Btu/ft^3, *Btu/lb, kJ/kg*)	320, 62050, 144000

Figure 15: Properties for hydrogen at 25°C and atmospheric pressure
Source: The Engineering Toolbox [117]
`https://www.engineeringtoolbox.com/hydrogen-d_1419.html`

Additional chemical, physical and thermal values or units from [113]

Property	Value
Density	0.0824 $kg{\cdot}m^{-3}$
Viscosity	$9{\cdot}10^{-6}$ $kg{\cdot}ms^{-1}$
Boiling point-saturation atmsopheric pressure	20.4 K or -252.6°C

Table 21: Additional values or units
Source: Sunden, B. [113]
`https://doi.org/10.1016/B978-0-12-816950-6.00003-8`

Useful conversion factors and thermodynamic properties

- Btu = 1055 J
- Litre = 0.2642 gallons U.S.
- 1 kg_{H_2} = 11.13 N·m^3 (at 0°C and 1 atm)
- Hydrogen HHV (ΔH) = -286 kJ·$(mol)^{-1}$ (HHV = Higher heating value)
- Hydrogen LHV (ΔH) = -242 kJ·$(mol)^{-1}$ (LHV = Lower heating value)
- Energy content of 1 kg_{H_2} = 141.9 MJ (HHV) // 120.1 MJ (LHV) = 39.4 kWh // 33.3 kWh
- Energy content of 1 N·m^3 $_{H_2}$ = 12.7 MJ (HHV)

Source: The hydrogen economy: opportunities, costs, barriers, and R&D needs [36]
`https://doi.org/10.17226/10922`

The main parameters used for the values in the framework analysis from [26]

Isentropic Compressor Efficiency	$\eta_{comp,is}$ = 0.8 [16]
Mechanical Compressor Efficiency	$\eta_{comp,mech}$ = 0.9 [16]
Isentropic Pump Efficiency	$\eta_{pump,is}$ = 0.8 [16]
Mechanical Pump Efficiency	$\eta_{pump,mech}$ = 0.9 [16]
Operating Temperature PEM	T_{PEM} = 80°C [19]
Operating Temperature AWE	T_{AWE} = 90°C [127]
Base cost for a reference PEM electrolyser	$C_{0,PEM}$ = 36 000€·m^{-2} [99]
Base active area size for a reference PEM electrolyser	$A_{0,PEM}$ = 28 m^2 [5]
Base cost for a reference AWE electrolyser	$C_{0,AWE}$ = 8 300€·m^{-2} [99]
Base active area size for a reference AWE electrolyser	$A_{0,AWE}$ = 97 m^2 [127]
Cost of Wind (for all time periods)	EP = 40€·MW^{-1} [63]

Table 22: Parameters from the framework analysis
Source: Cooper, N. [26]
`https://doi.org/10.1016/j.ijhydene.2021.12.225`

C - List of standards and ongoing hydrogen projects

European Projects:

- H2SusBuild
- HySafe
- HyApproval
- European Integrated Hydrogen Project (EIHP2)
- HyWays
- Zemships
- Hytrec (Hydrogen Technology Research Centre)
- HyREADY (JIP: Joint Industry Project) [48]

Standards that could be of interest:

- ISO 14692
- ISO TC197 (Hydrogen technologies)
- EIGA (IGC Doc 121/04, Pipeline)
- Local US regulations: ASME B31.12 [12] // ASME B31.3 [13]

D - Matlab codes for reproducing graphs shared by *Strohm*

Code for the mechanical graphs

```
%%
clc
clear all
close all

figure(1)
y11 = [6, 6, 6, 6, 6, 6]*10^3 ;
y21 = [11, 11, 11, 11, 11, 11]*10^3 ;
y31 = [16.5, 16.5, 16.5, 16.5, 16.5, 16.5]*10^3 ;
y41 = [26.5, 26.5, 26.5, 26.5, 26.5, 26.5]*10^3 ;
yyaxis left
x11 = [0, 5, 10, 15, 20, 25] ;
x011 = linspace(0,25,100) ;
y011 = 0.208*10^3 * x011 ;
y021 = (800/7)*x011 ;
y031 = (550/7)*x011 ;
y041 = (325/7)*x011 ;

p11 = plot(x11,y11,'-','color',[1 0 0],'LineWidth',2);
grid on    %red 1 0 0 ; green 0 1 0 ; blue 0 0 1 ;
hold on    % cyan 0 1 1 ; pink 1 0 1 ; yellow 0 1 1 ;
% black 0 0 0 ; white 1 1 1
p21 = plot(x11,y21,'-','color',[0 1 0],'LineWidth',2) ;
p31 = plot(x11,y31,'-','color',[0 1 1],'LineWidth',2) ;
p41 = plot(x11,y41,'-','color',[0 0 1],'Linewidth',2) ;
p51 = plot(x011,y011,'--','color',[1 0 0], 'LineWidth'
              , 2) ;
p61 = plot(x011,y021,'--','color',[0 1 0], 'LineWidth'
              , 2) ;
p71 = plot(x011,y031,'--','color',[0 1 1], 'LineWidth'
              , 2) ;
p81 = plot(x011,y041,'--','color',[0 0 1], 'LineWidth'
              , 2) ;
title('Axial Stiffness and Strain for the 4"TCP at
            50 bar')
```

```
xlabel('Axial Force $$F_{axial}$$ (kN)','interpreter'
            ,'latex')
ylabel('Axial Stiffness $$EA\hspace{0.1cm}(kN)$$'
            ,'interpreter','latex')

x51 = [25,25,25,25,25,25] ;
y51 = [0,0.5,1,1.5,2,2.5] ;
yyaxis right
plot(x51,y51)
ylabel('Axial strain $$\varepsilon\hspace{0.1cm}(\%)$$'
            ,'interpreter','latex')
legend([p11 p21 p31 p41 p51 p61 p71 p81],{'EA (60 C )',
            'EA (40 C )', 'EA (20 C )', 'EA (0 C )',
            '   (60 C )', '   (40 C )', '   (20 C )',
            '   (0 C )'},'Location','northeast')

%%

figure (2)
vx_red01 = [(51/2660),(0.05),(33/532)];
vy_red01 = [(13.75), (13.75), (13.75)];
x_red = linspace(33/532,0.40,100);
y_red = 73.6352*(x_red).^2 -52.5144*(x_red) + 16.7241;
vx_green01 = [51/2660, 0.05];
vy_green01 = [26.25, 26.25];
x_green = linspace(0.05,0.40,100);
y_green = 130.9523809523809*(x_green).^2
            - 99.4047619047619*(x_green)
            + 30.8928571428571;
vx_cyan01 = [51/2660, 3/76]; vy_cyan01 = [475/12; 475/12];
x_cyan = linspace(3/76,0.40,100);
y_cyan = 220.0600295161741*(x_cyan).^2
            - 159.1193510430378*(x_cyan)
            + 45.5214690279606;
vx_blue01 = linspace(51/2660, 0.05, 100);
vy_blue01 =  611.8332186456612*(vx_blue01).^2
            - 109.9035986441367*(vx_blue01)
            + 65.6322635522593;
x_blue = linspace(0.05, 0.40, 100);
y_blue = 339.2857142857143*(x_blue).^2
```

```
            - 251.4880952380952*(x_blue)
            + 73.3928571428571;

x_red2 = linspace(51/2660, 0.40, 100);
y_red2 = -43.8440091697742*(x_red2).^2
            + 53.3897388351979 *(x_red2)
            + 0.242479266418062 ;
x_green2 = x_red2 ;
y_green2 = -78.7372439642924*(x_green2).^2
            + 90.9923463785754*(x_green2)
            + 0.784353816189947 ;
x_cyan2 = x_red2;
y_cyan2 = -113.050441283413*(x_cyan2).^2
            + 126.163598103381*(x_cyan2)
            + 1.78929803066032 ;
x_blue2 = x_red2 ;
y_blue2 = -211.929770912989*(x_blue2).^2
            + 214.657862547793*(x_blue2)
            + 2.21228499362754 ;

p= plot(vx_red01, vy_red01,'-', 'color',[1 0 0],
            'LineWidth',2); grid on
hold on
m12 = plot(x_red, y_red,'-', 'color',[1 0 0],
            'LineWidth',2);
m22 = plot(vx_green01,vy_green01,'-','color',
            [0 1 0],'LineWidth',2);
plot(x_green,y_green,'color',[0 1 0],'LineWidth',2); hold on
m32 = plot(vx_cyan01,vy_cyan01,'-','color',[0 1 1],'LineWidth',2);
plot(x_cyan,y_cyan,'color',[0 1 1],'LineWidth',2) ; hold on
m42 = plot(vx_blue01,vy_blue01,'-','color',[0 0 1],'LineWidth',2);
plot(x_blue,y_blue,'color',[0 0 1],'LineWidth',2); %hold on
p52 = plot(x_red2, y_red2,'--','color',[1 0 0],
            'LineWidth',2);
p62 = plot(x_green2, y_green2,'--','color',[0 1 0],
            'LineWidth',2);
p72 = plot(x_cyan2, y_cyan2,'--','color',[0 1 1],
            'LineWidth',2);
p82 = plot(x_blue2, y_blue2,'--','color',[0 0 1],
            'LineWidth',2);
```

```
yyaxis left
title('Bending Stiffness and Reaction Moment for
            the 4"TCP at 50 bar');
xlabel('Curvature $$(m^{-1})$$' ,'interpreter',
            'latex');
ylabel('Bending Stiffness $$EI (kN\cdot m^2) $$',
            'interpreter','latex');

x52 = [0.4,0.4,0.4,0.4,0.4,0.4,0.4,0.4] ;
y52 = [0,2,4,6,8,10,12,14] ;
yyaxis right
plot(x52,y52)
ylabel('Bending Reaction Moment $$BRM (kN\cdot m) $$',
            'interpreter','latex');


legend([m12 m22 m32 m42 p52 p62 p72 p82],
            {'EI (60 C )','EI (40 C )','EI (20 C )',
            'EI(0 C )','BRM (60 C )','BRM (40 C )',
            'BRM (20 C )','BRM (0 C )'},'Location',
            'north')

%%

figure(3)
y13 = [880/21,880/21,880/21,880/21,880/21] ;
y23 = [50,50,50,50,50] ;
y33= [410/7,410/7,410/7,410/7,410/7] ;
y43 = [530/7,530/7,530/7,530/7,530/7] ;
yyaxis left
x13 = [0, 0.5, 1.0, 1.5, 2.0] ;
x013 = linspace(0,2.0,100) ;
y013 = (205/21) * x013 ;
y023 = (35/3)*x013 ;
y033 = (290/21)*x013 ;
y043 = (125/7)*x013 ;

p13 = plot(x13,y13,'-','color',[1 0 0],
            'LineWidth',2);
grid on   %red 1 0 0 ; green 0 1 0 ; blue 0 0 1 ;
```

```
hold on    %cyan 0 1 1 ; pink 1 0 1 ; yellow 0 1 1 ;
           %black 0 0 0 ; white 1 1 1
p23 = plot(x13,y23,'-','color',[0 1 0],
             'LineWidth',2) ; % green 0 1 0
p33 = plot(x13,y33,'-','color',[0 1 1],
             'LineWidth',2) ; % cyan 0 1 1
p43 = plot(x13,y43,'-','color',[0 0 1],
             'Linewidth',2) ; % blue 0 0 1
p53 = plot(x013,y013,'--','color',[1 0 0],
             'LineWidth', 2) ; % red 1 0 0
p63 = plot(x013,y023,'--','color',[0 1 0],
             'LineWidth', 2) ; % green 0 1 0
p73 = plot(x013,y033,'--','color',[0 1 1],
             'LineWidth', 2) ; % cyan 0 1 1
p83 = plot(x013,y043,'--','color',[0 0 1],
             'LineWidth', 2) ; % blue 0 0 1
title('Torsional Stiffness and Reaction Moment
             for the 4"TCP at 50 bar')
xlabel('Torsion angle $$ \Theta_{Torsion}
             \hspace{0.1cm} (degree \cdot m^{-1})$$',
             'interpreter','latex')
ylabel('Torsional Stiffness $$GJ \hspace{0.1cm}
             (kN\cdot m^2)$$','interpreter','latex')

x53 = [2,2,2,2,2,2,2] ;
y53 = [0,1,2,3,4,5,6] ;
yyaxis right
plot(x53,y53,'-')
ylabel('Torsional Reaction Moment
            $$T\hspace{0.1cm}(kN\cdot m)$$ ',
             'interpreter','latex')
legend([p13 p23 p33 p43 p53 p63 p73 p83],
             {'GJ (60 C )', 'GJ (40 C )', 'GJ (20 C )',
             'GJ (0 C )', 'T (60 C )', 'T (40 C )',
             'T (20 C )', 'T (0 C )'},
             'Location','northeast')
```

Code for the hydrogen permeation prediction

```
%%
```

```
clc
close all
clear all

figure(1)

x1 = [20,40,60];
y1 = [0.000178,0.00238,0.00715];
plot(x1,y1,'*-g','LineWidth',3)
xlim([10 70])
ylim([-0.0004 0.008])
title('Permeation results: 4" pipe from data of
            Strohm''s technical note')
xlabel('Temperature ( C )')
ylabel('TCP Permeation $$(g\cdot (day\cdot m)^{-1} )$$',
            'interpreter','latex')
grid on
% P = 50bar


hold on
x2 = [20,40,60];
y2 = [0.000326,0.00205,0.00653];
plot(x2,y2,'*-b','LineWidth',3) % P = 100 bar

x3 = [20,40,60];
y3 = [0.000259,0.00148,0.00445];
plot(x3,y3,'*-r','LineWidth',3) % P = 150 bar

x4 = [20,40,60];
y4 = [0.000251,0.00126,0.00402];
plot(x4,y4,'*-k','LineWidth',3) % P = 200 bar


legend('P=50bar','P=100bar','P=150bar','P=200bar',
            'Location','northwest')

%%
figure(2)

```

```
x5 = [20,40,60];
y5 = [0.0000965,0.00141,0.00437];
plot(x5,y5,'*-g','LineWidth',3)
xlim([10  70])
ylim([-0.0004  0.008])
title('Permeation results: 6" pipe from data of
            Strohm''s technical note') % P = 50bar
xlabel('Temperature ( C )')
ylabel('TCP Permeation $$(g\cdot (day\cdot m)^{-1} )$$',
            'interpreter','latex')
grid on

hold on
x6 = [20,40,60];
y6 = [0.000136,0.000899,0.00277];
plot(x6,y6,'*-b','LineWidth',3) % P = 100 bar

x7 = [20,40,60];
y7 = [0.000119,0.000662,0.00203];
plot(x7,y7,'*-r','LineWidth',3) % P = 150 bar

x8 = [20,40,60];
y8 = [0.0000672,0.00038,0.00117];
plot(x8,y8,'*-k','LineWidth',3) % P = 200 bar


legend('P=50bar','P=100bar','P=150bar',
            'P=200bar','Location','northwest')
```

Code for the calculation of curves and lines

```
x111 = 51/2660 ; y111 = 25/4 ;
x222 = 0.20 ; y222 = 110/3 ;
x333 = 0.40 ; y333 = 325/6 ;


abc1 = inv([x111^2 x111 1 ;
    x222^2 x222 1;
    x333^2 x333 1]) *     [y111;
    y222 ;
```

```
10        y333]
11
12 format longg
```